FINAL REPORT

U.F. Project No: 49104504801-12
Contract No: BC-354
RPWO#: 36

EVALUATION OF SUPERPAVE MIXTURES WITH AND WITHOUT POLYMER MODIFICATION BY MEANS OF ACCELERATED PAVEMENT TESTING

Mang Tia
Reynaldo Roque
Okan Sirin
Hong-Joong Kim

November 2002

Department of Civil & Coastal Engineering
College of Engineering
University of Florida
Gainesville, Florida

ACKNOWLEDGMENTS

The Florida Department of Transportation (FDOT) is gratefully acknowledged for providing the financial support for this study. The FDOT Materials Office provided the additional testing equipment, materials and personnel needed for this investigation. Sincere thanks go to the project manager, Dr. Bouzid Choubane for providing the technical coordination and advices throughout the project. Sincere gratitudes are extended to the FDOT Materials Office personnel, particularly to Messrs. Gale C. Page, Tom Byron, Steve Ross, James Musselman, Patrick Upshaw, Greg Sholar, Howard Moseley, Ron McNamara and Natasha Seavers. The help of Messrs. Booil Kim, Sylvester Asiamah, Daniel D. Darku and Claude Villiers in the sampling of asphalt mixtures and installation of thermocouples, and Mr. Rajarajan Subramanian in the laboratory testing of the core samples are acknowledged. The technical inputs from Drs. David Bloomquist and Byron E. Ruth of the University of Florida are duly acknowledged.

TABLE OF CONTENTS

LIST OF TABLES

LIST OF FIGURES

TECHNICAL SUMMARY

Florida Department of Transportation (FDOT) started the use of Superpave mixtures on its highway pavements in 1996. Modified binders have also been used in some of the Superpave mixtures in an effort to increase the cracking and rutting resistance of these mixtures. Due to the short history of these mixtures, it is still too early to assess the long-term performance of these Superpave mixtures and the benefits from the use of the modified binders. There is a need to evaluate the long-term performance of these mixtures and the benefits obtained from the use of modified binders, so that the Superpave technology and the selection of modified binders to be used could be effectively applied.

The FDOT Materials Office has recently acquired a Heavy Vehicle Simulator (HVS) and constructed an Accelerated Pavement Testing (APT) facility which uses this Heavy Vehicle Simulator. The HVS can simulate 20 years of interstate traffic on a test pavement within a short period of time. Thus, a research study was started to evaluate the long-term performance of Superpave mixtures and modified Superpave mixtures using the APT facility. The main objectives of this study are as follows:

(1) To evaluate the operational performance of the Heavy Vehicle Simulator, and to determine its most effective test configurations for use in evaluating the rutting performance of pavement materials and/or designs under typical Florida traffic and climate conditions.

(2) To evaluate the rutting performance of a typical Superpave mixture used in Florida and that of the same Superpave mixture modified with a SBS polymer.

(3) To evaluate the relationship between mixture properties and the rutting performance.

(4) To evaluate the difference in rutting performance of a pavement using two lifts of modified mixture versus a pavement using one lift of modified mixture on top of one lift of unmodified mixture.

Five trial runs with the HVS were made using a super single tire with a load of 9,000 lbs (40 kN), tire pressure of 115 psi (792 kPa) and a wheel traveling speed of 8 mph (12.9 km/hr). These five trial runs used different combinations of wheel traveling direction (uni-directional or bi-directional), total wheel wander and wander increments.

The uni-directional loading was found to be a more efficient mode for evaluation of rutting performance using the HVS. As compared with the bi-directional loading mode, the uni-directional mode produced substantially higher rut depths for the same number of wheel passes and also for the same testing time duration. When the bi-directional loading with no wander was used, imprints of the tire treads were observed on the wheel track. It was found that using a loading mode with wander smoothened out the imprints of the tire treads considerably. The uni-directional loading mode with 4-inch (10.2-cm) wander using 1-inch (2.54-cm) increments was selected to be used in the main field testing program for evaluation of rutting performance based on consideration of testing efficiency and realistic rutting results.

Results from the HVS tests showed that the pavement sections with two lifts of SBS-modified mixture clearly outperformed those with two lifts of unmodified mixture, which had two to two and a half times the rut rate. The pavement sections with a lift of SBS-modified mixture over a lift of unmodified mixture practically had about the same

performance as the sections with two lifts of SBS-modified mixture, and had only about 20% higher rutting than those with two lifts of modified mixture when tested at 50° C. The test section with two lifts of SBS-modified mixture and tested at 65° C still outperformed the test sections with two lifts of unmodified mixture and tested at 50° C.

The mixtures with a higher rut depth in the APA also rutted more in the HVS tests. The mixtures with a GSI of more than 1.0 as measured by the GTM rutted more than one with a GSI close to 1.0. Rutting of the unmodified mixture was observed to be due to a combination of densification and shoving, while that of the SBS-modified mixture was due primarily to densification.

CHAPTER 1
INTRODUCTION

1.1 Background

Florida Department of Transportation (FDOT) started the use of Superpave mixtures on its highway pavements in 1995. Modified binders have also been used in some of the Superpave mixtures in an effort to increase the cracking and rutting resistance of these mixtures. Due to the short history of these mixtures, it is still too early to assess the long-term performance of these Superpave mixtures and the benefits from the use of the modified binders. There is a need to evaluate the long-term performance of these mixtures and the benefits obtained from the use of modified binders, so that the Superpave technology and the selection of modified binders to be used could be effectively applied.

The FDOT Materials Office recently acquired a Heavy Vehicle Simulator (HVS), Mark IV Model, and constructed an Accelerated Pavement Testing (APT) facility, which uses this Heavy Vehicle Simulator. The HVS can simulate 20 years of interstate traffic on a test pavement within a short period of time. Thus, a research study was undertaken to evaluate the long-term performance of Superpave mixtures and SBS-modified Superpave mixtures with particular emphasis on the rutting resistance of these mixtures using the FDOT APT facility. This research work was a cooperative effort between the FDOT and the University of Florida. The main objectives of this study are as follows:

To evaluate the operational performance of the Heavy Vehicle Simulator, and to determine its most effective test configurations for use in evaluating the long term

performance of pavement materials and/or designs under typical Florida traffic and climate conditions.

To evaluate the rutting performance of a typical Superpave mixture used in Florida and that of the same Superpave mixture modified with a SBS polymer.
To evaluate the relationship between mixture properties and the rutting performance.
To evaluate the difference in rutting performance of a pavement using two lifts of modified mixture versus a pavement using one lift of SBS-modified mixture on top of one lift of unmodified mixture.

1.2 Scope of Report

The description of the planning, design and construction of the test sections for this study have previously been presented in an interim report entitled "Evaluation of Superpave and Modified Superpave Mixtures by Means of Accelerated Pavement Testing – Planning and Design Phase." However, some changes were made to the experimental design and instrumentation as the experiment progressed. Thus, in order to have an updated description of the experimental design and instrumentation used in the study and for ease of reference for the readers, this report describes this study in its entirety. The main report includes descriptions of (1) the materials and mix designs used for the test pavement sections, (2) the design of experiment, (3) the instrumentation and data acquisition system, (4) the construction of the test sections, (5) the experimental program for determination of the optimum HVS test configurations, (6) the main HVS testing program, (7) the laboratory testing program, (8) test and analysis results, and (9) findings from this study.

The following information are included in the appendices: (1) detailed mix design data, (2) detailed nuclear density data obtained from the test sections, (3) thickness profiles of cores obtained from the test sections, (4) literature review on full-scale accelerated testing and methods for measurement of rutting, and (5) description of the Heavy Vehicle Simulator, Mark IV Model.

CHAPTER 2
EXPERIMENTAL DESIGN AND INSTRUMENTATION

2.1 Test Track Layout

The layout of the test track, which was constructed at the FDOT APT facility for this study, is shown in Figure 2.1. The test track consisted of seven test lanes. The locations for these test lanes were selected such that they could fit around the two existing concrete conduit boxes. Their widths varied from 12 to 13.5 feet. Each test lane was divided into three test sections, which were identified as Sections A, B and C. Each test section was to be 30 feet long, with 20 feet of test area and 5 feet at each end for acceleration and deceleration of the test wheel. Adjacent to the test lanes was a 94 feet long area, which was to be used for maneuvering of the HVS.

The test track had a 10.5-inch limerock base placed on top of a 12-inch limerock stabilized subgrade. Lanes 1 and 2 were paved with two 2-inch lifts of the SBS-modified Superpave mixture. Lane 3 had a 2-inch lift of the modified Superpave mix over a 2-inch lift of unmodified Superpave mix. Lanes 4 through 7 were paved with two 2-inch lifts of the unmodified Superpave mix. All Sections C in Lane 1 through 5 was named as Phase I, and all Sections A and B in Lane 1 through 5 was named as Phase II.

2.2 Testing Parameters and Sequence

The main testing program was to be run on Test Lanes 1 through 5, which had a total of 15 test sections. Test Lane 6 was set aside for additional testing deemed necessary or desirable at the end of the main testing program. Test Lane 7 was to be

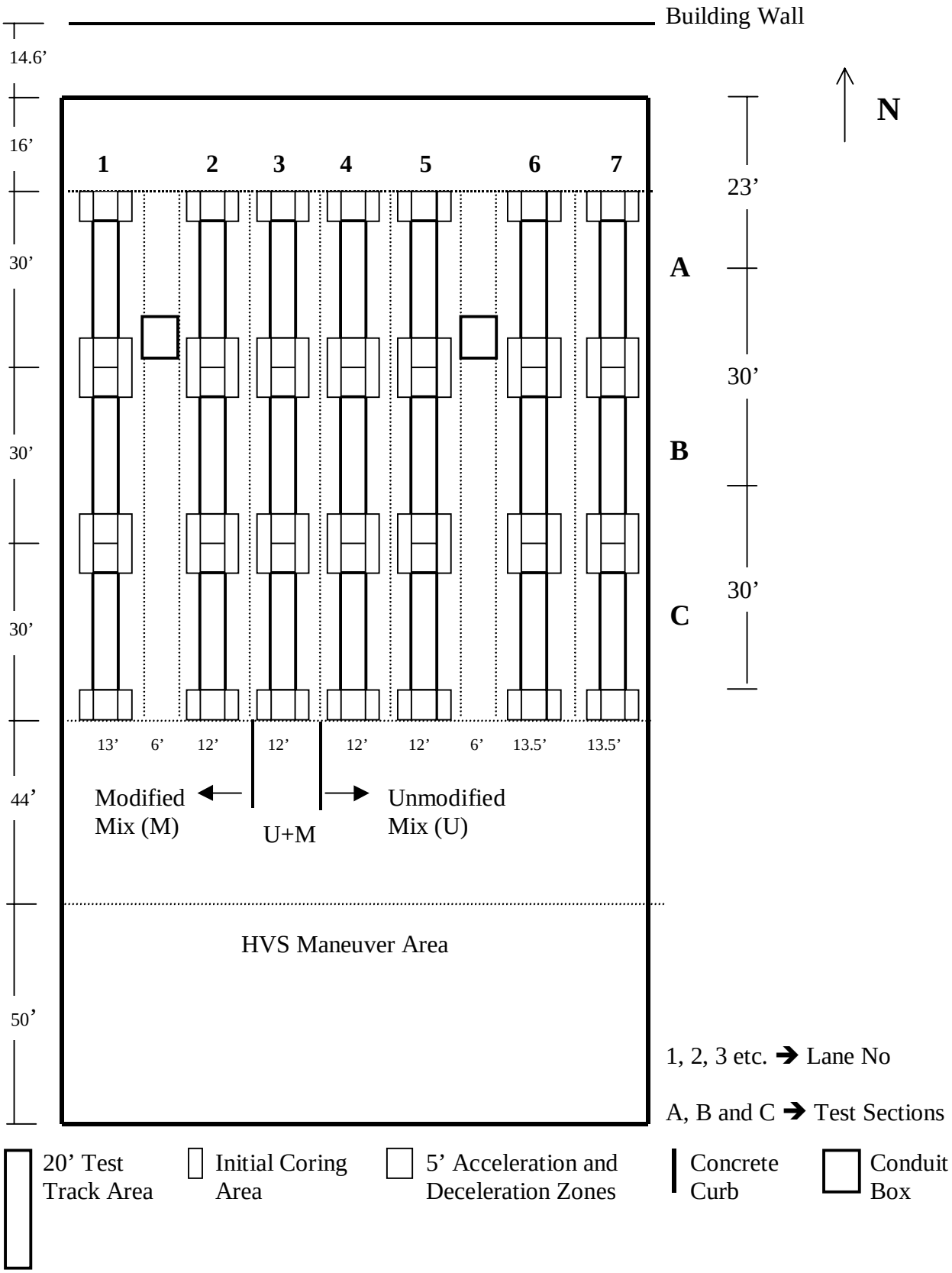

Figure 2.1 APT Test Track Layout

used for trial runs to evaluate the performance characteristics of the HVS and to determine the most effective test configuration to be used in the testing program.

The testing parameters and sequence to be used for the main testing program are shown in Figure 2.2. The testing program was divided into two phases. Phase I was conducted at ambient condition on five test sections, 1C through 5C. Phase II was conducted with temperature control on the other ten test sections. In Phase II, Lanes 1 and 2, which have two 2-inch lifts of SBS-modified Superpave mixture were tested at controlled pavement temperatures of 50° C and 65° C. The rest of the test sections in Phase II were tested at only one temperature, namely 50° C. The testing sequence was arranged such that the effects of time on each lane could be averaged out. It was also arranged such that the HVS vehicle would not have to drive over a test section, which has not been tested in order to minimize damage to the test sections.

The wheel load to be used is a 9-kip super single tire. The type and amount of wheel wander to be used were to be determined after all the trial tests on Lane 7 were completed and evaluated.

2.3 Temperature Monitoring System

The temperature distributions in the test pavements were monitored by means of Type K thermocouples installed at various depths and locations in the test pavements. Type K thermocouple was selected to be used in consideration of its relatively high sensitivity (40 μV/°C), high range of operation (-200 to 1250° C), reliability and low cost. Figure 2.3 shows the plan and cross section views of the thermocouples for each test section. A total of eight thermocouples were installed for each test section. For each

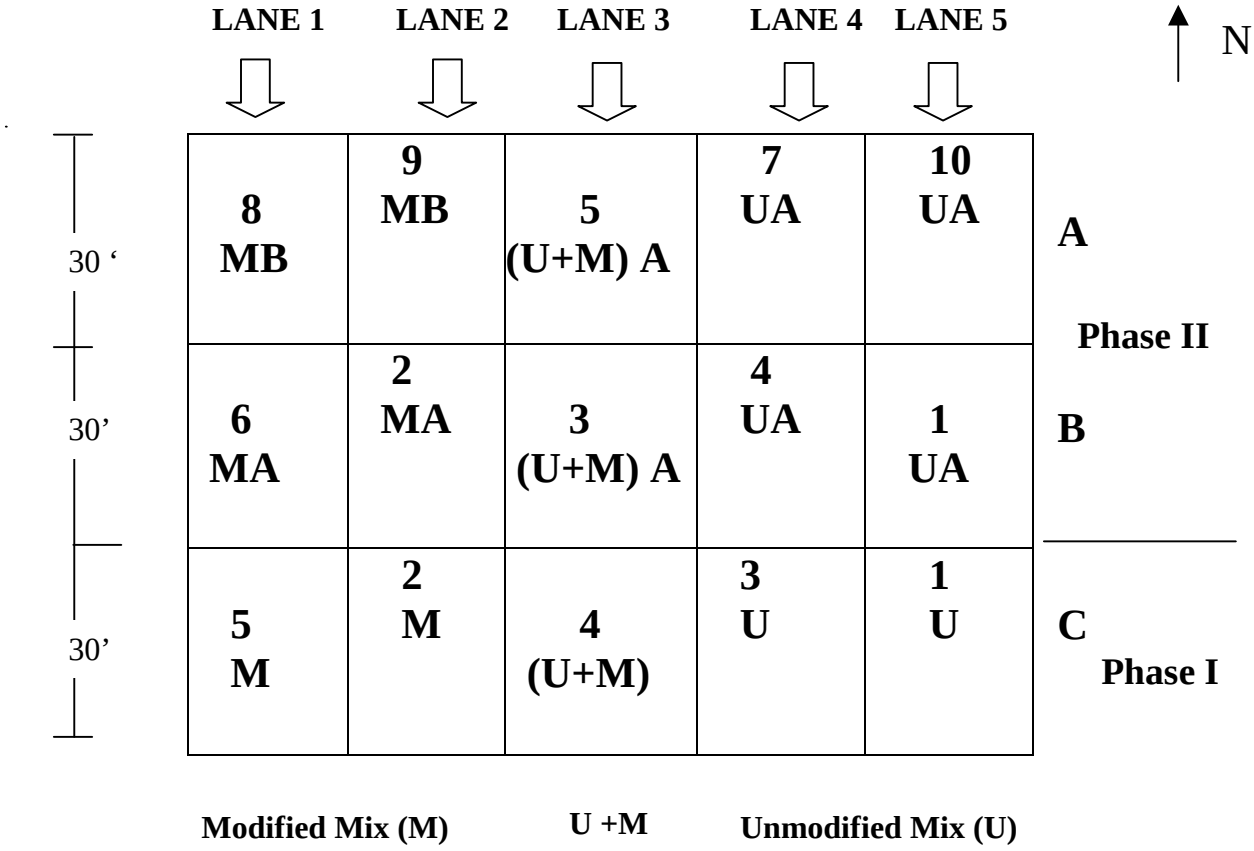

U → Unmodified Mix
M → Modified Mix
U+M →Unmodified +Modified Mix

A → Test Temperature of 50°C
B → Test Temperature of 65°C
1, 2, 3 …→ Testing sequence number

Figure 2.2 Testing Sequence

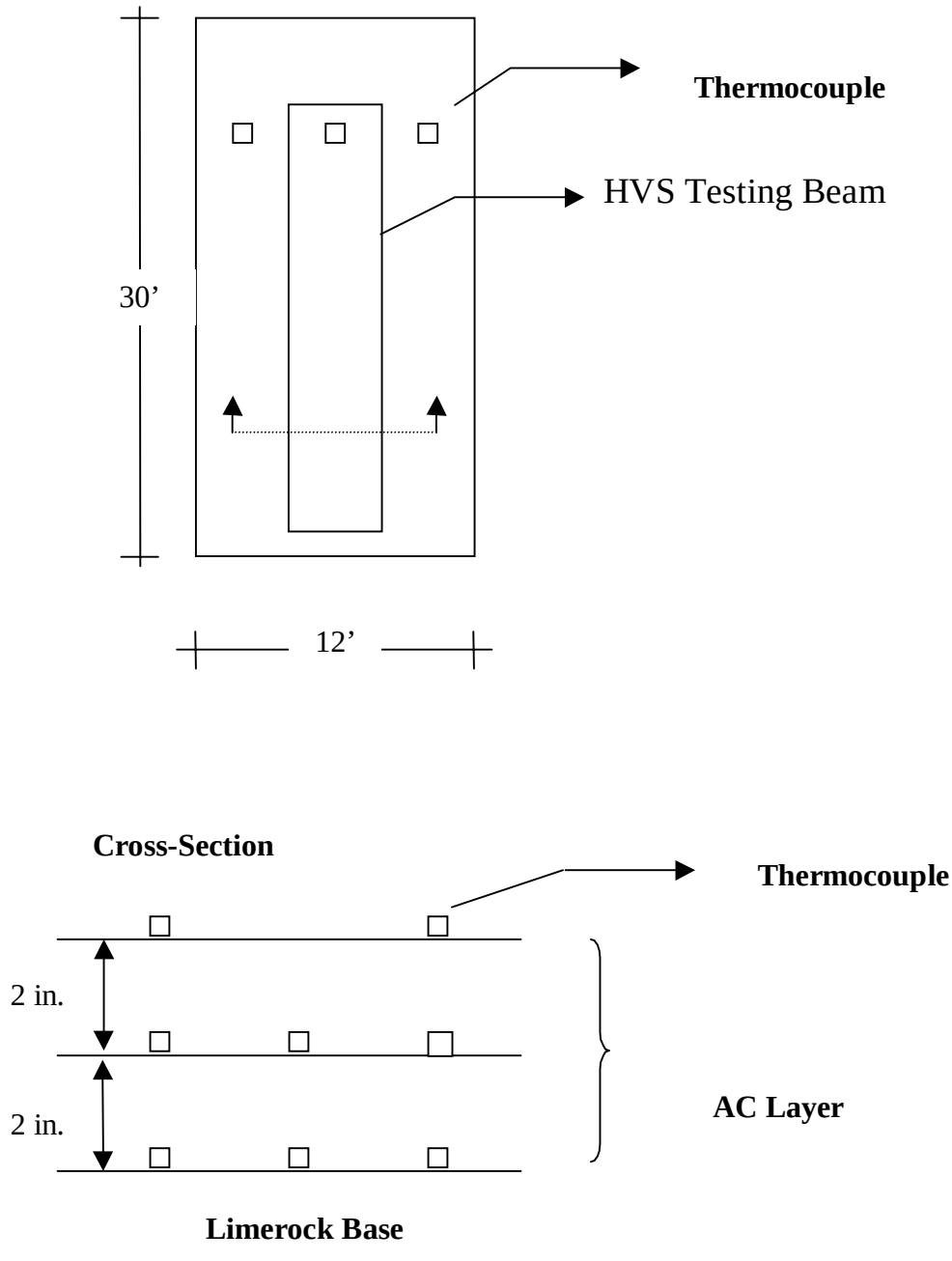

Figure 2.3 Plan and Cross Section View of Thermocouples per Test Section

test section, three thermocouples were placed on top of the base course, three were placed on top of the first lift of asphalt mixture, and two were placed on the surface. These thermocouples were conducted to a PC data acquisition system. Temperature readings were taken every 15 minutes and recorded in the PC during each test.

2.4 Pavement Temperature Control System

A temperature control system to control the temperature of the HVS test pavements was installed at the end of Phase I and used in Phase II of the testing program. It consisted mainly of (1) insulating panels to cover the pavement area to be tested, (2) radiant heaters to heat the pavement surface, and (3) thermocouples to monitor the pavement temperature and to control the heaters.

The insulating panels were made of 3-inch thick Styrofoam boards, which were covered with 0.08-inch thick aluminum sheeting. The roof panels were installed directly under the longitudinal beam of the HVS frame to cover the top of the test pavement area. Each panel was approximately 12 feet wide and 7 feet long. A total of 6 roof panels were used. Five sidewall panels were installed on each side of the HVS to cover the sides of the enclosed test area. Figure 2.4 shows a picture of the HVS covered with the sidewall panels. The total enclosed test area was approximately 3,675 cubic feet.

Three pairs of radiant heaters (Watlow's Raymax 1525) were used to heat the test pavement surface as needed. Figure 2.5 shows the locations and dimensions of a pair of heaters, and the ranges of their heat flux inside the insulating area. Each heater was supported by a 480-volt power and had a maximum capacity of 7500 watts. Figure 2.6 shows a picture of the Raymax radiant heater unit.

Figure 2.4 Photo of Sidewall-Paneled HVS

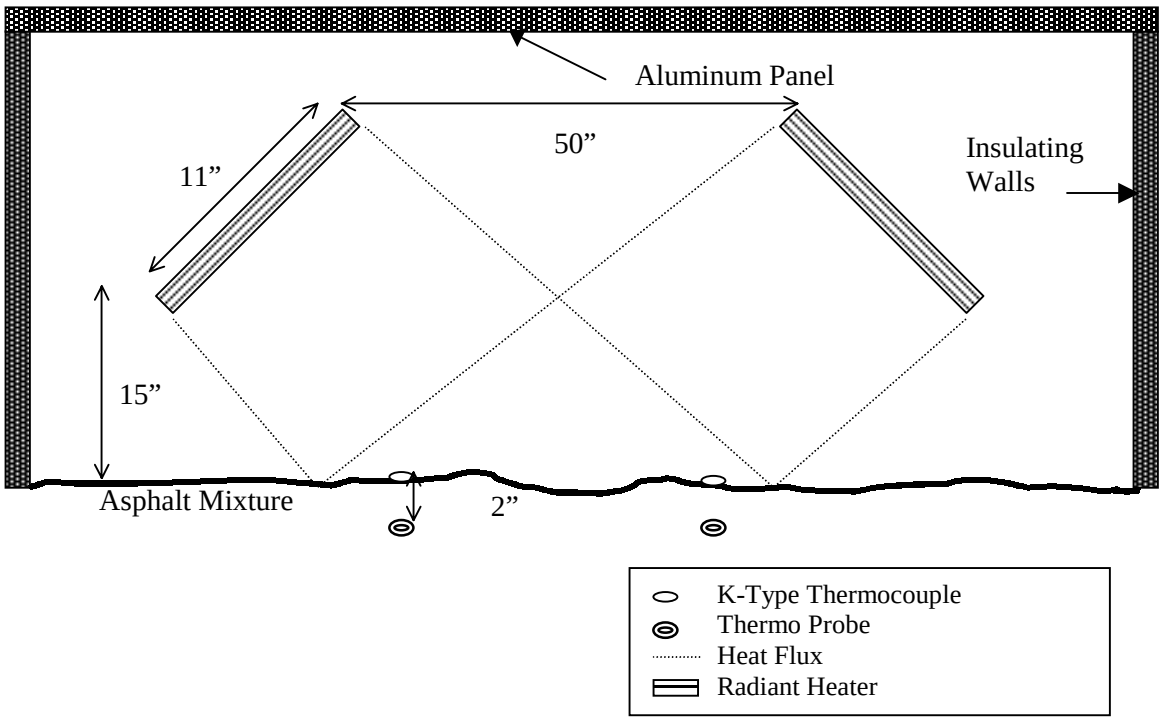

Figure 2.5 The Dimensions and Heat Flux Ranges of Radiant Heaters

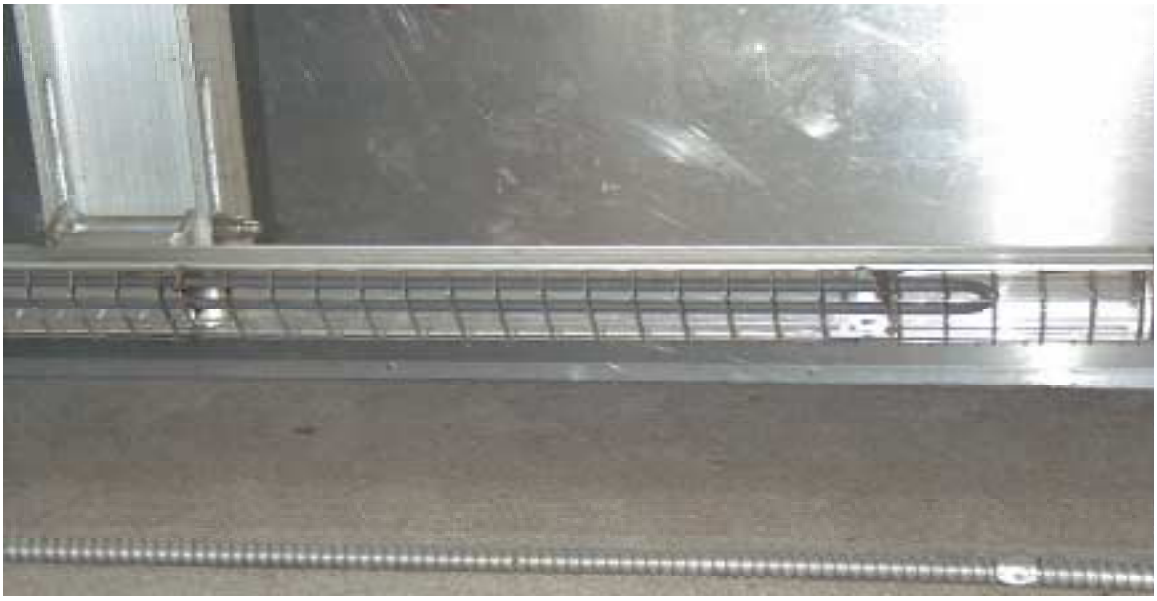

Figure 2.6 Photo of RAYMAX Hairpin Radiant Heater Unit

Each radiant heater was controlled by a pair of thermocouples. Figure 2.7 shows the locations for these six pairs of thermocouples (K-type). At each location, one thermocouple was glued on the surface by means of a high thermal conductivity paste (Omegatherm 201). Another thermocouple was placed at a depth of 2 inches. This was done by drilling a hole to a depth of 2 inches, placing the thermocouple inside a thermal probe, and inserting the thermal probe into the drilled hole. A high thermal conductivity paste (Omegatherm 201) was placed at the bottom of the drilled hole to ensure good thermal contact between the tip of the thermal probe and the asphalt concrete at 2-inch depth. Figure 2.8 shows the location of the thermo probe at a 2-inch depth. Figure 2.9 shows a picture of the pavement inside the insulating area.

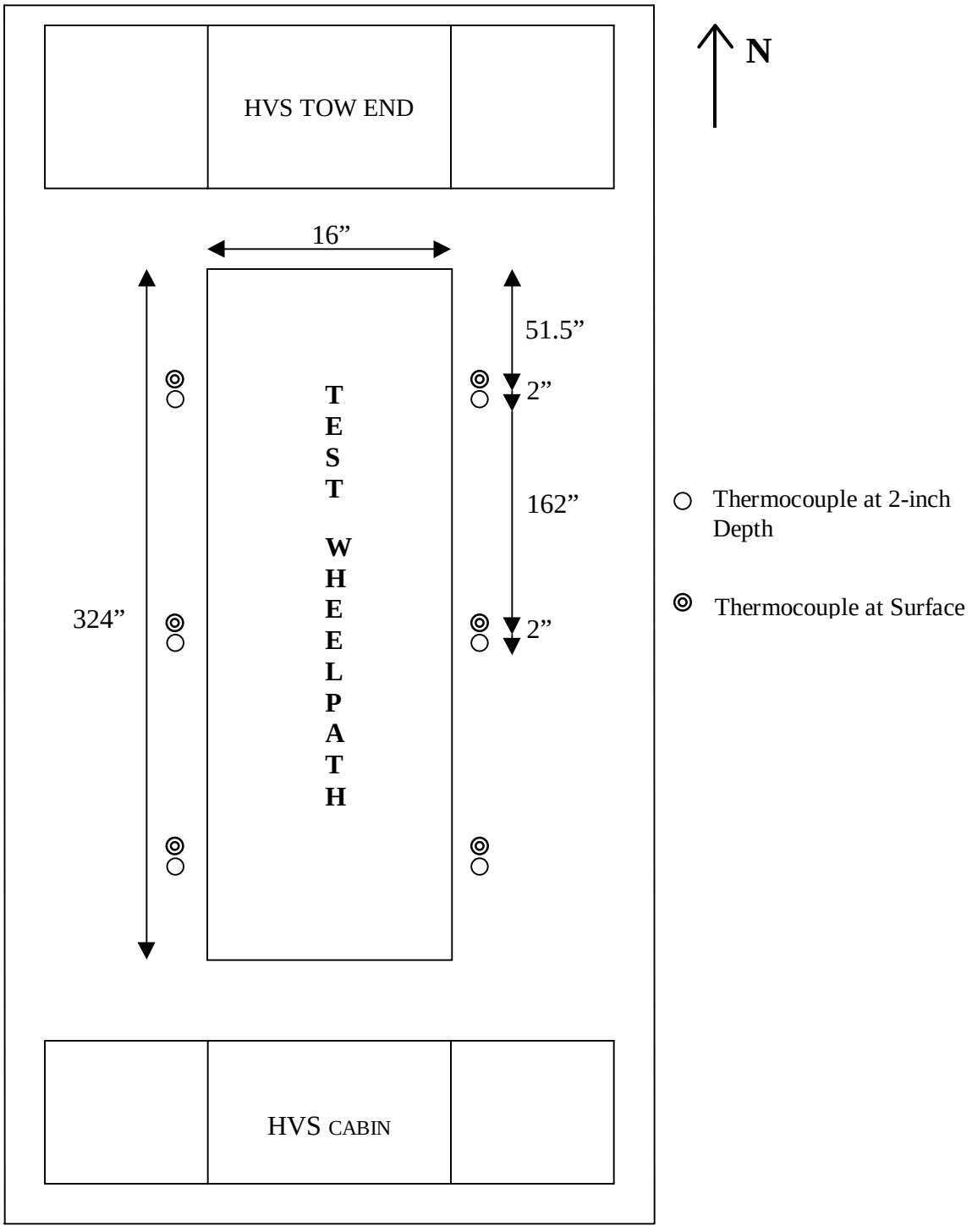

Figure 2.7 Locations of Thermocouples for Temperature Control

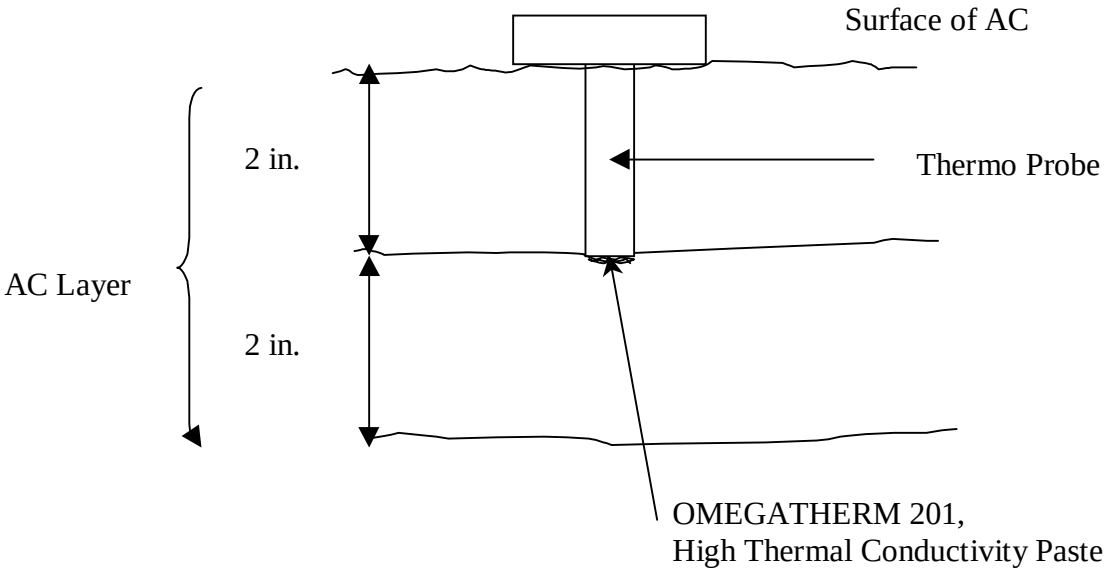

Figure 2.8 The Installation of Thermo Probe at 2-inch Depth from the Surface

Figure 2.9 Photo of Pavement Inside of Insulating Area

2.5 Laser Profiler

A laser profiler was installed on the HVS at the end of Phase I and used in Phase II of the testing program in order to enable more frequent and consistent measurement of the pavement profile during the HVS tests. The laser profiler used was a SLS 5000 ™ manufactured by LMI Selcom. It consisted of two lasers. The specified ambient temperature surrounding the laser should be 0 to 50° C, while the temperature of objects to be measured can be below 0° C and up to 1,600° C. Each of the two lasers was mounted on each side of the test carriage as shown in Figure 2.10. The two lasers were placed at a distance of 30 inches away from one another.

Figure 2.10 Photo of Lasers Mounted onto Two Sides of the Test Carriage

Figure 2.11 shows the paths of the two lasers in making a profile measurement of a tested pavement. In making a profile measurement of a tested pavement, the test carriage holding the two lasers would travel (240 inches) longitudinally from one end to

another, and then move diagonally back to the other end with a lateral incremental shift of 1 inch. In each pass, 58 data points would be collected, with each data point representing the average reading from every 4-inch sweep. This process would be repeated 30 ½ times (with a total of 61 sweeps) until that each laser would sweep over a lateral distance of 30 inches. The last sweep of the right laser would overlap with the first sweep of the left laser. The total lateral distance covered by the two lasers would be 60 inches.

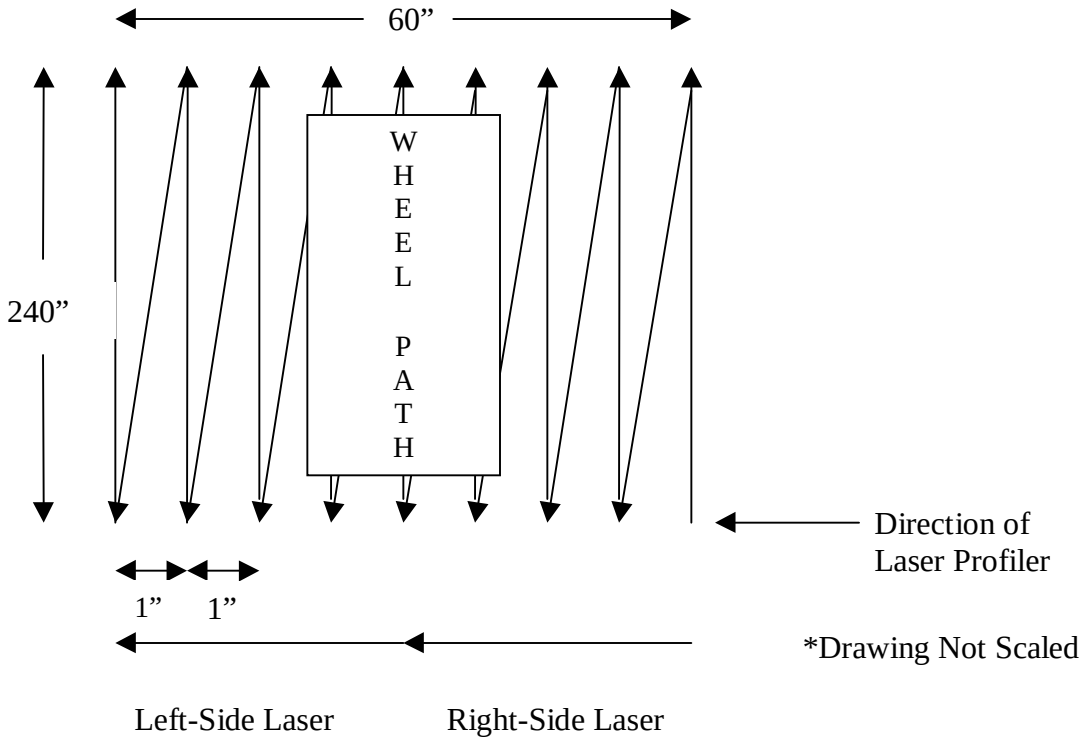

Figure 2.11 The Paths of Laser Profiler in Measuring Pavement Surface Profile

The longitudinal profiles as measured would be used to determine the lateral profiles, which would in turn be used to determine the rut depth. The procedures for determination of rut depths from lateral profiles are described in Chapter 7.

CHAPTER 3
MATERIALS

The two asphalt mixtures, which were placed in the test pavements, were (1) a Superpave mixture using PG67-22 asphalt and (2) a Superpave mixture using PG67-22 asphalt modified with a SBS polymer, which had an equivalent grading of PG76-22. Both mixtures were made with the same aggregate blend having the same gradation, and had the same effective asphalt content. The types and gradation of the aggregate blend used were similar to those of an actual Superpave mixture, which had recently been placed down in Florida. These mixtures can be classified as 12.5 mm fine Superpave mixes, with a nominal maximum aggregate size of 12.5 mm and the gradation plotted above the restricted zone. The properties of the aggregates used are shown in Table 3.1.

Designs for these two mixtures were done by the personnel of the Bituminous Section of the FDOT Materials Office. The optimum binder content was determined according to the Superpave mix design procedure and criteria using a design traffic level of 10 to 30×10^6 ESALs. The mix design data for these two mixtures are also given in Tables A.1 through A.3 in the Appendix A. The binder contents and volumetric properties for these two mixtures are shown in Table 3.2.

Table 3.1 Properties of Aggregate Used in the Asphalt Mixture

Type Material	FDOT Code	Producer	Pit No	Date Sampled
1. S-1-A Stone	41	Rinker Mat. Corp	TM-489 87-089	9/11/00
2. S-1-B Stone	51	Rinker Mat. Corp	TM-489 87-089	9/11/00
3. Screenings	20	Anderson Mining Corp	29-361	9/11/00
4. Local Sand		V.E.Whitehurst & Sons, Inc	Starvation Hill	9/11/00

Percentage by Weight of Total Aggregate Passing Sieves								
Blend		12%	25%	48%	15%	JMF	Control Points	Restricted Zone
Number		1	2	3	4			
Sieve Size	¾" 19.0mm	99	100	100	100	100	100	
	½" 12.5mm	45	100	100	100	93	90-100	
	3/8" 9.5mm	13	99	100	100	89	-90	
	No. 4 4.75mm	5	49	90	100	71		
	No. 8 2.36mm	4	10	72	100	53	28-58	39.1-39.1
	No. 16 1.18mm	4	4	54	100	42		25.6-31.6
	No. 30 600µm	4	3	41	96	35		19.1-23.1
	No. 50 300µm	4	3	28	52	22		
	No. 100 150µm	3	2	14	10	9		
	No. 200 75µm	2.7	1.9	5.9	2.2	4.5	2-10	
G_{sb}		2.327	2.337	2.299	2.546	2.346		

Table 3.2 Volumetric Properties of the Asphalt Mixtures

Mix Type	Asphalt Binder	% Binder	V_a @ N_{des}	VMA	VFA	P_{be}	G_{mm}
Superpave Mix (Compacted at 300° F)	PG67-22	8.2	4.0	14.5	72	4.97	2.276
Modified Superpave Mix (Compacted at 325° F)	PG76-22	7.9	3.8	14.2	73	4.90	2.273

CHAPTER 4
CONSTRUCTION OF THE TEST TRACK

4.1 Construction of Control Strip

Before the Superpave and the SBS-modified Superpave mixtures were placed on the test track, a control strip was constructed using the Superpave mixture. This was done in order to determine the appropriate rolling pattern needed to achieve the desired density and to calibrate the two nuclear density gauges to be used for checking the density of the test pavements. The target density for the compacted mixture was 93±1% of G_{mm} (maximum theoretical density). The density of the compacted mixture was measured by means of the two nuclear density gauges using a reading time of one minute, and cores taken from the compacted pavement. The density measurements from the cores were used to calibrate the two nuclear density gauges.

The two rollers used by the paving contractor were 25,000-lb rollers, which could be used in either a static mode or a vibratory mode. From the results of the test strip, it was determined that the target density could be achieved by three passes of the vibratory roller followed by three passes of the static roller. This rolling pattern was thus used in the compaction of the asphalt mixtures in the test track.

4.2 Placement of Thermocouples

As described in Section 2.3, for each of the 21 test sections, three K-type thermocouples were to be placed on top the limerock base course, three were to be placed between the two lifts of asphalt layers, and two were to be placed on the surface of the pavement. There were a total of 63 thermocouples to be placed on the limerock base.

This task was completed by October 16, 2000, one day before the placement of the asphalt mixture on the test track. The end of each thermocouple wire was placed at its designated location on the limerock base and secured by means of a U-shaped two-ended nail, as shown in Figure 4.1. Each thermocouple wire was run from its designated location to the nearest concrete conduit box. These thermocouple wires were secured to the limerock by means of the U-shaped nails.

Figure 4.1 Photo of K-Type Thermocouple Installed on the Limerock Base

There were a total of 63 thermocouples to be placed on top of the first lift of asphalt mixture. This task was done in the afternoon of October 17, 2000 and in the morning of October 18, 2000, between the time of the placement of the first lift and the placement of the second lift. The thermocouples were secured to the asphalt layer by mean of the U-shaped nails in a similar fashion as that for the limerock base. Figure 4.2 shows a picture of the thermocouples placed on top of the first lift of asphalt mixture.

Figure 4.2 Photo of the Thermocouples Installed on the First Lift of HMA

4.3 Placement of the Asphalt Mixtures

The placement of the asphalt mixtures on the test track was started on October 17, 2000 and completed on October 18, 2000. The first 2-inch lift of unmodified Superpave mixture was placed on Lanes 3 through 7 on the first day. The second lift of unmodified Superpave mixture was placed on Lanes 4 through 7 on the second day. The bottom lift of SBS-modified Superpave mixture was placed on Lanes 1 and 2 in the morning of the second day. The top lift of SBS-modified Superpave Mixture was placed in the afternoon of the second day.

Each lift of asphalt mixture was compacted by three passes of the vibratory followed by three passes of the static roller, as determined from the results of the test strip. Figure 4.3 shows a picture of the 25,000-lb roller used. Additional passes of the static rollers were made to smoothen the surface of the pavement as needed. Figure 4.4 shows the finished test pavement.

Figure 4.3 Photo of Steel-Wheel Roller Used for Compaction

Figure 4.4 Photo of Test Track

4.4 Density of the Compacted Pavement

The two calibrated nuclear density gauges were used to check the density of the compacted mixtures after the completion of these six roller passes. After the nuclear density measurements were taken, core samples were taken from the same locations. The coring and nuclear density testing plan for the test track is shown in Figure 4.5. A total of four cores and thirteen nuclear density measurements were taken per lift per lane after each lift was completed. Coring and nuclear density readings were performed by FDOT personnel. Core and nuclear density data taken at the same locations for lifts 1 and 2 are given in Tables 4.1 and 4.2, respectively. It can be seen that the density of each lift was within the target range. Nuclear density at each location was the average of four readings. The completed nuclear density data are presented in Tables B.1 through B.14 in Appendix B.

4.5 Volumetric Properties and Binder Contents

The Superpave and SBS-modified Superpave mixtures that were placed down on the test track were sampled at the hot-mix plant and tested for their volumetric properties and binder contents by FDOT personnel. One set of tests was run for every lift and every lane. Thus, a total of 14 sets of samples were collected and 14 sets of tests were run. The asphalt mixture samples were compacted in a Superpave gyratory compactor using the same test parameters as used in the mix design procedure, and the volumetric properties of the compacted mixtures were determined. Binder contents were determined by means of the Ignition Oven test. Sieve analyses were performed on the recovered aggregate after the ignition oven test.

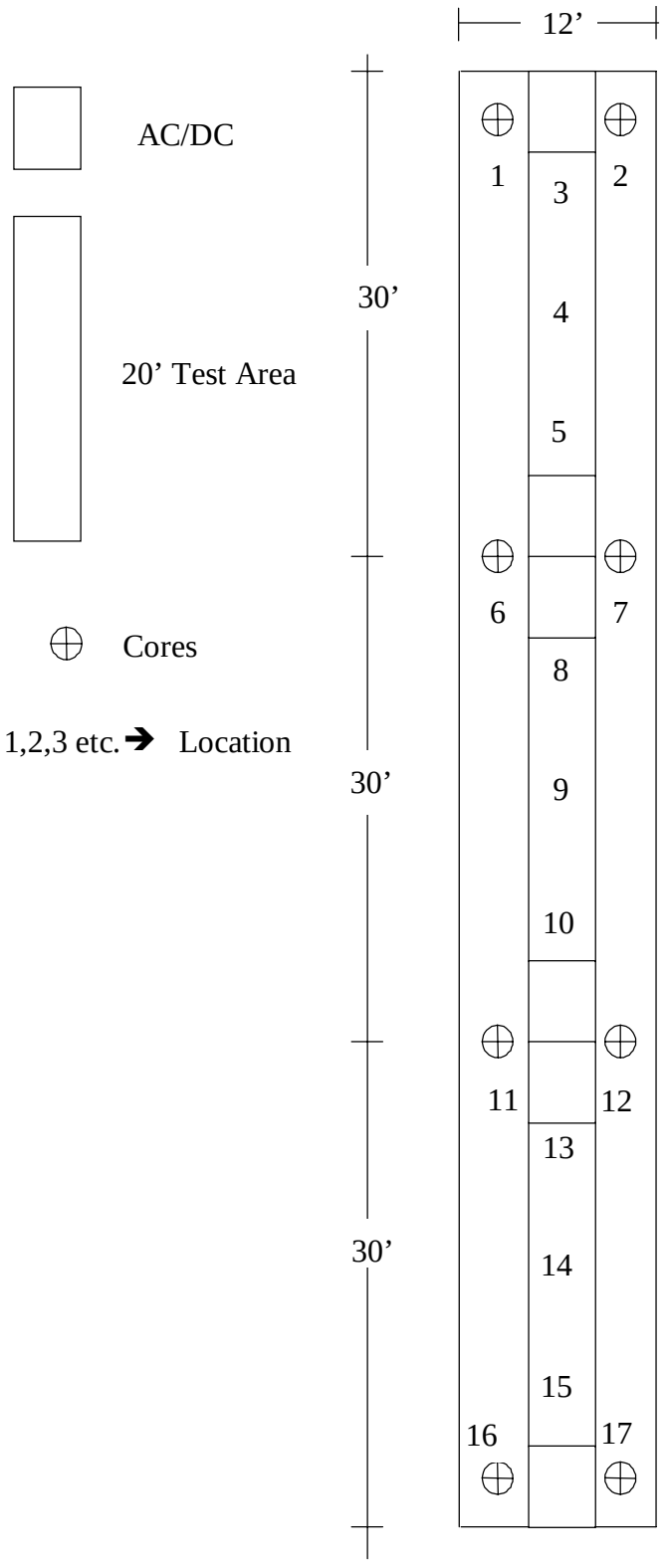

Cores and Nuclear density to be taken at the following lane:

First Lift Coring

1, 7, 11 and 17

Second Lift Coring

2, 6, 12 and 16

Nuclear Density measurements

First Lift

1, 3, 4, 5, 7, 8, 9, 10, 11, 13, 14, 15 and 17

Second Lift

2, 3, 4, 5, 6, 8, 9, 10, 12, 13, 14, 15 and 16

Figure 4.5 Coring and Nuclear Density Testing Plan

Table 4.1 Core and Nuclear Density Data for Lift 1

Core Data							Nuclear Density Data
Lane	Location	Height (in)	Gmb	Gmm	% Gmm	Measured Density (lb/cf)	Density Avg. (lb/cf)
1	1	1.92	2.137	2.268	94.2%	133.4	130.6
1	7	1.96	2.138	2.268	94.3%	133.4	131.9
1	11	2.04	2.149	2.268	94.7%	134.1	133.4
1	17	1.88	2.102	2.268	92.7%	131.2	130.6
1	**Average**	**1.95**	**2.132**		**94.0%**	**133.0**	**131.6**
2	1	1.83	2.128	2.263	94.0%	132.8	130.7
2	7	2.04	2.072	2.263	91.6%	129.3	127.2
2	11	1.75	2.123	2.263	93.8%	132.5	130.7
2	17	1.83	2.077	2.263	91.8%	129.6	127.5
2	**Average**	**1.86**	**2.100**		**92.8%**	**131.0**	**129.0**
3	1	1.35	2.115	2.271	93.1%	132.0	128.1
3	7	1.71	2.080	2.271	91.6%	129.8	127.3
3	11	1.27	2.120	2.271	93.4%	132.3	132.4
3	17	1.38	2.081	2.271	91.7%	129.9	128.5
3	**Average**	**1.43**	**2.099**		**92.4%**	**131.0**	**129.1**
4	1	1.71	2.132	2.280	93.5%	133.1	133.3
4	7	1.46	2.089	2.280	91.6%	130.4	127.7
4	11	1.67	2.141	2.280	93.9%	133.6	130.3
4	17	1.63	2.086	2.280	91.5%	130.2	127.3
4	**Average**	**1.62**	**2.112**		**92.6%**	**131.8**	**129.7**
5	1	1.60	2.134	2.276	93.7%	133.1	131.2
5	7	1.71	2.125	2.276	93.4%	132.6	132.6
5	11	1.60	2.141	2.276	94.1%	133.6	134.3
5	17	1.92	2.108	2.276	92.6%	131.5	130.7
5	**Average**	**1.71**	**2.127**		**93.4%**	**132.7**	**132.2**
6	1	1.81	2.108	2.261	93.2%	131.5	130.2
6	7	1.77	2.138	2.261	94.6%	133.4	134.7
6	11	1.90	2.141	2.261	94.7%	133.6	132.5
6	17	1.54	2.127	2.261	94.1%	132.7	138.8
6	**Average**	**1.75**	**2.129**		**94.1%**	**132.8**	**134.0**
7	1	1.92	2.145	2.264	94.7%	133.9	134.6
7	7	1.75	2.168	2.264	95.8%	135.3	135.5
7	11	1.88	2.176	2.264	96.1%	135.8	137.0
7	17	1.67	2.134	2.264	94.3%	133.2	133.6
7	**Average**	**1.80**	**2.156**		**95.2%**	**134.5**	**135.2**

Table 4.2 Core and Nuclear Density Data for Lift 2

Core Data							Nuclear Density Data
Lane	Location	Height (in)	Gmb	Gmm	% Gmm	Measured Density (lb/cf)	Density Avg. (lb/cf)
1	2	2.13	2.088	2.272	91.9%	130.3	131.1
1	6	1.92	2.129	2.272	93.7%	132.9	131.3
1	12	2.21	2.112	2.272	92.9%	131.8	131.4
1	16	1.75	2.113	2.272	93.0%	131.8	132.4
1	**Average**	**2.00**	**2.110**		**92.9%**	**131.7**	**131.5**
2	2	1.75	2.081	2.272	91.6%	129.9	130.2
2	6	1.42	2.120	2.272	93.3%	132.3	131.1
2	12	1.25	2.102	2.272	92.5%	131.2	129.8
2	16	1.83	2.122	2.272	93.4%	132.4	131.2
2	**Average**	**1.56**	**2.106**		**92.7%**	**131.4**	**130.6**
3	2	2.13	2.096	2.278	92.0%	130.8	128.6
3	6	1.92	2.124	2.278	93.3%	132.6	131.9
3	12	2.21	2.074	2.278	91.0%	129.4	132.0
3	16	1.75	2.120	2.278	93.0%	132.3	132.0
3	**Average**	**2.00**	**2.104**		**92.3%**	**131.3**	**131.1**
4	2	2.04	2.125	2.276	93.3%	132.6	131.0
4	6	1.88	2.139	2.276	94.0%	133.5	130.4
4	12	2.00	2.132	2.276	93.7%	133.0	130.2
4	16	1.58	2.133	2.276	93.7%	133.1	133.1
4	**Average**	**1.87**	**2.132**		**93.7%**	**133.0**	**131.2**
5	2	2.04	2.099	2.278	92.2%	131.0	129.1
5	6	1.88	2.117	2.278	92.9%	132.1	134.3
5	12	1.88	2.102	2.278	92.3%	131.2	134.0
5	16	1.92	2.116	2.278	92.9%	132.0	130.7
5	**Average**	**1.93**	**2.108**		**92.6%**	**131.6**	**132.0**
6	2	2.13	2.103	2.267	92.8%	131.2	128.8
6	6	2.38	2.133	2.267	94.1%	133.1	131.1
6	12	2.25	2.131	2.267	94.0%	133.0	130.4
6	16	2.00	2.123	2.267	93.6%	132.4	130.2
6	**Average**	**2.19**	**2.122**		**93.6%**	**132.4**	**130.1**
7	2	1.79	2.089	2.275	91.8%	130.4	130.1
7	6	1.50	2.129	2.275	93.6%	132.8	132.3
7	12	1.96	2.098	2.275	92.2%	130.9	128.4
7	16	1.63	2.121	2.275	93.2%	132.3	130.6
7	**Average**	**1.72**	**2.109**		**92.7%**	**131.6**	**130.4**

Tables 4.3 and 4.4 show the comparison of the aggregate gradations, volumetric properties and binder contents of these sampled mixes with those of the job mix design for lifts 1 and 2, respectively. It can be seen that the recovered aggregates from the ignition oven tests were finer than the job mix formula. This difference might be caused by the loss of aggregate materials due to the ignition process.

The binder contents for the mixtures in Lanes 1, 3, 4, and 5 of Lift 1 were very close to the design binder content. However, the mixtures in Lanes 2, 6 and 7 of Lift 1 had higher binder contents than that of the design. Binder contents for all lanes of Lift 2 were close to the design value.

The air voids of all the compacted samples were lower than the design value of 4%. Particularly low air voids were observed for samples from Lanes 2, 6 and 7 of Lift 1. The low air voids for these mixtures can be explained by the high binder contents of these mixtures.

4.6 Additional Asphalt Mixture Samples

Additional samples of asphalt mixtures were collected at the hot-mix plant by the University of Florida investigators for additional laboratory testing. Four sets of samples were obtained. One set of samples was obtained for each lift of the unmodified Superpave mixture and each lift of the SBS-modified mixture.

A laboratory testing program was performed to characterize these mixtures to evaluate potential performance of these mixes based on the laboratory results, and to evaluate the correlation between the laboratory test results with the performance of the test sections.

Table 4.3 Comparisons of Volumetric Properties of Asphalt Mixtures for Lift 1

Sieve Size	Design Job Mix Formula	PG 76-22		Sieve Size	Design Job Mix Formula	PG 67-22				
		Truck 1	Truck 3			Truck 7	Truck 6	Truck 4	Truck 3	Truck 1
		Lane 1	Lane 2			Lane 3	Lane 4	Lane 5	Lane 6	Lane 7
1"		100.0	100.0	1"		100.0	100.0	100.0	100.0	100.0
3/4"	**100**	100.0	100.0	3/4"	**100**	100.0	100.0	100.0	100.0	100.0
1/2"	**93**	97.8	97.4	1/2"	**93**	97.6	98.8	96.9	97.8	97.5
3/8"	**89**	95.8	95.7	3/8"	**89**	95.1	96.7	93.4	96.0	94.9
#4	**71**	77.8	75.4	#4	**71**	74.9	76.8	74.3	76.0	74.1
#8	**53**	54.6	51.9	#8	**53**	54.3	54.0	53.9	55.9	53.8
#16	**42**	44.6	42.4	#16	**42**	44.6	44.1	45.2	46.0	43.7
#30	**35**	39.2	36.4	#30	**35**	38.1	37.8	39.4	39.3	36.7
#50	**22**	24.5	23.6	#50	**22**	24.2	23.4	24.3	24.5	23.9
#100	**9**	8.8	9.4	#100	**9**	9.4	8.3	8.5	9.1	10.2
#200	**4.5**	4.0	4.3	#200	**4.5**	4.2	3.6	3.7	4.2	5.0
AC content	**7.9**	8.0	8.3	AC content	**8.2**	8.0	8.2	8.0	8.4	8.7
G_{mm}	**2.273**	2.268	2.263	G_{mm}	**2.276**	2.271	2.280	2.276	2.261	2.264
G_{mb} @ N_{des}	**2.186**	2.196	2.215	G_{mb} @ N_{des}	**2.185**	2.200	2.196	2.197	2.204	2.220
Air Voids	**3.8**	3.2	2.1	Air Voids	**4**	3.1	3.7	3.5	2.5	1.9
VMA	**14.2**	13.9	13.4	VMA	**14.5**	13.7	14.0	13.9	14.0	13.6
VFA	**73**	77.2	84.2	VFA	**72.0**	77.2	73.6	74.9	81.8	85.7
P_{be}	**4.9**	5.1	5.3	P_{be}	**4.97**	5.0	4.9	4.9	5.4	5.4
Dust Ratio	**0.9**	0.8	0.8	Dust Ratio	**0.9**	0.8	0.7	0.7	0.8	0.9
% G_{mm} @ N_{ini}	**89.1**	90.6%	90.8%	% G_{mm} @ N_{ini}	**88.8**	90.2%	89.8%	90.5%	91.0%	90.8%

Table 4.4 Comparisons of Volumetric Properties of Asphalt Mixtures for Lift 2

Sieve Size	Design Job Mix Formula	PG 76-22			Sieve Size	Design Job Mix Formula	PG 67-22			
		Truck 3	Truck 2	Truck 1			Truck 1	Truck 3	Truck 4	Truck 6
		Lane 1	Lane 2	Lane 3			Lane 4	Lane 5	Lane 6	Lane 7
1"		100.0	100.0	100.0	1"		100.0	100.0	100.0	100.0
3/4"	**100**	100.0	100.0	100.0	3/4"	**100**	100.0	100.0	100.0	100.0
1/2"	**93**	97.5	97.1	98.9	1/2"	**93**	98.0	97.9	97.4	97.2
3/8"	**89**	95.4	94.6	96.9	3/8"	**89**	96.3	96.1	95.7	95.7
#4	**71**	76.1	76.5	76.0	#4	**71**	76.7	76.0	76.3	76.6
#8	**53**	54.4	55.2	54.0	#8	**53**	54.6	53.9	54.2	54.7
#16	**42**	45.1	45.3	44.4	#16	**42**	44.4	44.2	44.1	44.4
#30	**35**	38.5	39.2	38.1	#30	**35**	37.5	37.9	37.8	37.7
#50	**22**	23.9	24.0	24.3	#50	**22**	24.0	23.6	23.7	24.3
#100	**9**	8.8	8.8	9.3	#100	**9**	9.7	8.8	8.9	10.2
#200	**4.5**	3.9	3.9	4.1	#200	**4.5**	4.6	3.9	4.2	4.9
AC content	**7.9**	8.0	7.9	7.8	AC content	**8.2**	7.9	8.0	7.9	7.9
G_{mm}	**2.273**	2.272	2.272	2.278	G_{mm}	**2.276**	2.276	2.278	2.267	2.275
G_{mb} @ N_{des}	**2.186**	2.201	2.202	2.200	G_{mb} @ N_{des}	**2.185**	2.199	2.196	2.202	2.214
Air Voids	**3.8**	3.1	3.1	3.4	Air Voids	**4**	3.4	3.6	2.9	2.7
VMA	**14.2**	13.7	13.6	13.5	VMA	**14.5**	13.7	13.9	13.6	13.1
VFA	**73**	77.0	77.3	74.7	VFA	**72**	75.1	73.9	78.9	79.3
P_{be}	**4.9**	5.0	4.9	4.8	P_{be}	**4.97**	4.8	4.8	5.0	4.8
Dust Ratio	**0.9**	0.8	0.8	0.9	Dust Ratio	**0.9**	1.0	0.8	0.8	1.0
% G_{mm} @ N_{ini}	**89.1**	90.4%	90.5%	90.2%	% G_{mm} @ N_{ini}	**88.8**	89.7%	89.7%	90.4%	90.5%

The laboratory testing program for characterization of these mixtures and the results from this testing program are presented in Chapter 8.

CHAPTER 5
TRIAL TESTS FOR DETERMINATION OF OPTIMUM HVS TEST CONFIGURATION

5.1 Testing Configurations

Five trial tests with the HVS were run on test Lane 7 in order to determine the optimum HVS test configuration to be used in the main testing program. All five trial runs with the HVS used a super single tire with a load of 9,000 lbs, tire pressure of 115 psi and a wheel traveling speed of 8 mph. These five trial runs used different combinations of wheel traveling direction (uni-directional or bi-directional), total wheel wander and wander increments as follows:

(1) Bi-directional travel with no wander

(2) Uni-directional travel with no wander

(3) Uni-directional travel with 4-inch wander in 2-inch increments

(4) Bi-directional travel with 4-inch wander in 2-inch increments

(5) Uni-directional travel with 4-inch wander in 1-inch increments

Trial Run 1 was run on Test Section 7C. Trial Runs 2 and 3 were run on the western and the eastern sides, respectively, of Test Section 7B, and were designated as 7B-W and 7B-E. The edges of wheel tracks from these two tests were separated by a distance of about 15 inches. Trial Runs 4 and 5 were run on the eastern and western sides, respectively, of Test Section 7C, and were designated as 7A-E and 7A-W. The edges of wheel tracks from these tests were separated by a distance of about 11 inches.

5.2 Temperature Measurement

Since the temperature control system was not ready yet at the time of these trial runs, the temperature of the test pavements was not controlled. The temperature distribution in each test pavement was monitored by eight thermocouples. For each test section, three thermocouples (#1, 2 & 3) were placed on top of the base course, three (#4, 5 & 6) were placed between the two lifts of asphalt mixture, and two (#7 & 8) were placed on the surface. During each of the trial runs, the temperature readings for the test section were taken every 15 minutes and recorded by a PC data acquisition system. Table 5.1 displays (1) the average of the daily minimum temperatures, (2) the average of the daily maximum temperatures, (3) the overall minimum temperature, and (4) the overall maximum temperature as recorded by the three thermocouples between the two lifts of asphalt mixtures for each test. The averages of the values from the three thermocouples are also given in the table.

5.3 Rut Measurement

For each test pavement, five transverse profiles were measured on a daily basis by means of a straight edge placed across the pavement at five fixed locations evenly spaced across the test section. A ruler was used to measure the relative elevation (or profile) of the pavement surface with respect to the straight edge. Figure 5.1 shows how this measurement was done.

Rut depths were determined by two different methods. In the first method, the initial surface profile of the pavement before the test was subtracted from the measured surface profile at specified times to give the "differential surface deformations." This method is termed the "Differential Surface Deformation Method" in this report.

Table 5.1 Temperatures of Test Pavement in Trial Sections as Measured by Thermocouples Placed between the Two 2-inch Lifts of Asphalt Mixture

Section 7C	Bi-Directional Loading with No Wander			
	Thermo.4	Thermo.5	Thermo.6	**Average**
Avg. Daily Min. Temp (°C)	20.6	20.4	20.3	**20.4**
Avg. Daily Max. Temp (°C)	31.3	31.6	33.3	**32.1**
Overall Min. Temp (°C)	18.9	20.1	18.0	**18.0**
Overall Max. Temp (°C)	34.2	33.7	37.5	**37.5**
Section 7BW	Uni-Directional Loading with No Wander			
	Thermo.4	Thermo.5	Thermo.6	**Average**
Avg. Daily Min. Temp (°C)	19.2	18.9	19.0	**19.0**
Avg. Daily Max. Temp (°C)	33.1	28.4	27.7	**29.7**
Overall Min. Temp (°C)	13.3	12.7	13.1	**12.7**
Overall Max. Temp (°C)	36.7	31.9	32.4	**36.7**
Section 7BE	Uni-Directional Loading with 4-inch Wander in 2-inch Increments			
	Thermo.4	Thermo.5	Thermo.6	**Average**
Avg. Daily Min. Temp (°C)	14.5	15.3	14.1	**14.6**
Avg. Daily Max. Temp (°C)	16.3	23.0	22.9	**20.7**
Overall Min. Temp (°C)	7.4	8.8	7.0	**7.0**
Overall Max. Temp (°C)	32.2	28.6	28.9	**32.2**
Section 7AE	Bi-Directional Loading with 4-inch Wander in 2-inch Increments			
	Thermo.4	Thermo.5	Thermo.6	**Average**
Avg. Daily Min. Temp (°C)	9.0	9.4	9.2	**9.2**
Avg. Daily Max. Temp (°C)	21.6	19.6	17.9	**19.7**
Overall Min. Temp (°C)	2.9	3.6	2.9	**2.9**
Overall Max. Temp (°C)	30.2	36.1	26.4	**36.1**
Section 7AW	Uni-Directional Loading with 4-inch Wander in 1-inch Increments			
	Thermo.4	Thermo.5	Thermo.6	**Average**
Avg. Daily Min. Temp (°C)	13.1	12.7	13.1	**13.0**
Avg. Daily Max. Temp (°C)	25.0	23.1	22.4	**23.5**
Overall Min. Temp (°C)	3.2	3.3	4.3	**3.2**
Overall Max. Temp (°C)	34.6	29.8	34.1	**34.6**

Figure 5.1 Photo of Straight Edge Used for Measuring Rut Depth

In the second method, the measured profile was plotted, and a straight line was drawn on the plot such that it touched the highest point on each side of the wheel track. The maximum distance between the straight line and the measured profile was determined as the rut depth. This procedure is similar to how rut depths are usually determined in the field. Figure 5.2 illustrates how this was done. This method is termed the "Surface Profile Method" in this report.

5.4 Comparison Between Bi-Directional and Uni-Directional Loading with No Wander

Trial Test No. 1 (bi-directional loading with no wander, Test Section 7C) was run for 12 days with a total of 315,299 wheel passes. Figure 5.3 shows a picture of the rutted pavement at the end of the test. With this mode of loading, the wheel appeared to travel along the exact tire print as it moved back and forth without lifting itself off the ground. As a result, imprints of the tire treads could be clearly seen on the wheel track. This is not representative of pavement rutting in the field.

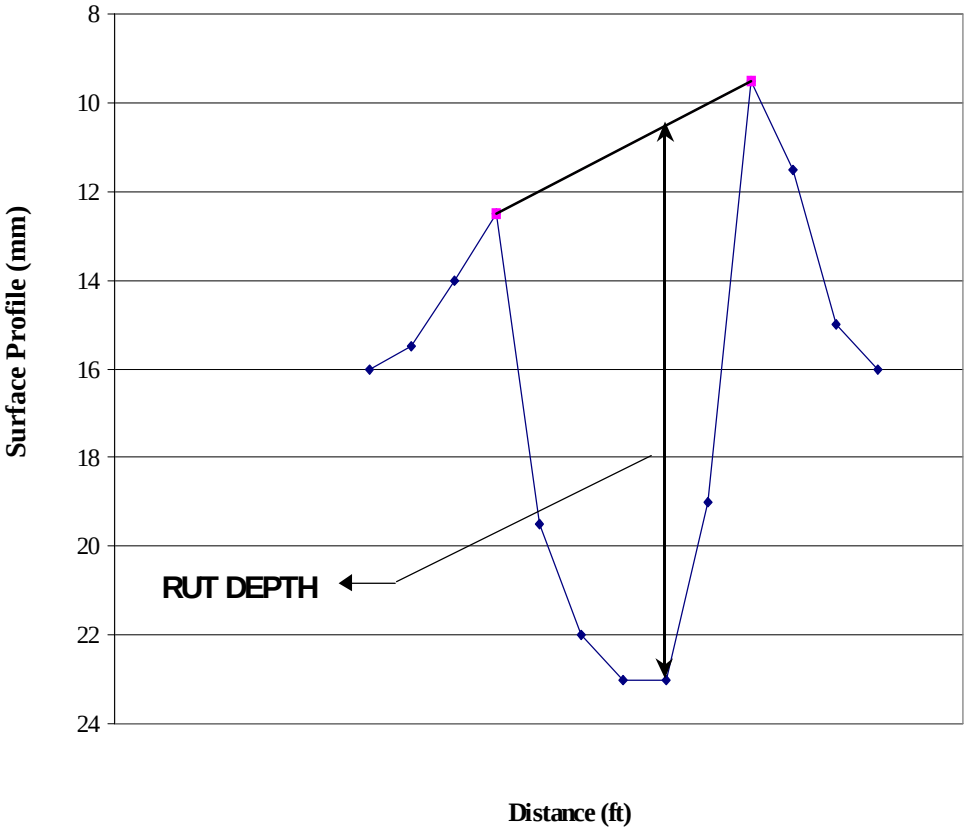

Figure 5.2 Determination of Rut Depth in the Surface Profile Method

Figure 5.3 Photo of Section 7C

Trial Test No. 2 (uni-directional loading with no wander, Test Section 7B-W) was run for 8 days with a total of 101,414 passes. Figure 5.4 shows a picture of the rutted pavement at the end of the test. It can be seen that the imprints of the tire treads were smoothened out considerably in this loading mode. However, continuous ridges were observed along the wheel track. Although the observed rutted pavement surface represents an improvement over that observed in the bi-directional loading case, it is still not representative of pavement rutting in the field.

Figure 5.4 Photo of Section 7B-W

It was also observed that the loading wheel experienced more wear when run in the uni-directional mode. Accumulation of rubber, which was rubbed off from the tire, was observed on the surface of the wheel track, and mostly at the starting location. Figure 5.5 shows the comparison of rut depths as measured by the differential surface deformation method as a function of number of wheel passes between these two modes of loading. Figure 5.6 shows similar comparison of rut depths as measured by the surface

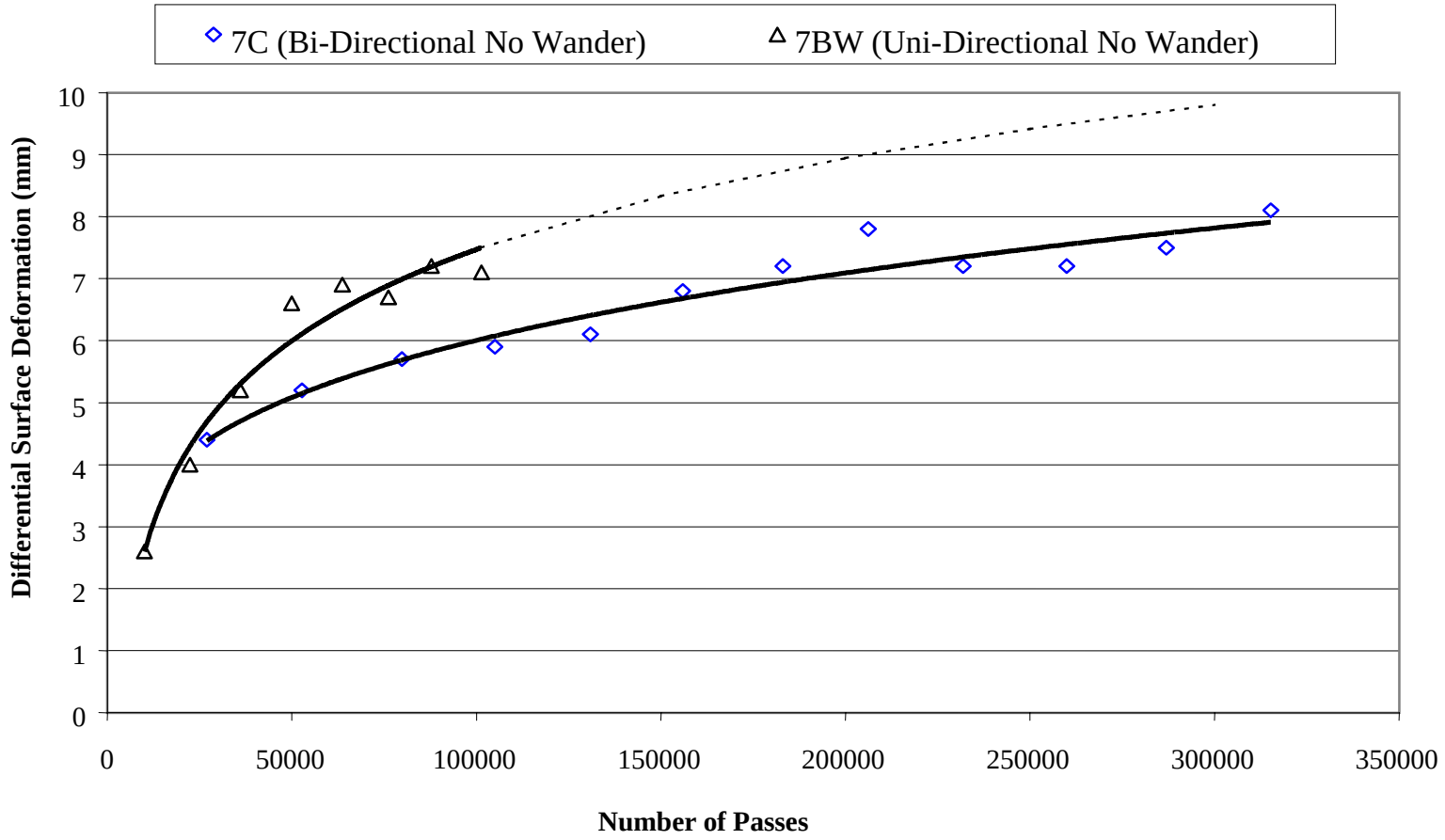

Figure 5.5 Comparison of Differential Surface Deformation versus Number of Passes between Bi-Directional and Uni-Directional Loading with No Wander

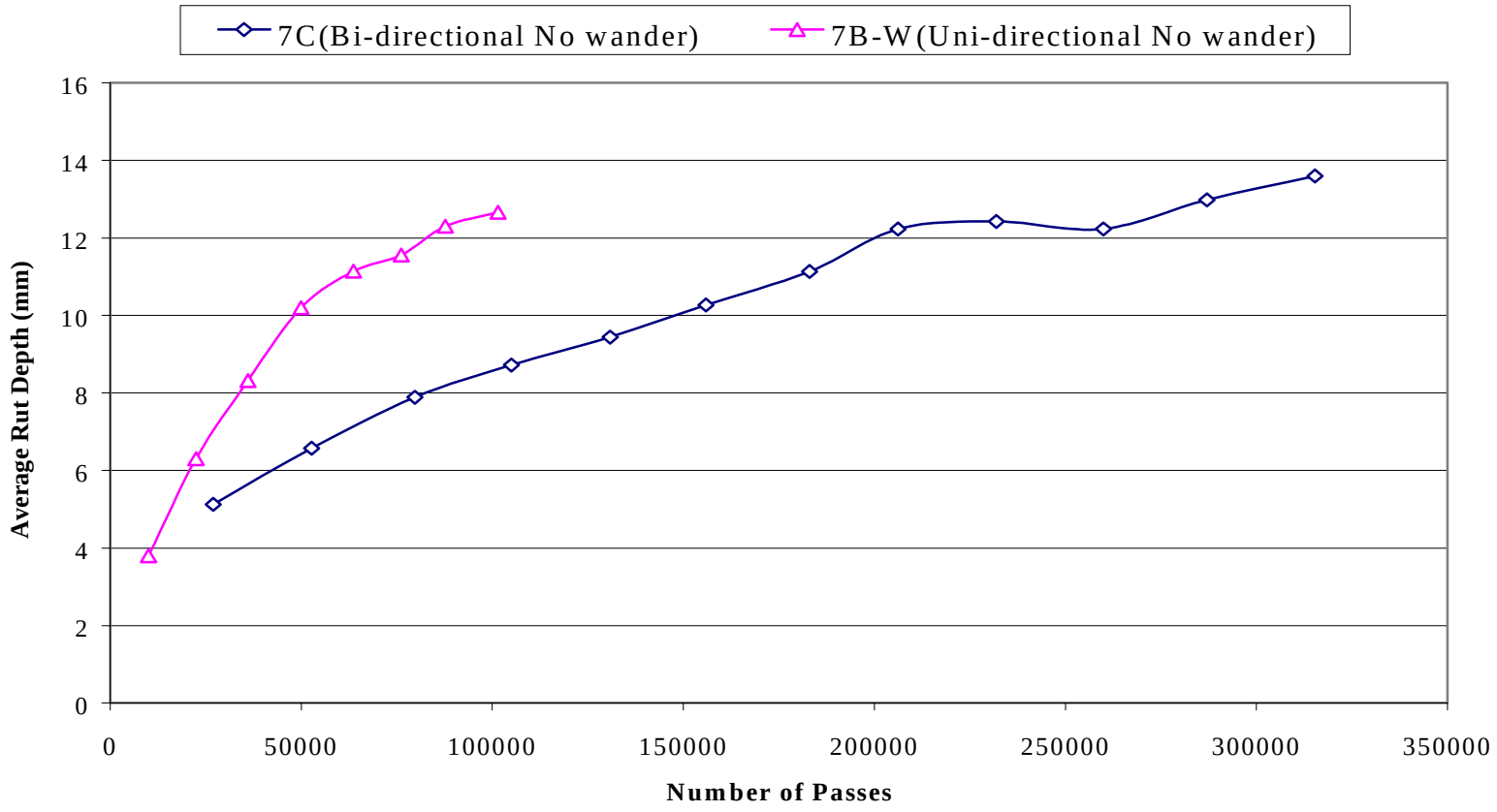

Figure 5.6 Comparison of Average Rut Depth as Measured by the Surface Profile Method versus Number of Passes Between Bi-Directional and Uni-Directional Loading with No Wander

profile method. It can be seen from both figures that for the same number of wheel passes, the uni-directional loading produced substantially higher rut depths than those by the bi-directional loading.

Figures 5.7 and 5.8 show the comparisons of rut depths versus testing time between these two modes of loading, using the differential surface deformation method and surface profile method, respectively. Although the bi-directional mode can apply almost twice the number of wheel passes per day as compared with the unidirectional mode, the uni-directional mode of loading still produced slightly higher rut depths for the same testing duration.

A comparison between the recorded pavement temperatures for these two tests shows that both the average daily maximum temperature and the overall maximum temperature during the bi-directional test were higher than those during the uni-directional test. Although the pavement temperature was relatively lower during the uni-directional test, rutting was still observed to be higher. Thus, it can be concluded that the uni-directional loading is a more efficient mode for evaluation of rutting performance using the HVS.

5.5 Comparison Between Bi-Directional and Uni-Directional Loading with 4-inch Wander

Trial Test No. 3 (uni-directional loading with 4-inch wander in 2-inch increments, Test Section 7B-E) was run for 25 days with a total of 310,620 wheel passes. Figure 5.9 shows a picture of the rutted pavement at the end of the test. Trial Test No. 4 (bi-directional loading with 4-inch wander in 2-inch increments, Test Section 7A-E) was run for 33 days with a total of 843,151 passes. Figure 5.10 shows a picture of the rutted

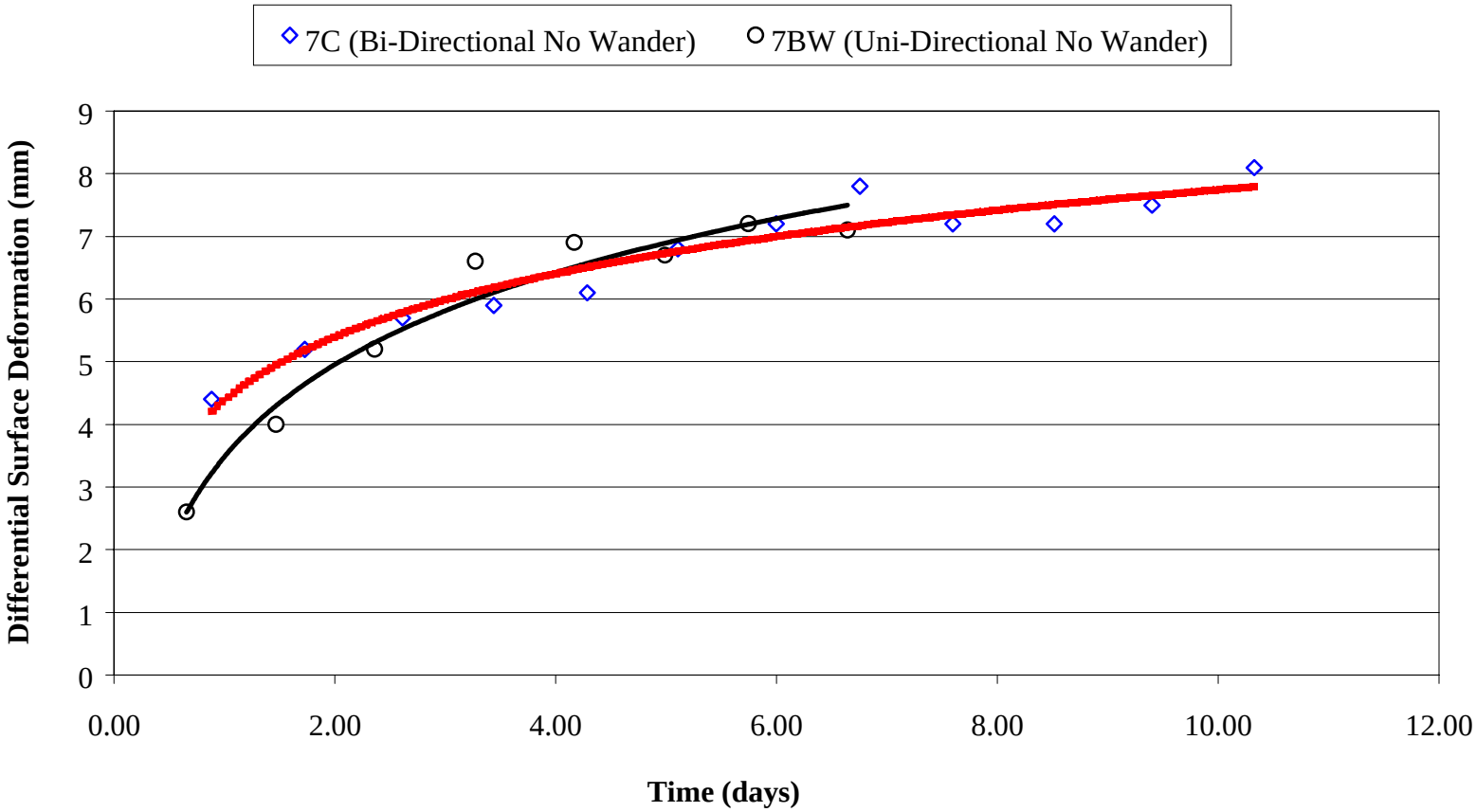

Figure 5.7 Comparison of Differential Surface Deformation versus Time between Bi-Directional and Uni-Directional Loading

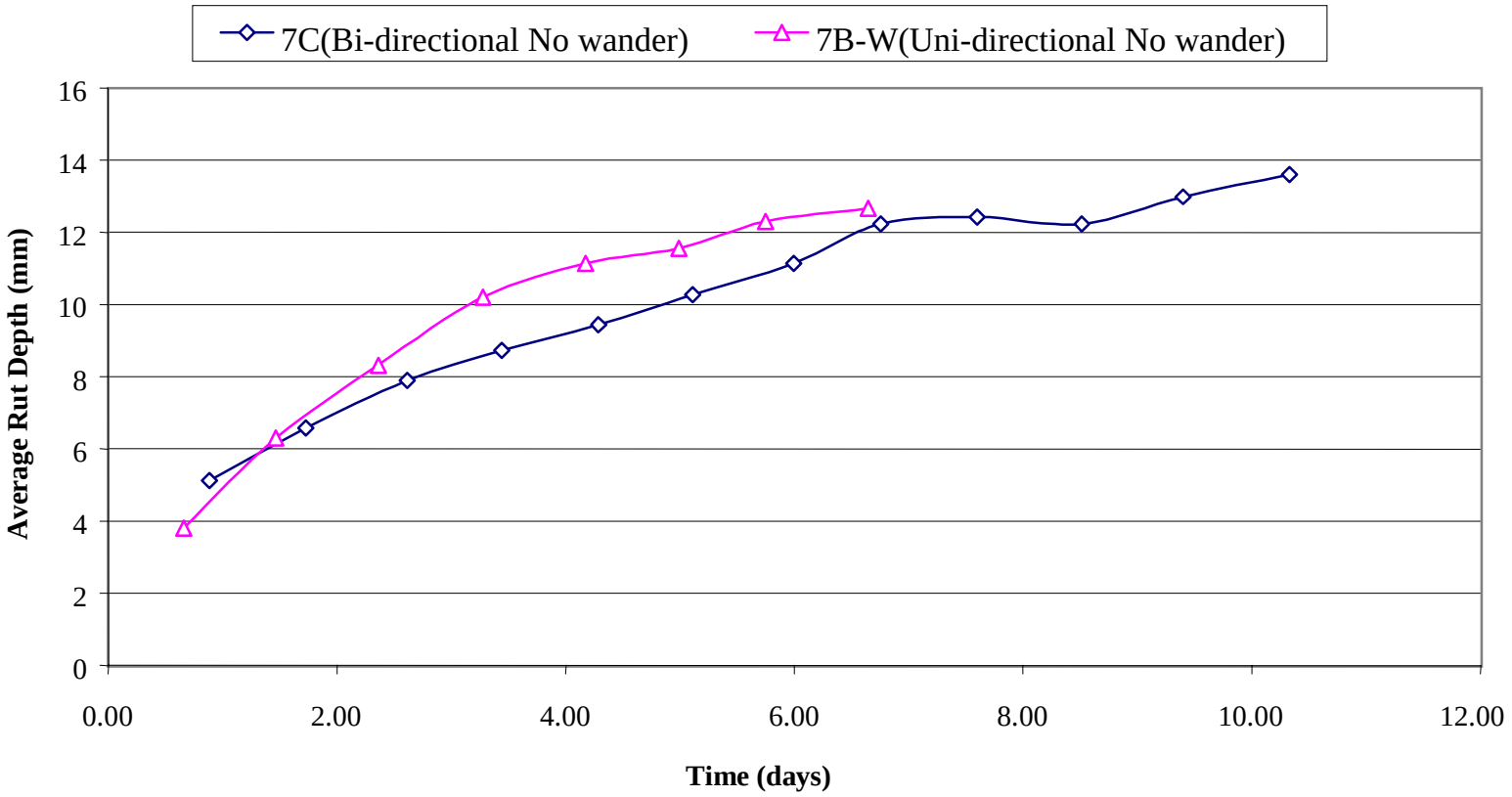

Figure 5.8 Comparison of Average Rut Depth as Measured by the Surface Profile Method versus Time Between Bi-Directional and Uni-Directional Loading with No Wander

Figure 5.9 Photo of Section 7B-E

Figure 5.10 Photo of Section 7A-E

pavement at the end of the test. In both cases, the rutted wheel tracks were observed to be much smoother than those in Trial Tests 1 and 2 (with no wander). However, continuous ridges were still observed along the wheel track. Accumulation of rubber on the surface of the wheel track was also observed in Trial Test 3 (with uni-directional loading).

Figure 5.11 shows the comparison of rut depths as measured by the differential surface deformation method as a function of number of wheel passes between these two modes of loading. Figure 5.12 shows similar comparison of rut depths as measured by the surface profile method. It can be seen from both figures that for the same number of wheel passes, the uni-directional loading produced substantially higher rut depths than those by the bi-directional loading.

Figures 5.13 and 5.14 show the comparisons of rut depths versus testing time between these two modes of loading, using the differential surface deformation method and surface profile method, respectively. It can be seen that for the same testing time, the uni-directional loading produced higher rut depths than those by the bi-directional loading.

5.6 Comparison Between Uni-Directional Loading with 4-inch Wander in 2-inch Increments and Uni-Directional Loading with 4-inch Wander in 1-inch Increments

Trial Test No. 5 (uni-directional loading with 4-inch wander in 1-inch increments, Test Section 7A-W) was run for 39 days with a total of 443,489 wheel passes. Figure 5.15 shows a picture of the rutted pavement at the end of the test. The rutted wheel track

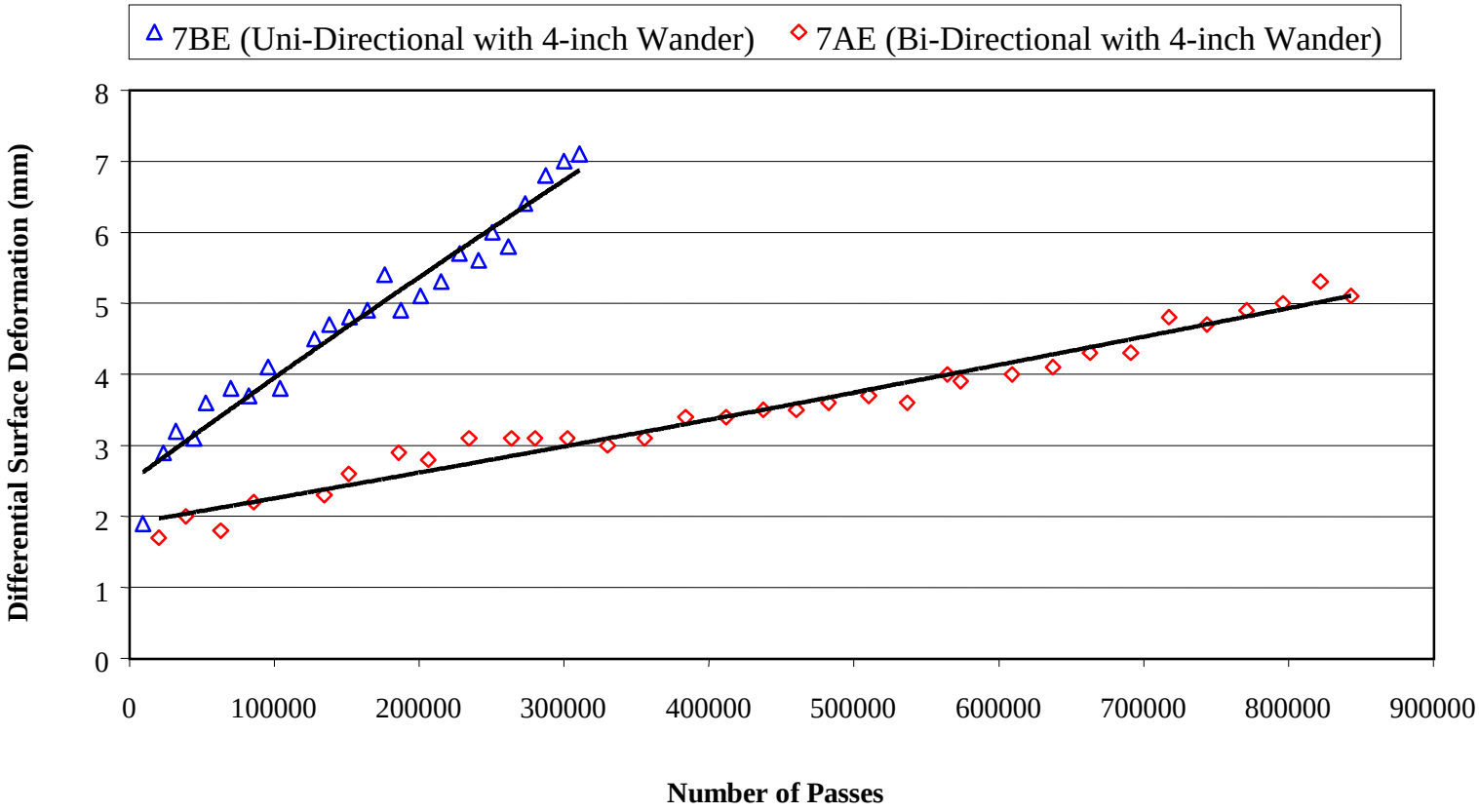

Figure 5.11 Comparison of Differential Surface Deformation versus Number of Passes Between Uni-Directional and Bi-Directional Loading with 4-inch Wander

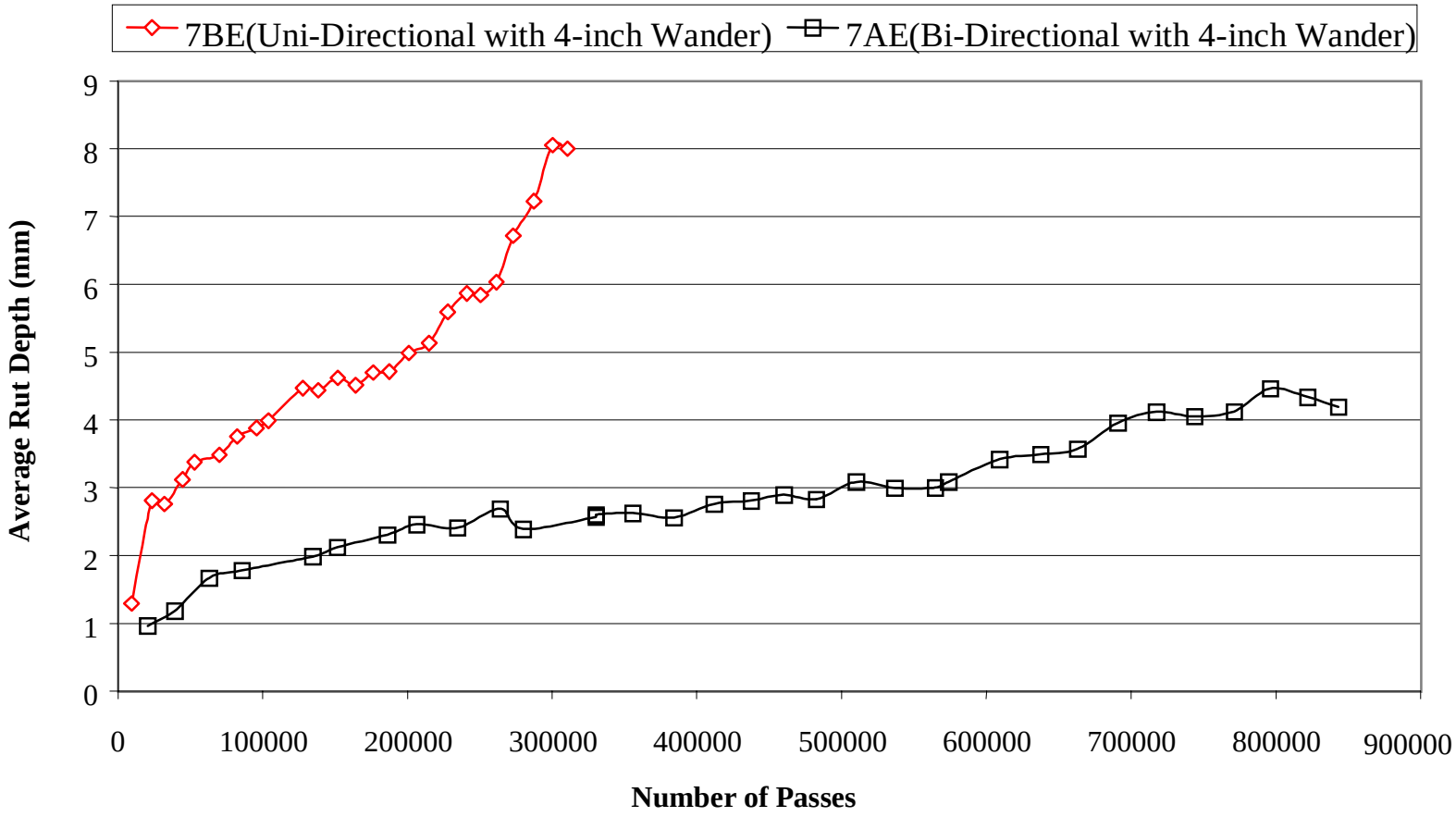

Figure 5.12 Comparison of Average Rut Depth by Profile Method versus Number of Passes Between Uni-Directional and Bi-Directional Loading with 4-inch Wander

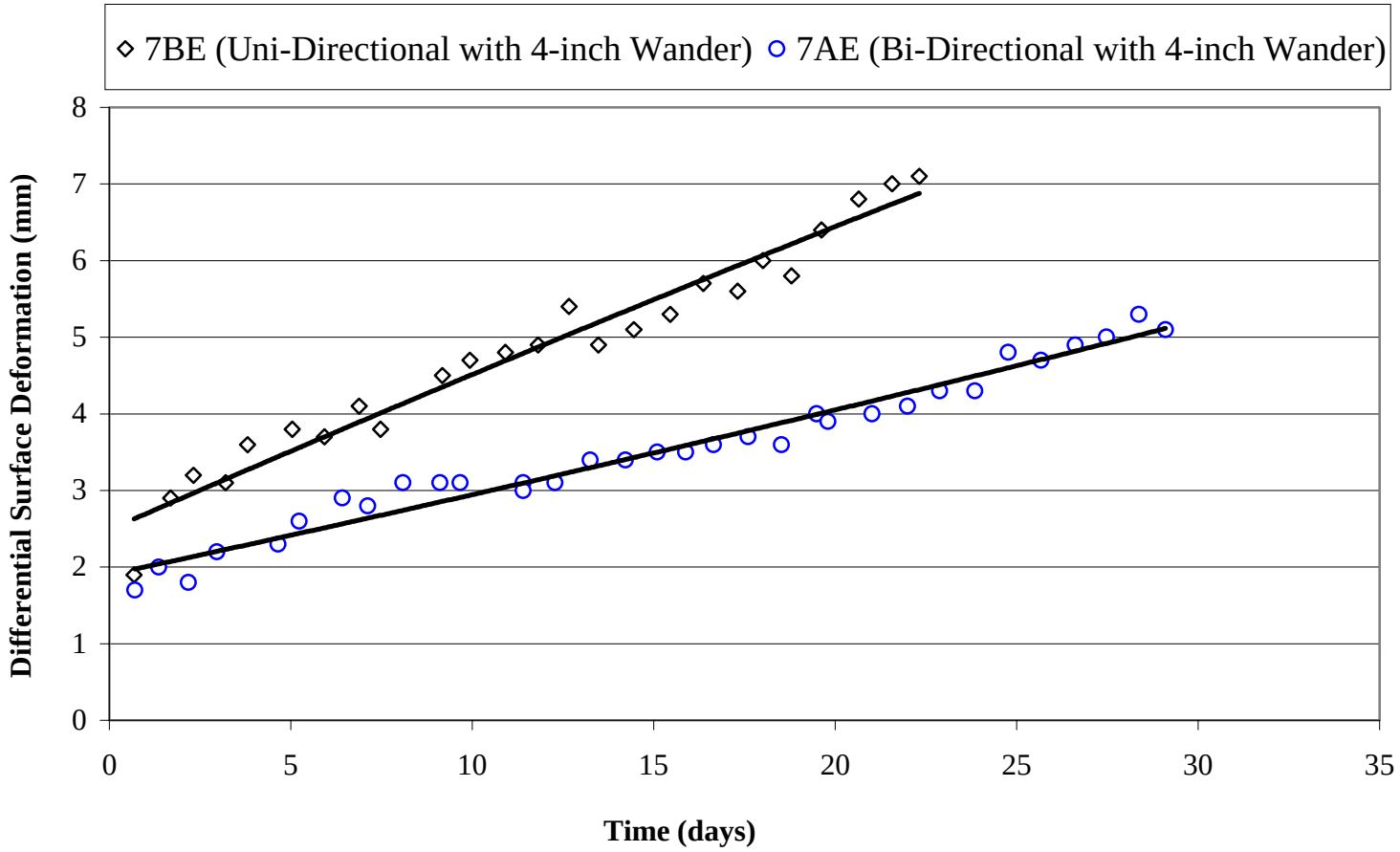

Figure 5.13 Comparison of Differential Surface Deformation versus Time Between Uni-Directional and Bi-Directional Loading with 4-inch Wander

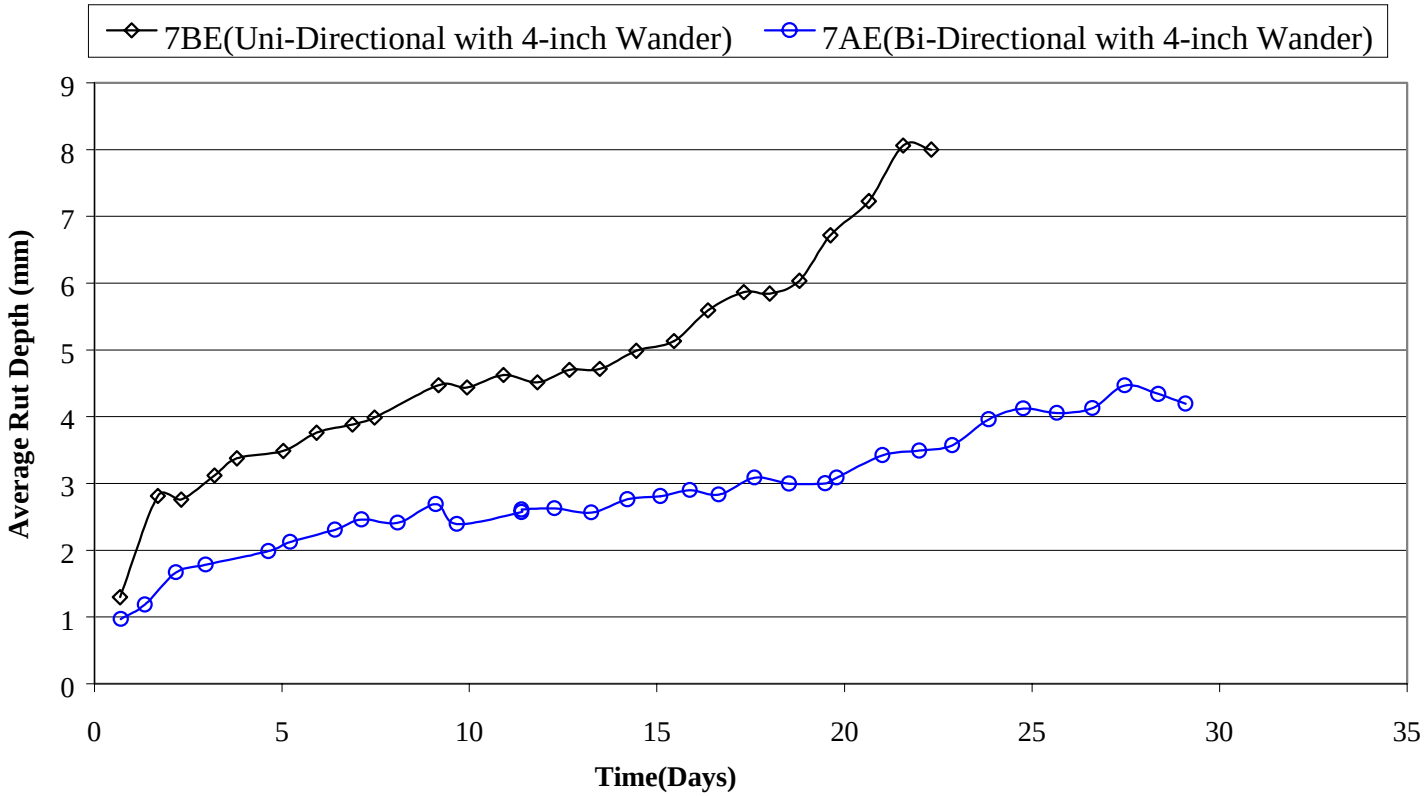

Figure 5.14 Comparison of Average Rut Depth by the Profile Method versus Time Between Uni-Directional and Bi-Directional Loading with 4-inch Wander

Figure 5.15 Photo of Section 7A-W

was observed to be much smoother than those in Trial Tests 3 and 4 (with 4-inch wander in 2-inch increments). Accumulation of rubber on the surface of the wheel track was also observed in this test but was much less than that in the other tests using uni-directional loading.

Figure 5.16 shows the comparison of rut depths as measured by the differential surface deformation method as a function of number of wheel passes between uni-directional loading with 4-inch wander in 2-inch increments and uni-directional loading with 4-inch wander in 1-inch increments. It can be seen that for the same number of wheel passes, the loading with wander in 2-inch increments gave slightly higher differential deformations than those by the loading with wander in 1-inch increments. Figure 5.17 shows similar comparison of rut depths as measured by the surface profile method. In this comparison, the case using 1-inch increments appears to give slightly

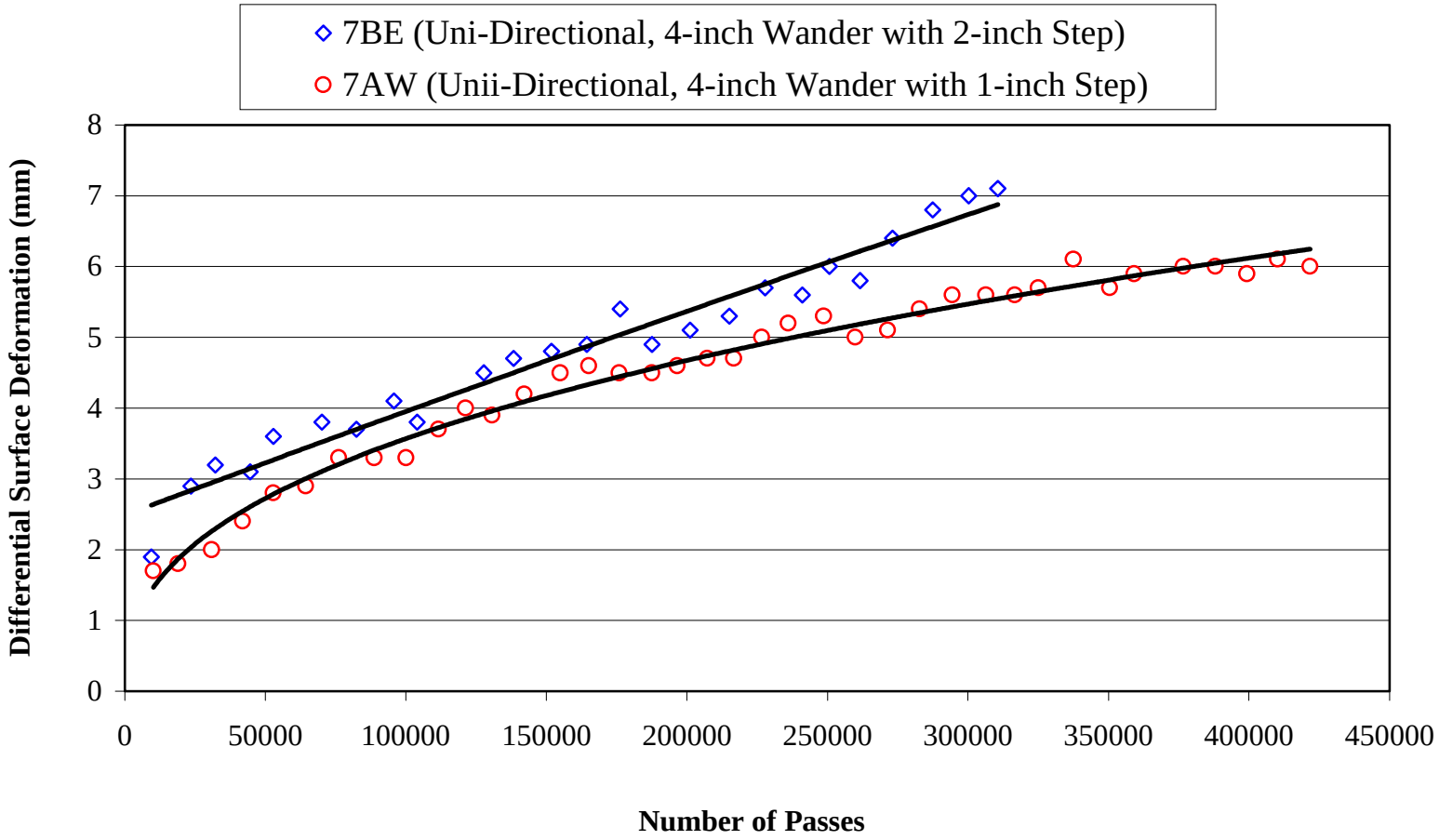

Figure 5.16 Comparison of Differential Surface Deformation versus Number of Passes Between Uni-Directional Loading with 4-inch Wander in 1-inch Increments and 2-inch Increments

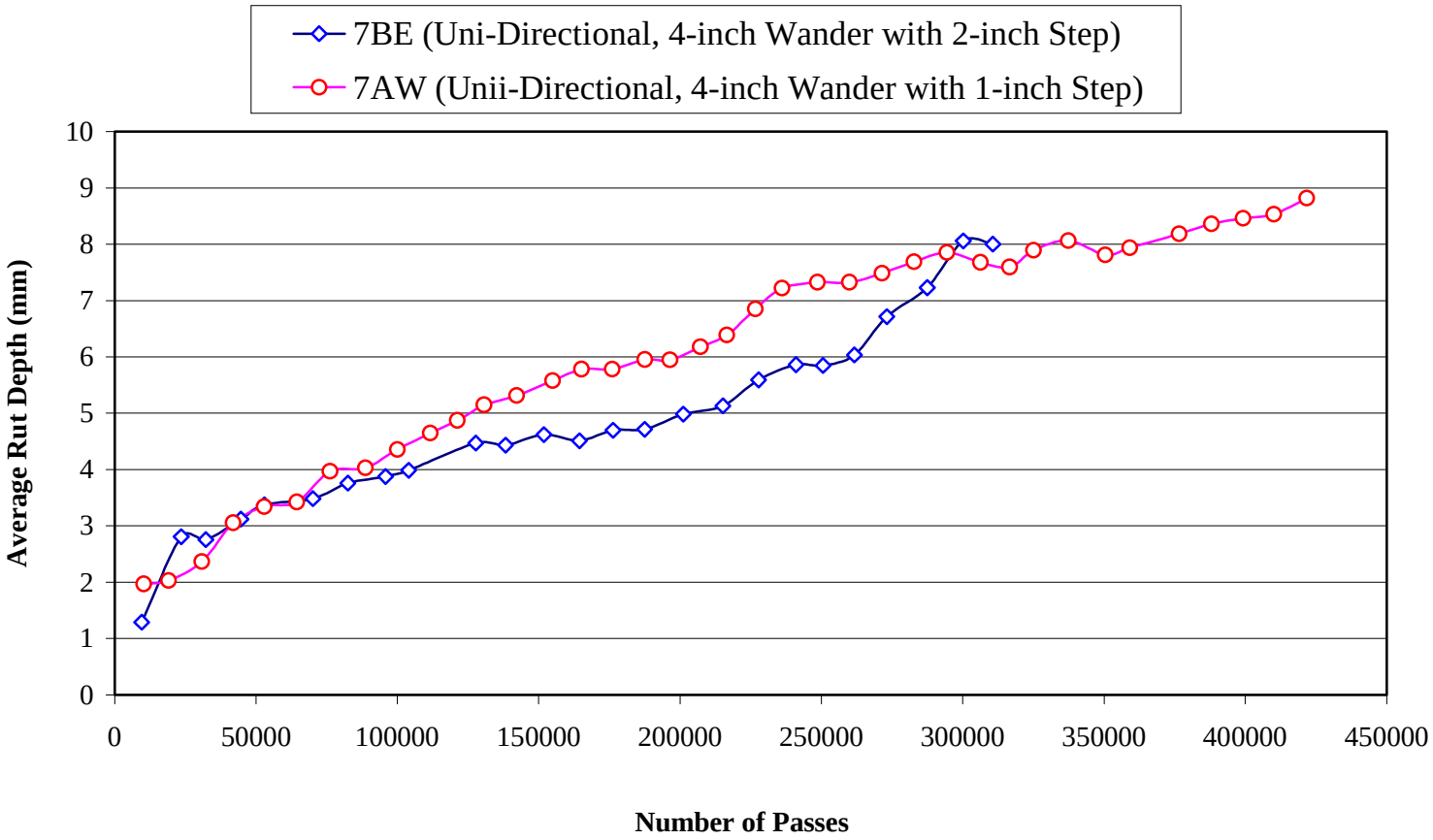

Figure 5.17 Comparison of Average Rut Depth by the Profile Method versus Number of Passes Between Uni-Directional Loading with 4-inch Wander in 1-inch Increments and 2-inch Increments

higher rut depths than those in the case using 2-inch increments. This may be explained by the fact that the case using 1-inch increments produced more heaving at the edge of the wheel track and thus resulted in higher rut depths as measured by the surface profile method.

5.7 HVS Test Configuration Chosen

The test configuration of uni-directional loading with 4-inch wander in 1-inch increments was chosen to be used in the main testing program. Using this test configuration produced wheel track profiles, which did not have the wavy transverse pattern due to tire treads, and which were more representative of observed rut profiles in the field.

CHAPTER 6
PHASE I OF HVS FIELD TESTING PROGRAM

6.1 Testing Configuration

The main HVS testing program was run using a mode of uni-directional travel with 4-inch wander in 1-inch increments, which was determined to be an effective testing configuration from the trial tests. The applied load was a 9000-lb super single wheel traveling at a speed of 6 mph. There was no temperature control on the test pavement in Phase I of the main testing program. The testing sequence has been presented in Figure 2.2 in Chapter 2.

6.2 Temperature Measurement

Table 6.1 presents the average pavement temperatures of all of the five test sections in Phase I as measured by thermocouples placed between the two 2-inch lifts of asphalt mixtures on the test sections. It can be seen that the average daily maximum temperatures of Section 2C through 5C were very close to one another, while the average daily maximum temperature of Section 1C was slightly lower than the rest.

6.3 Rut Measurement

Section 1C, which had two 2-inch lifts of SBS-modified Superpave mixture, received 329,953 wheel passes over a 31-day period. Section 2C, which had the same mixture as Section 1C, was tested for 28 days with a total of 295,950 wheel passes. Section 3C, which had a 2-inch lift of SBS-modified Superpave mixture over a 2-inch lift of unmodified Superpave mixture, was trafficked for 25 days with a total of 253,425

Table 6.1 Temperatures of Test Pavement in Phase I as Measured by Thermocouples Placed Between the Two 2-inch Lifts of Asphalt Mixture

Section 1C	Uni-Directional Loading with 4-inch Wander in 1-inch Increments			
	Thermocouple 4	Thermocouple 5	Thermocouple 6	**Average**
Avg. Daily Min. Temp (°C)	23.8	23.2	22.5	**23.2**
Avg. Daily Max. Temp (°C)	30.4	30.5	32.2	**31.0**
Overall Min. Temp (°C)	19.1	17.3	16.6	**17.7**
Overall Max. Temp (°C)	34.2	34.7	39.0	**36.0**
Section 2C	Uni-Directional Loading with 4-inch Wander in 1-inch Increments			
	Thermocouple 4	Thermocouple 5	Thermocouple 6	**Average**
Avg. Daily Min. Temp (°C)	27.6	27.2	27.8	**27.5**
Avg. Daily Max. Temp (°C)	39.5	35.7	40.0	**38.4**
Overall Min. Temp (°C)	25.5	25.6	24.9	**25.3**
Overall Max. Temp (°C)	46.9	39.4	46.0	**44.1**
Section 3C	Uni-Directional Loading with 4-inch Wander in 1-inch Increments			
	Thermocouple 4	Thermocouple 5	Thermocouple 6	**Average**
Avg. Daily Min. Temp (°C)	26.5	26.8	27.9	**27.1**
Avg. Daily Max. Temp (°C)	40.5	34.2	35.8	**36.8**
Overall Min. Temp (°C)	21.5	21.9	24.0	**22.5**
Overall Max. Temp (°C)	48.4	54.0	48.2	**50.2**
Section 4C	Uni-Directional Loading with 4-inch Wander in 1-inch Increments			
	Thermocouple 4	Thermocouple 5	Thermocouple 6	**Average**
Avg. Daily Min. Temp (°C)	37.4	28.8	29.4	**31.9**
Avg. Daily Max. Temp (°C)	39.5	37.9	39.5	**39.0**
Overall Min. Temp (°C)	30.6	30.7	31.3	**30.9**
Overall Max. Temp (°C)	44.1	41.7	44.5	**43.4**
Section 5C	Uni-Directional Loading with 4-inch Wander in 1-inch Increments			
	Thermocouple 4	Thermocouple 5	Thermocouple 6	**Average**
Avg. Daily Min. Temp (°C)	27.1	26.2	26.9	**26.7**
Avg. Daily Max. Temp (°C)	41.9	39.1	37.8	**39.6**
Overall Min. Temp (°C)	25.0	23.8	24.2	**24.3**
Overall Max. Temp (°C)	48.5	46.4	41.8	**45.6**

wheel passes. Section 4C, which had two 2-inch lifts of unmodified Superpave mixture, was tested for 27 days with a total of 281,123 wheel passes. Finally, Section 5C, which had the same mixture as Section 4C, was applied with a total of 164,525 wheel passes over 14 test days.

For each test pavement, five transverse profiles were measured on a daily basis by means of a transverse profiler placed across the pavement at five fixed locations evenly spaced across the test section. Figure 6.1 shows the transverse profiler used for this purpose. The transverse profiler plotted a transverse profile of the pavement as the contact wheel of the transverse profiler was traveled transversely across the pavement.

Figure 6.1 Picture of Transverse Profiler

The recorded transverse profiles were then used to determine the rut depths. The two methods of rut determination as used in the analysis of the trial test sections, and as described in Chapter 5, were used.

Figure 6.2 shows the comparison of the differential surface deformation versus number of passes. Figure 6.3 also shows the comparison of the change in rut depth (as measured by the surface profile method) versus number of wheel passes for all of the five test sections in Phase I. It can be seen that Section 4C and 5C, which had two lifts of unmodified mixture, had substantially (2 to 3 times) higher rate of rut development than the other three test sections which had an SBS-modified mixture at the top lift. Section 3C, which had a lift of SBS-modified mixture over a lift of unmodified mixture, had similarly low rut rate as that of Sections 1C and 2C, which had two lifts of SBS-modified mixture. It is also noted that the difference between the modified and the unmodified mixtures are more pronounced when the surface profile method is used. This is because the surface profile method for determining rut depth accounts also for the heaving of the mixture at the edges of the wheel paths which are caused by the shoving of the unmodified mixture.

Figure 6.4 shows a picture of Section 5C (with the unmodified mixture), while Figure 6.5 shows a picture of Section 2C (with the SBS-modified mixture) after HVS testing. It can be seen that Section 5C had greater heaving at the edges of the wheel path.

6.4 Summary of Findings

The test results from Phase I clearly indicate that the SBS-modified mixture outperformed by far the unmodified mixture in rutting resistance. There were not much

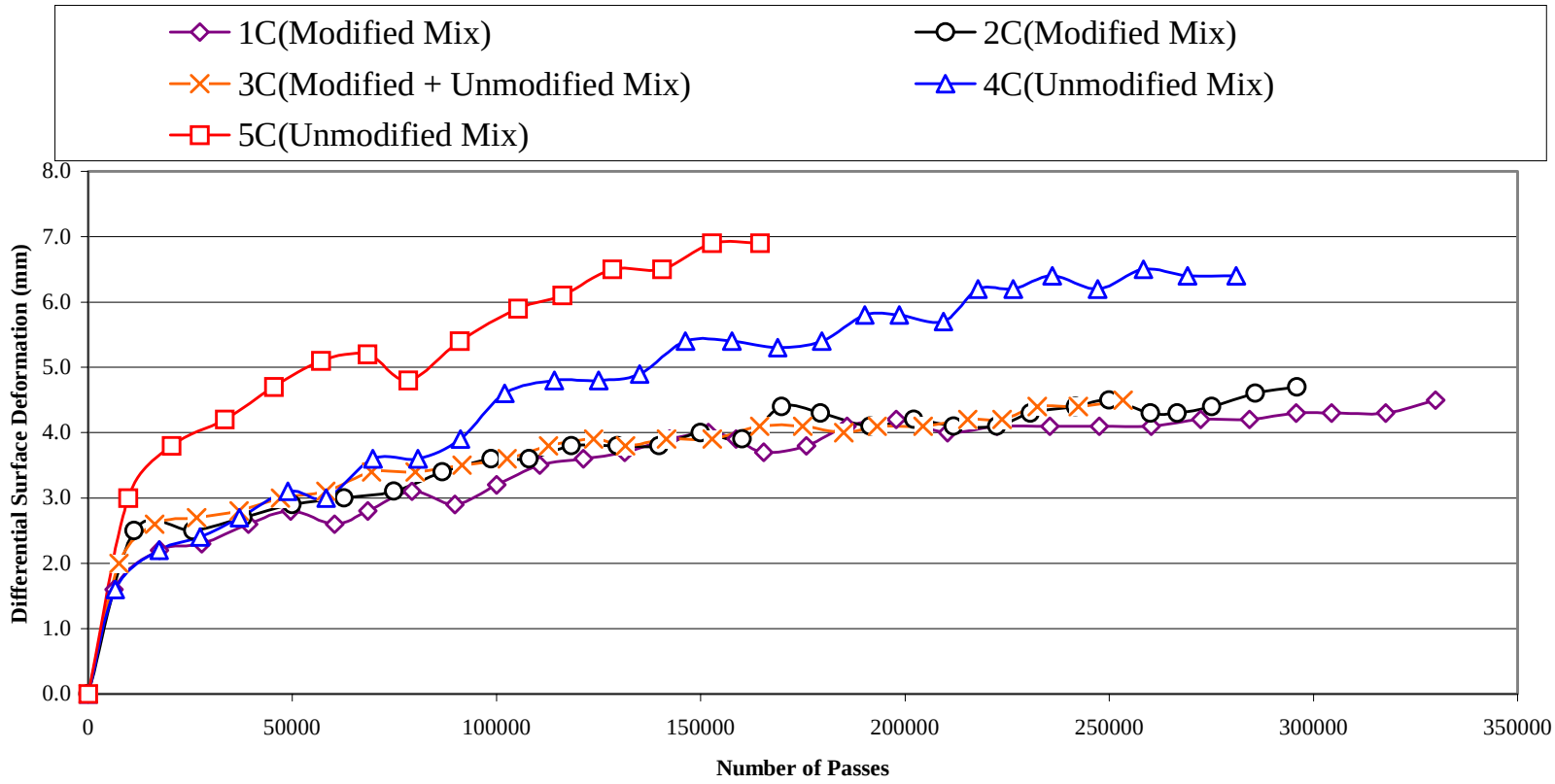

Figure 6.2 Comparison of Differential Surface Deformation versus Number of Passes for Test Sections in Phase I

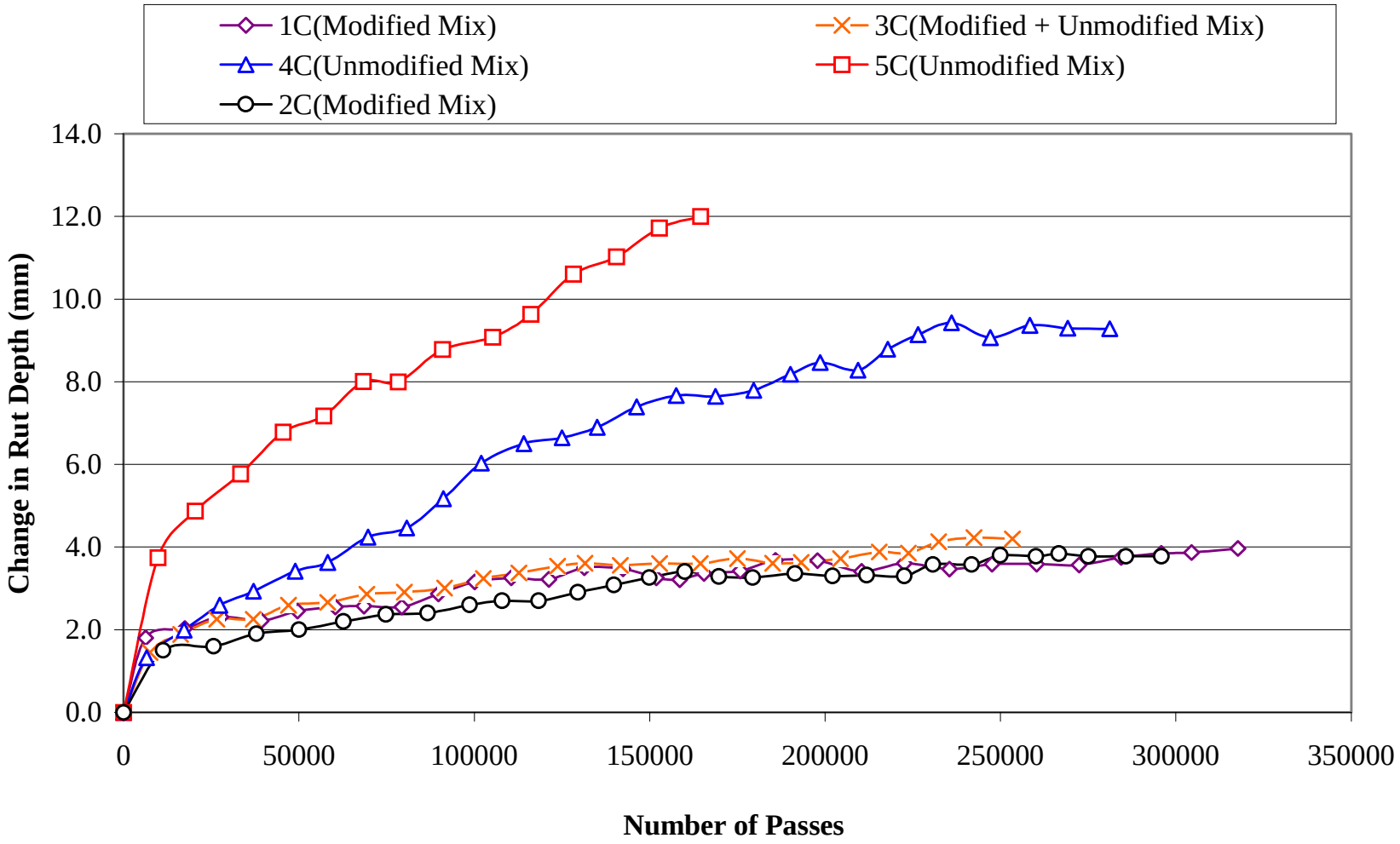

Figure 6.3 Comparison of Change in Rut Depth as Measured by the Surface Profile Method versus Number of Passes for Test Sections in Phase I

Figure 6.4 Section 5C (Unmodified Mixture) after HVS Testing

Figure 6.5 Section 2C (SBS-Modified Mixture) after HVS Testing

observed difference in rutting performance between the pavement with a lift of SBS-modified mixture over a lift of unmodified mixture and the pavement with two lifts of SBS-modified mixture.

CHAPTER 7
PHASE II OF HVS FIELD TESTING PROGRAM

7.1 Testing Configurations

The HVS was run on the test sections using the same testing configurations as used in Phase I. The applied load was a 9000-lb super single wheel traveling at a speed of 6 mph, in a uni-directional mode with 4-inch wander in 1-inch increments. For each test section, HVS loading was applied until the rut depth was judged to be more than 0.5 inch (12 mm). The testing sequence has been presented in Figure 2.2 in Chapter 2.

7.2 Temperature Measurement

The temperature of each test section was monitored by six pairs of thermocouples placed at six evenly spaced locations on the test pavement. At each location, a thermocouple was placed on the surface and another thermocouple was placed at a depth of 2 inches. Each pair of thermocouples was used to control a separate heater, which was turned on and off depending on the readings from these two thermocouples. The target pavement temperature measured at a depth of 2 inches was 50° C for eight test sections and 65° C for the other two, as shown Figure 2.2.

Before each HVS testing, the pavement was pre-heated until the desired temperature was reached. Figure 7.1 shows typical plots of the temperature versus time during pre-heating of a test section before test. HVS testing was started when the temperature at 2-inch depth reached the target temperature in a steady condition. Table 7.1 shows the minimum, maximum and average temperatures as measured by the six pairs of thermocouples during the testing of Section 3B and 5B. It can be seen that the

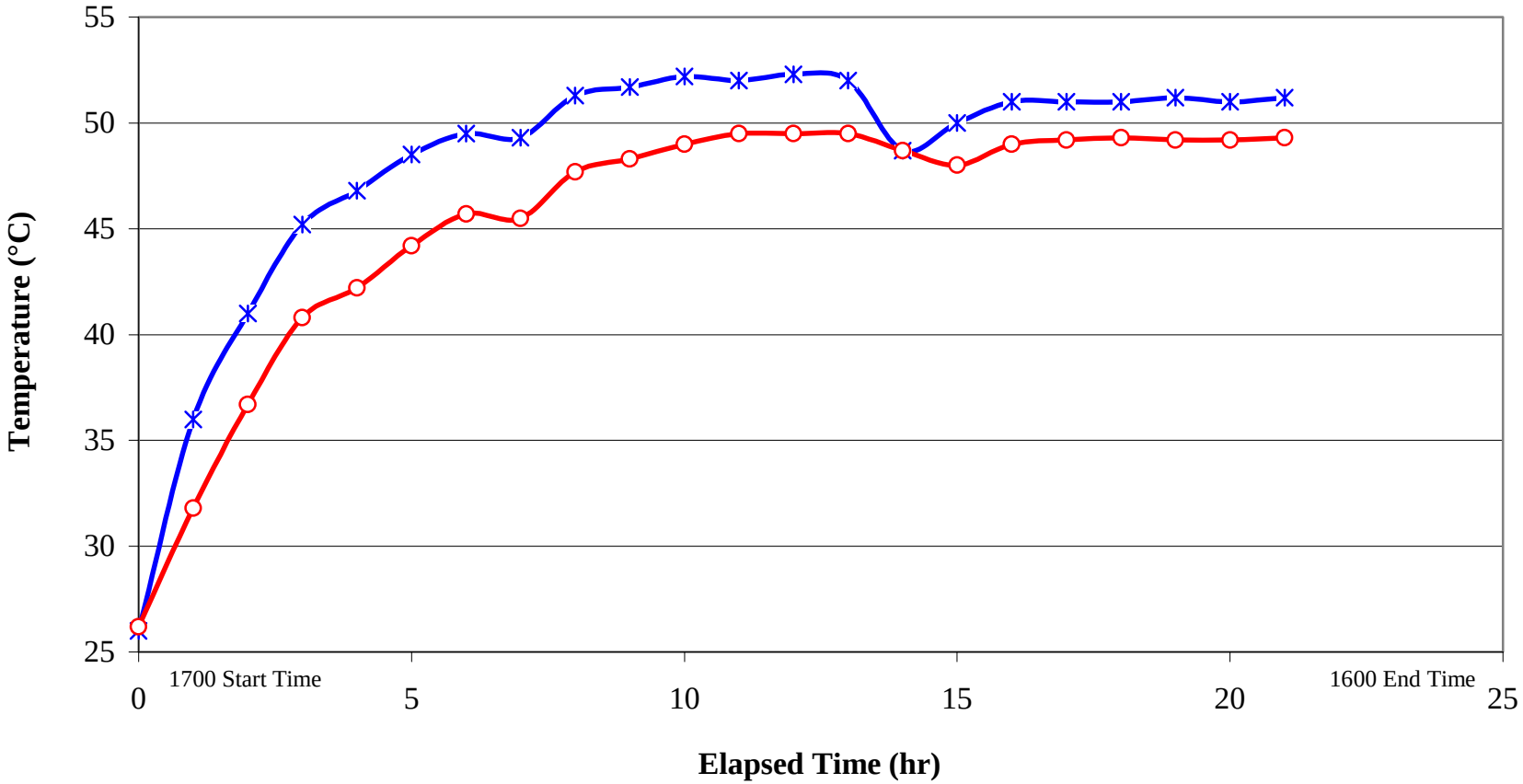

Figure 7.1 Pavement Temperatures versus Time during Pre-Heating before Start of Test

Table 7.1 Temperatures of Test Pavements in Section 3B and 5B as Measured by Thermocouples Placed at the Surface and at 2-inch Depth

Section 3B	Uni-Directional loading, 4-inch wander with 1-inch Increment						
Surface	Thermo.1	Thermo.2	Thermo.3	Thermo.4	Thermo.5	Thermo.6	Average
Avg. Daily Temp (^{o} C)	51.7	52.1	52.2	51.1	52.0	51.9	51.8
Overall Min. Temp (^{o} C)	50.0	51.0	51.0	50.0	51.0	51.0	50.7
Overall Max. Temp (^{o} C)	53.0	53.0	53.0	53.0	54.0	54.0	53.3
2-inch below	Thermo.1	Thermo.2	Thermo.3	Thermo.4	Thermo.5	Thermo.6	Average
Avg. Daily Temp (^{o} C)	50.6	50.8	51.3	50.6	50.8	51.4	50.9
Overall Min. Temp (^{o} C)	49.0	50.0	50.0	49.0	50.0	50.0	49.7
Overall Max. Temp (^{o} C)	53.0	52.0	52.0	51.0	52.0	53.0	52.2
Section 5B	Uni-Directional loading, 4-inch wander with 1-inch Increment						
Surface	Thermo.1	Thermo.2	Thermo.3	Thermo.4	Thermo.5	Thermo.6	Average
Avg. Daily Temp (^{o} C)	51.9	51.8	51.9	50.6	51.1	51.8	51.5
Overall Min. Temp (^{o} C)	47.0	50.0	49.0	47.0	50.0	51.0	49.0
Overall Max. Temp (^{o} C)	55.0	54.0	54.0	53.0	53.0	54.0	53.8
2-inch below	Thermo.1	Thermo.2	Thermo.3	Thermo.4	Thermo.5	Thermo.6	Average
Avg. Daily Temp (^{o} C)	50.9	51.6	51.1	51.0	51.0	51.3	51.2
Overall Min. Temp (^{o} C)	48.0	49.0	49.0	49.0	47.0	50.0	48.7
Overall Max. Temp (^{o} C)	53.0	54.0	53.0	53.0	54.0	53.0	53.3

range of temperature at 2-inch depth was within 48.0 to 54.0° C. The temperature ranges were similar for the rest of test sections in Phase II.

7.3 Rut Measurement

A laser profiler was used to measure the pavement surface profiles of the test pavements before, during and after the HVS testing. Analysis of the profiler data was performed by Mr. Tom Byron of FDOT. Two different methods of analysis were used. In the first method, the initial transverse surface profile (before test) was subtracted from the transverse surface profile to obtain the "differential surface profile." A straight line is drawn over the "differential surface profile" and touching it at two highest points. The greatest distance between this straight line and the "differential surface profile" is taken to be the change in rut depth of the tested pavement relative to its initial condition. Figure 7.2 shows the plots of change in rut depth as determined by this method.

In the second method, a straight line was drawn over the measured surface profile and touching it at two highest points. The greatest distance between this straight line and the surface profile was taken to be the rut depth of the test pavement. The rut depth of the pavement at its initial condition (before testing) was also determined in the same manner. The change in rut depth of the tested pavement relative to its initial condition was determined by subtracting the initial rut depth from the determine rut depth at the specified time. Figure 7.3 shows the plots of change in rut depth as determined by this method.

Figures 7.4 and 7.5 show respectively the pictures of Sections 1B and 2B (with two lifts of SBS-modified mixture) after HVS testing at 50° C. Figures 7.6 and 7.7 show respectively the pictures of Sections 3A and 3B (with a lift of SBS-modified mixture over an unmodified mixture) after HVS testing at 50° C. Figures 7.8 through 7.11 show respectively the pictures of Sections 4A, 4B, 5A and 5B (with two lifts of unmodified

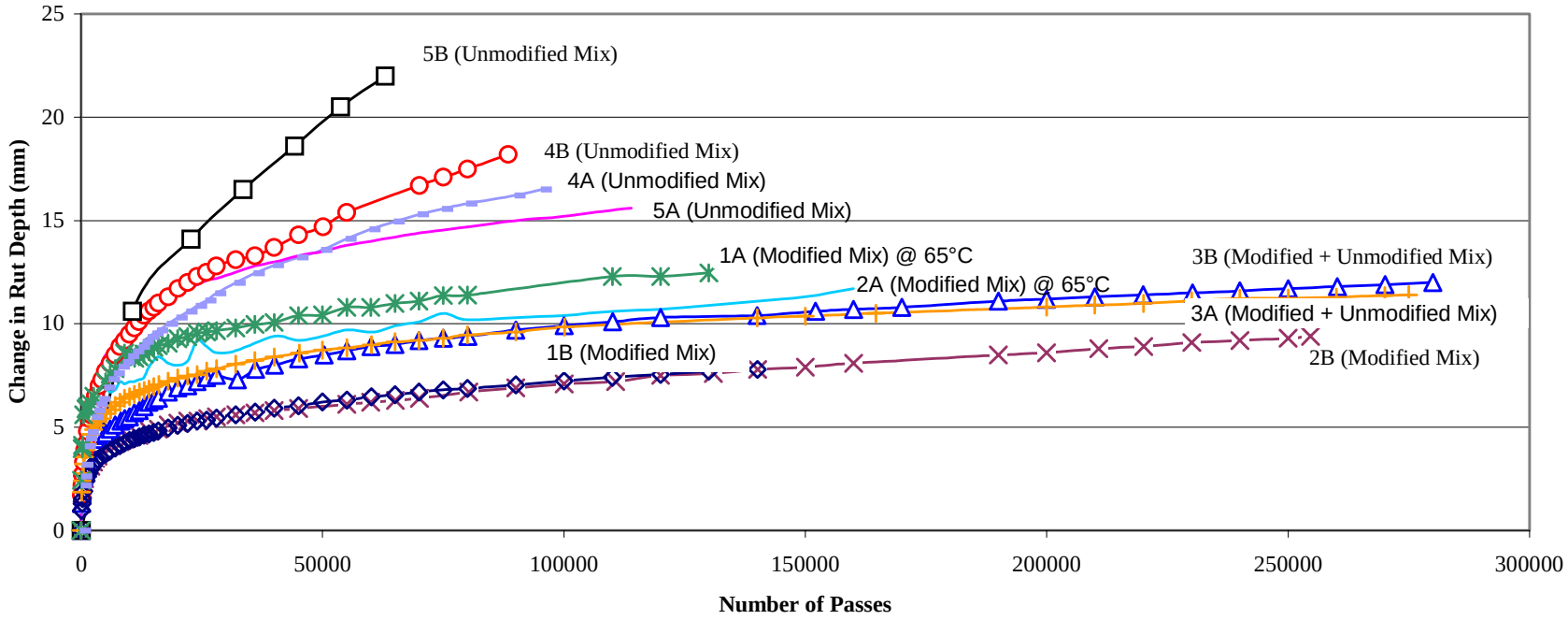

Figure 7.2 Comparison of Rut Depth as Measured by the Differential Surface Profile Method versus Number of Passes

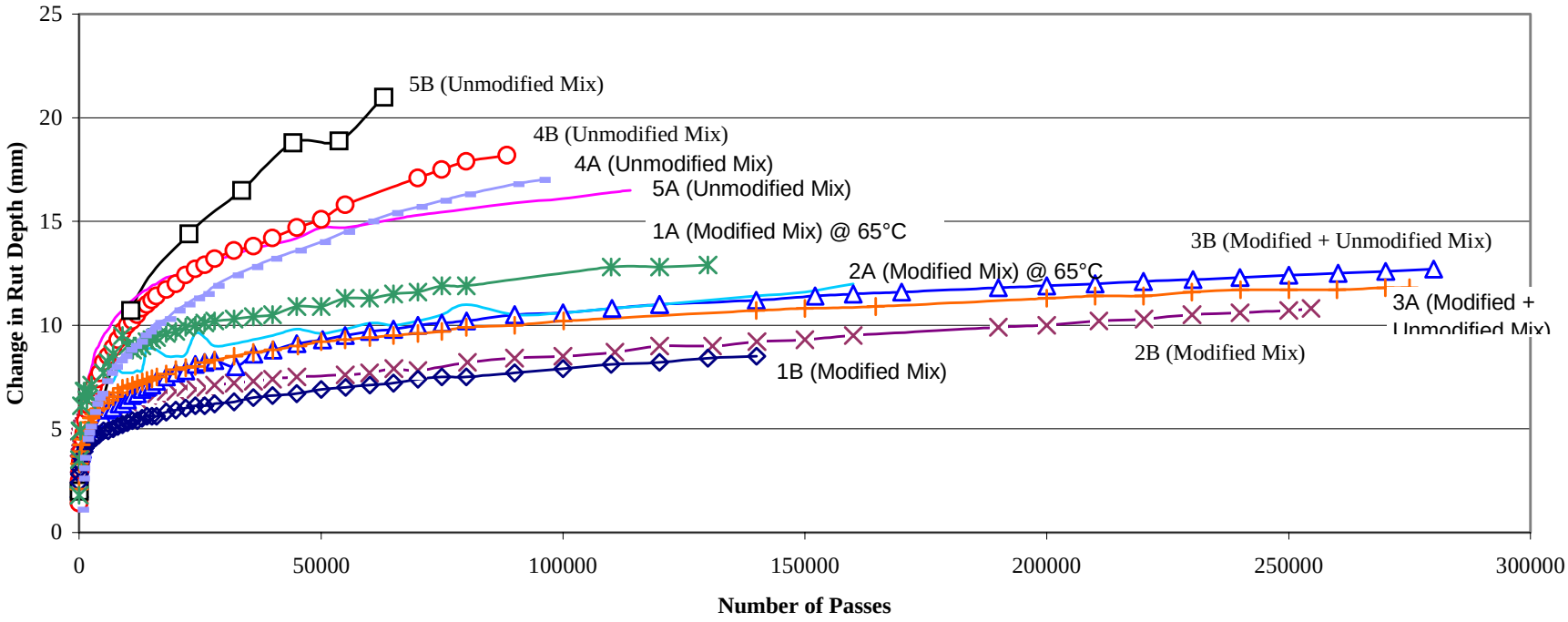

Figure 7.3 Comparison of Change in Rut Depth as Measured by the Surface Profile Method versus Number of Passes

Figure 7.4 Photo of Section 1B (SBS-Modified Mixture Tested at 50° C)

Figure 7.5 Photo of Section 2B (SBS-Modified Mixture Tested at 50° C)

Figure 7.6 Photo of Section 3A (SBS-Modified Mixture over Unmodified Mixture Tested at 50° C)

Figure 7.7 Photo of Section 3B (SBS-Modified Mixture over Unmodified Mixture Tested at 50° C)

Figure 7.8 Photo of Section 4A (Unmodified Mixture Tested at 50° C)

Figure 7.9 Photo of Section 4B (Unmodified Mixture Tested at 50° C)

Figure 7.10 Photo of Section 5A (Unmodified Mixture Tested at 50° C)

Figure 7.11 Photo of Section 5B (Unmodified Mixture Tested at 50° C)

mixture) after HVS testing at 50° C. Figures 7.12 and 7.13 show respectively the pictures of Sections 1A and 2A (with two lifts of SBS-modified mixture) after HVS testing at 65° C.

7.4 Summary of Findings

The following observations can be made from the rutting results as plotted in Figures 7.2 and 7.3:

1. Good repeatability of test results was generally observed between different test sections with the same pavement design and test temperature. Lanes 4 and 5, which had two lifts of unmodified mixture appeared to have relatively higher variability in rut development than the other test sections.
2. The pavement sections with two lifts of SBS-modified mixture clearly outperformed those with two lifts of unmodified mixture. Sections 4A , 4B, 5A and 5B (with two lifts of unmodified mixture and tested at 50° C) had about two to two and a half times the rut rate as compared with that of Sections 1B and 2B (with two lifts of modified mixture and tested at the same temperature.
3. The pavement sections with a lift of SBS-modified mixture over a lift of unmodified mixture (Sections 3A and 3B) had practically about the same rut rate as those with two lifts of modified mixture (1B and 2B) when tested at 50° C.
4. Test Sections 1A and 2A, which had two lifts of SBS-modified mixture and tested at 65° C still had much lower rutting than the test sections with the unmodified mixture and tested at 50° C (Sections 4A, 4B, 5A and 5B).

Figure 7.12 Photo of Section 1A (SBS-Modified Mixture Tested at 65° C)

Figure 7.13 Photo of Section 2A (SBS-Modified Mixture Tested at 65° C)

CHAPTER 8
LABORATORY TESTING PROGRAM ON PLANT-COLLECTED SAMPLES

8.1 Tests on Plant-Collected Samples

The asphalt mixtures sampled from the hot-mix plant during the construction of the test tracks were evaluated in the laboratory in order to determine the possible relationship between mixture properties and field performance.

The following tests were run on the asphalt mixtures in the laboratory:

1. Compaction and evaluation in the Gyratory Testing Machine (GTM);
2. Compaction and evaluation in the Servopac Gyratory Compactor using 1.25 and 2.5° gyratory angles; and
3. Evaluation in the Asphalt Pavement Analyzer (APA).

8.2 Gyratory Testing Machine (GTM) Results

Three samples from each lift of the unmodified and the SBS-modified mixtures were compacted to ultimate density (when the change in density is equal to or less than 0.5 lb/ft^3 per 50 revolutions) under a 120-psi vertical ram pressure in the Gyratory Testing Machine (GTM). The unmodified mixture samples were compacted at 300° F, whereas the SBS-modified asphalt mixtures were compacted at 325° F. These two different compaction temperatures were used to simulate the actual placement temperatures of these two mixtures at the test roads. The gyratory shear resistance (S_g) of the mixture was determined at every 10 revolutions until 50 gyrations, and after that every 25 revolutions until the ultimate density. The Gyratory Stability Index (the ratio of

the maximum gyratory angle to the minimum gyratory angle) was also determined at the end of the test.

The average gyratory shear resistance of the unmodified and modified asphalt mixtures versus number of gyrations was plotted in Figure 8.1. It can be seen that the gyratory shear value of the unmodified mix-lift 2, modified mix-lift 1 and lift 2 were very close to one another. The unmodified mix-lift 1 had slightly higher gyratory shear values than those of the other three mixtures.

The Gyratory Stability Index (GSI) value of each specimen was calculated from the gyrograph and displayed in Table 8.1. It can bee seen that the GSI values of the SBS-modified mixtures were very close to 1.0. The unmodified mixtures had GSI values of 1.18 and 1.21 for lift 1 and lift 2, respectively. An increase in the GSI value beyond 1.0 usually indicates instability of the mixture under the applied ram pressure. Therefore, this result could mean that the unmodified mixture (with a GSI of more than 1.0) was relatively less stable than the SBS-modified mixture (with a GSI close to 1.0).

Table 8.1 GSI values of the Four Mixtures Evaluated in the GTM

Sample No	Unmodified Mix	Unmodified Mix	Modified Mix	Modified Mix
	Lift 1	Lift 2	Lift 1	Lift 2
1	1.15	1.20	1.00	1.00
2	1.23	1.19	1.05	1.00
3	1.17	1.23	1.00	1.12
Average	**1.18**	**1.21**	**1.02**	**1.04**

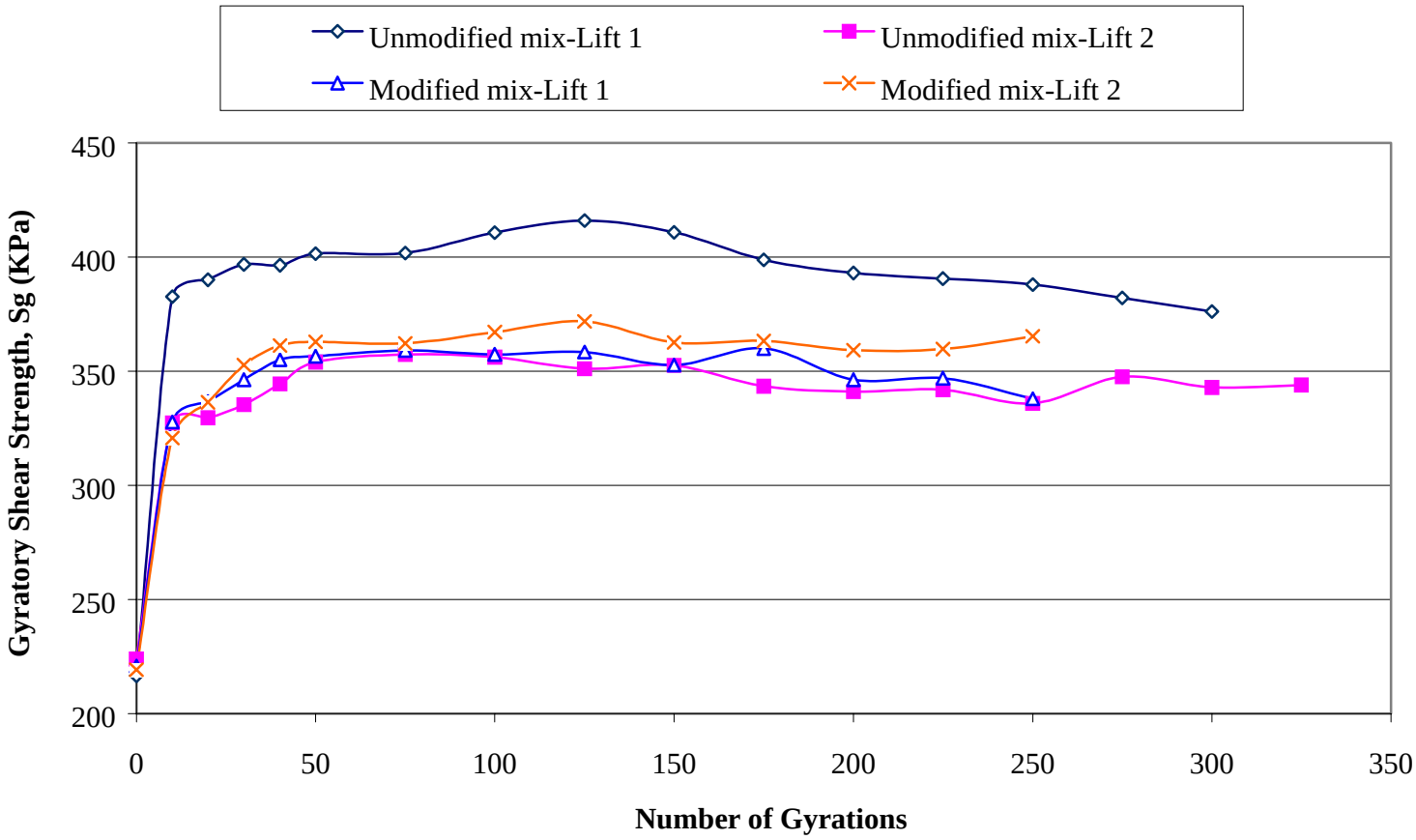

Figure 8.1 Gyratory Shear Resistance of the Unmodified and Modified Asphalt Mixtures versus Number of Gyrations

8.3 Servopac Gyratory Compactor (SGC) Results

Three asphalt specimens were compacted in the Servopac Gyratory Compactor for each of the following materials and testing configurations:

1. Unmodified Mixture-Lift 1 using 1.25° gyratory angle
2. Unmodified Mixture-Lift 1 using 2.5° gyratory angle
3. SBS-modified Mixture-Lift 1 using 1.25° gyratory angle
4. SBS-modified Mixture-Lift 1 using 2.5° gyratory angle
5. SBS-modified Mixture-Lift 2 using 1.25° gyratory angle
6. SBS-modified Mixture-Lift 2 using 2.5° gyratory angle

One specimen was compacted to N_{design} (100) gyrations, and two specimens were compacted to N_{max} (160) gyrations. The unmodified mixtures were compacted at 300 °F while the SBS-modified mixtures were compacted at 325 °F. The average gyratory shear values versus number of gyrations using 1.25° and 2.5° gyratory angles were plotted in Figure 8.2 and 8.3, respectively. It can be seen from these figures that the unmodified mixture had higher gyratory shear values than those of the SBS-modified mixtures. This could be due to the lower compaction temperature of the unmodified mixtures.
The volumetric properties of these mixtures compacted in the Servopac are given in Table 8.2. In the case of 1.25° gyratory angle, the modified mixture from lift 1 had the lowest air voids (2.05%) and VMA (13%) at N_{design}. The unmodified mixture from lift 1 had 2.35% air voids and 13.9% VMA at N_{design}. Similar trends were seen in the case of 2.5° gyratory angle. The modified mixture from lift 1 had the lowest air voids (0.22%) and VMA (11.4%) at N_{design}. The unmodified mixture from lift 1 had an air voids value (0.52%) between those of the two modified mixtures and higher VMA value (12.1%) than those of the two modified mixtures.

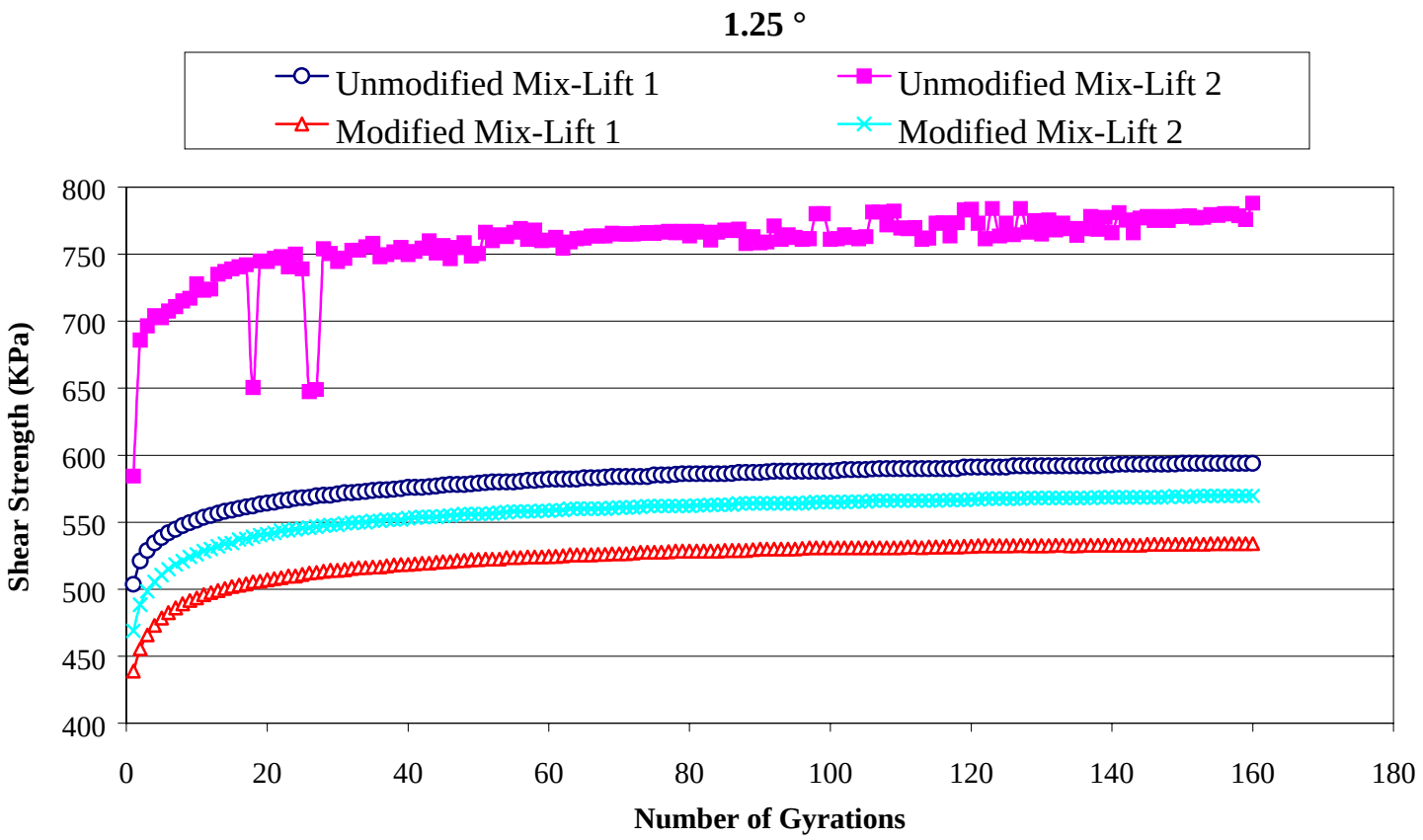

Figure 8.2 Gyratory Shear Values versus Number of Gyrations Using 1.25° Gyratory Angle

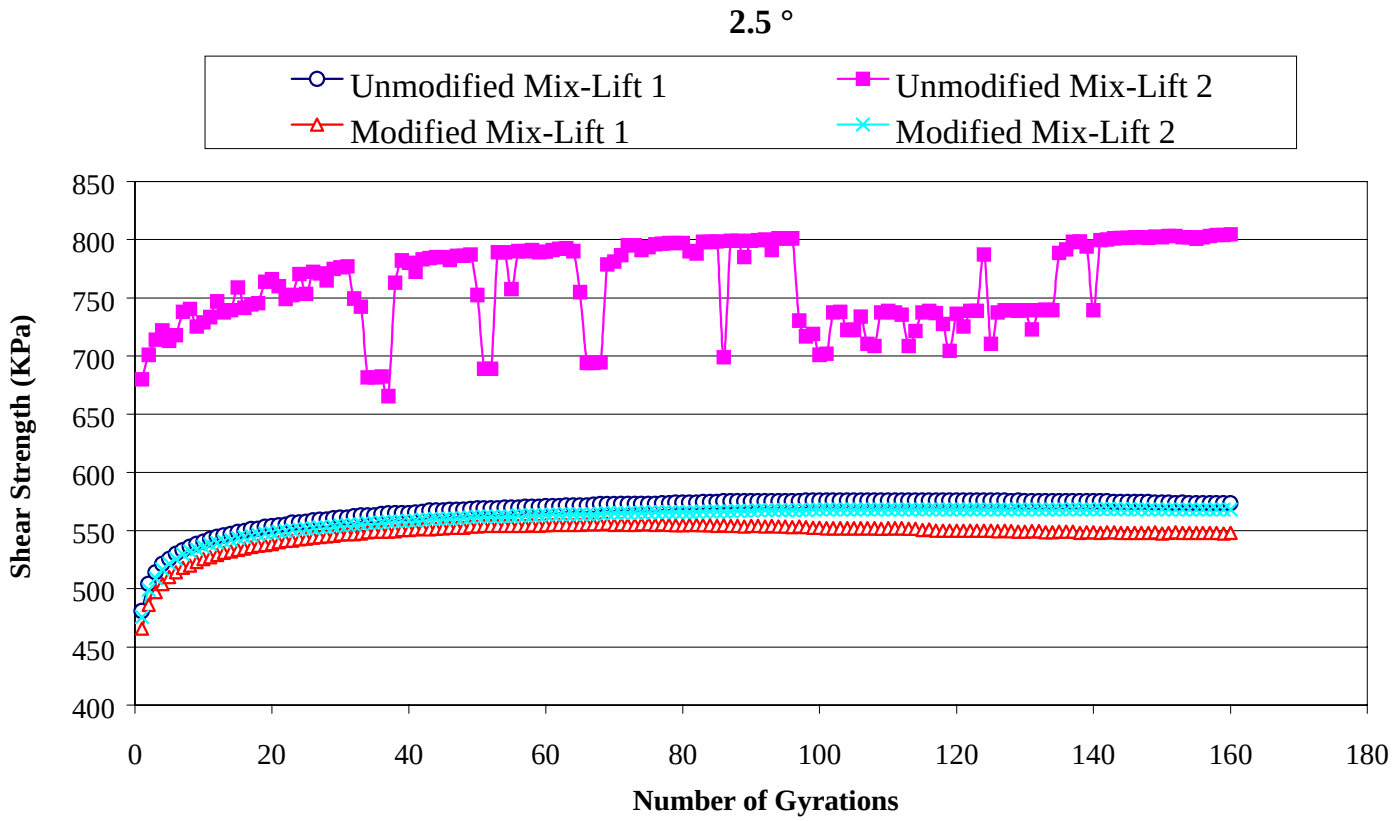

Figure 8.3 Gyratory Shear Values versus Number of Gyrations Using 2.5° Gyratory Angle

Table 8.2 Volumetric Properties of the Mixtures Compacted in the Servopac Gyratory Compactor Using 1.25 and 2.5° Gyratory Angles

Mix Type	% AC	% Air Voids	VMA	VFA	%Gmm (@Nini)	%Gmm (@Ndes)	%Gmm (@Nmax)	Dust Ratio
Unmod-Lift 1 (1.25°)	8.2	2.35	13.9	83.1	91.1	97.7	98.3	0.8
Unmod-Lift 2 (1.25°)	8.2	3.43	14.0	75.5	89.5	96.6	97.2	0.9
Mod-Lift 1 (1.25°)	7.9	2.05	13.0	84.2	90.6	97.9	98.5	0.9
Mod-Lift 2 (1.25°)	7.9	3.19	13.6	76.7	90.0	96.8	97.4	0.9
Unmod-Lift 1 (2.5°)	**8.2**	**0.52**	**12.1**	**95.7**	**92.5**	**99.5**	**100.0**	**0.8**
Unmod-Lift 2 (2.5°)	**8.2**	**1.05**	**11.9**	**91.2**	**91.6**	**98.9**	**99.6**	**0.8**
Mod-Lift 1 (2.5°)	**7.9**	**0.22**	**11.4**	**98.1**	**92.9**	**99.8**	**100.0**	**0.9**
Mod-Lift 2 (2.5°)	**7.9**	**0.91**	**11.6**	**92.2**	**92.4**	**99.1**	**99.7**	**0.9**

Figures 8.4 and 8.5 show the plots of gyratory shear versus log of number of gyrations between air voids of 7% to 4% at 1.25° and 2.5° gyratory angles, respectively. Some prior research results have indicated that the slope of the plot of gyratory shear versus log of number of gyrations between air voids of 7% to 4% may be related to the rutting resistance of the mixture. According to that hypothesis, a higher slope may indicate higher resistance to rutting. However, the slopes of the plots of gyratory shear versus log of number of gyrations as shown on Figures 8.4 and 8.5 do not support that hypothesis. The slopes for the SBS-modified mixture did not show significantly higher values than those for the unmodified mixtures.

Generally, the gyratory shear stress increases as air void decreases in compaction. Figures 8.6 and 8.7 show the plots of gyratory shear stress versus air void of SBS-modified and unmodified mixtures at 1.25 and 2.5° gyratory angles. It is clearly seen that

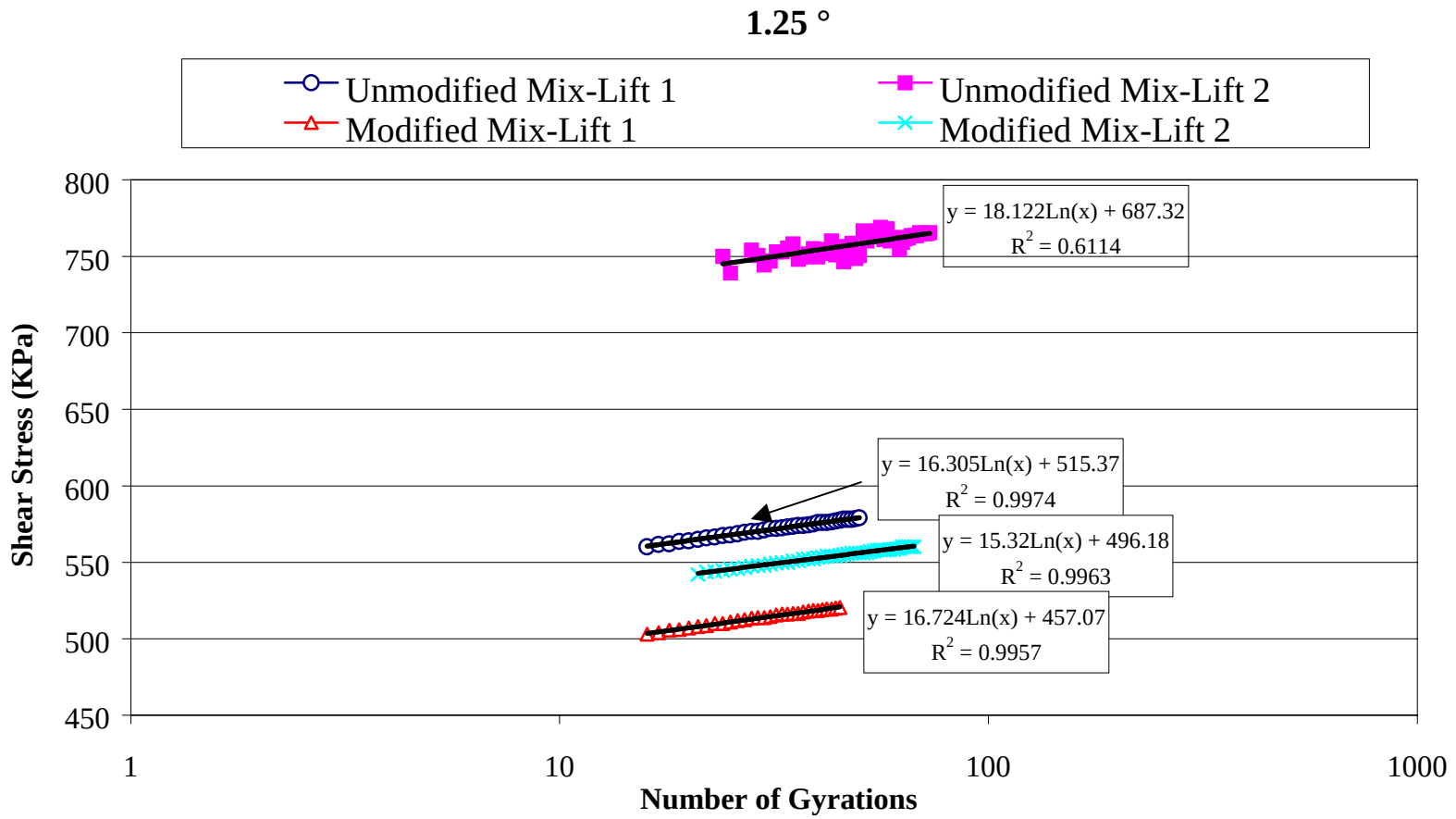

Figure 8.4 Gyratory Shear Strength versus Log Cycles for Gyrations between Air Voids of 7% to 4% at 1.25° Gyratory Angle

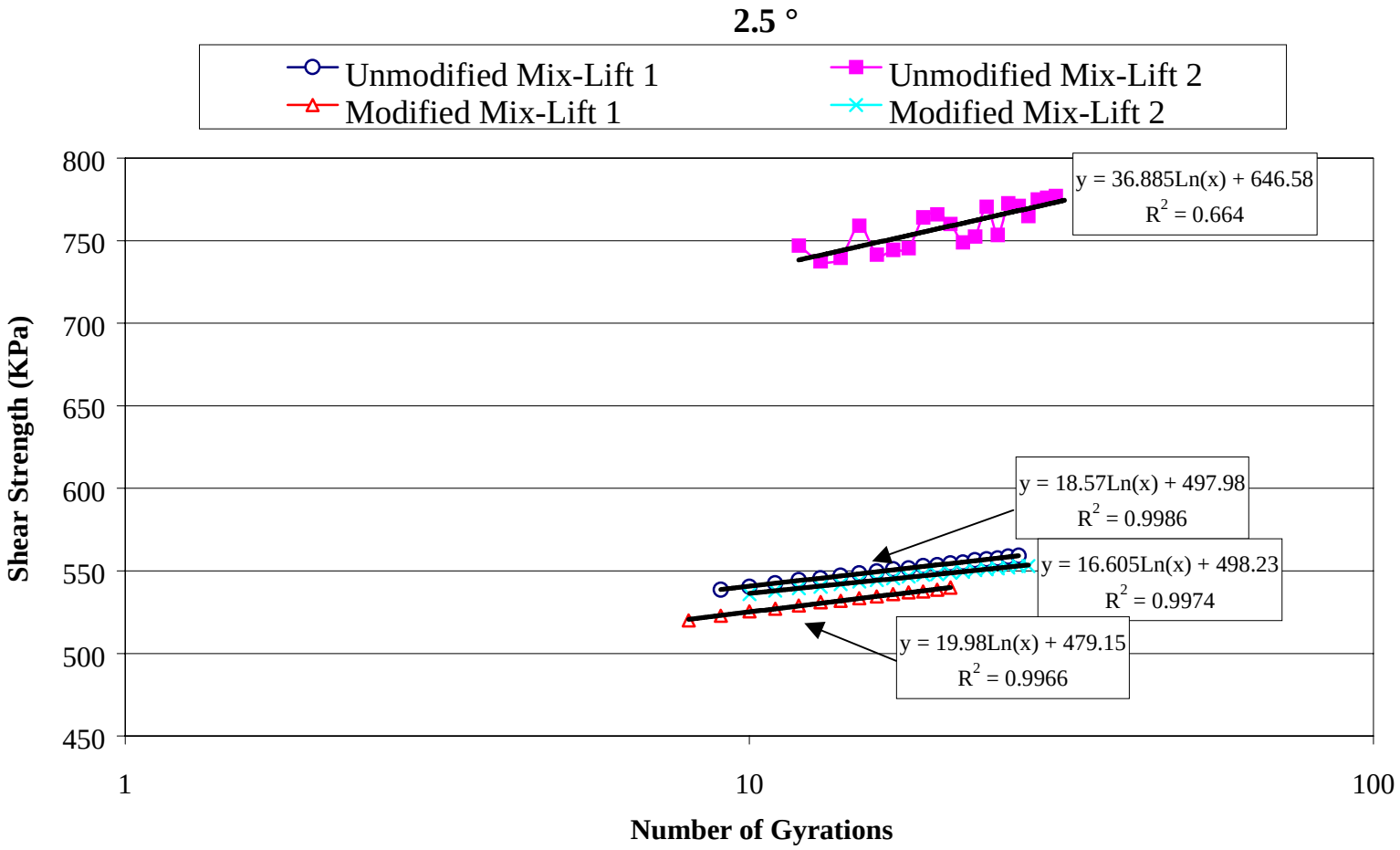

Figure 8.5 Gyratory Shear Strength versus Log Cycles for Gyrations between Air Voids of 7% to 4% at 2.5° Gyratory Angle

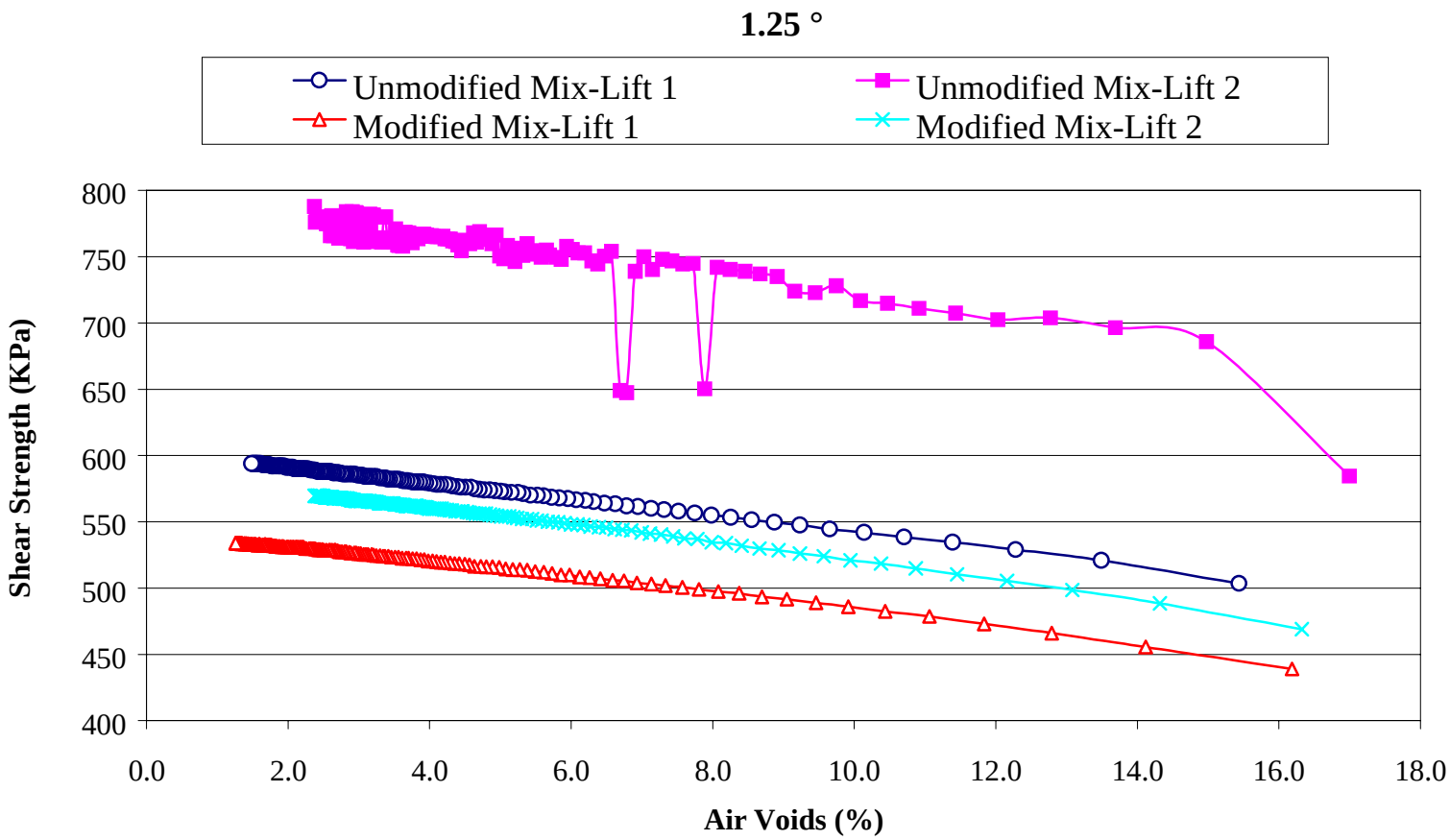

Figure 8.6 Gyratory Shear Strength versus Air Voids at 1.25° Gyratory Angle in the Servopac Gyratory Compactor

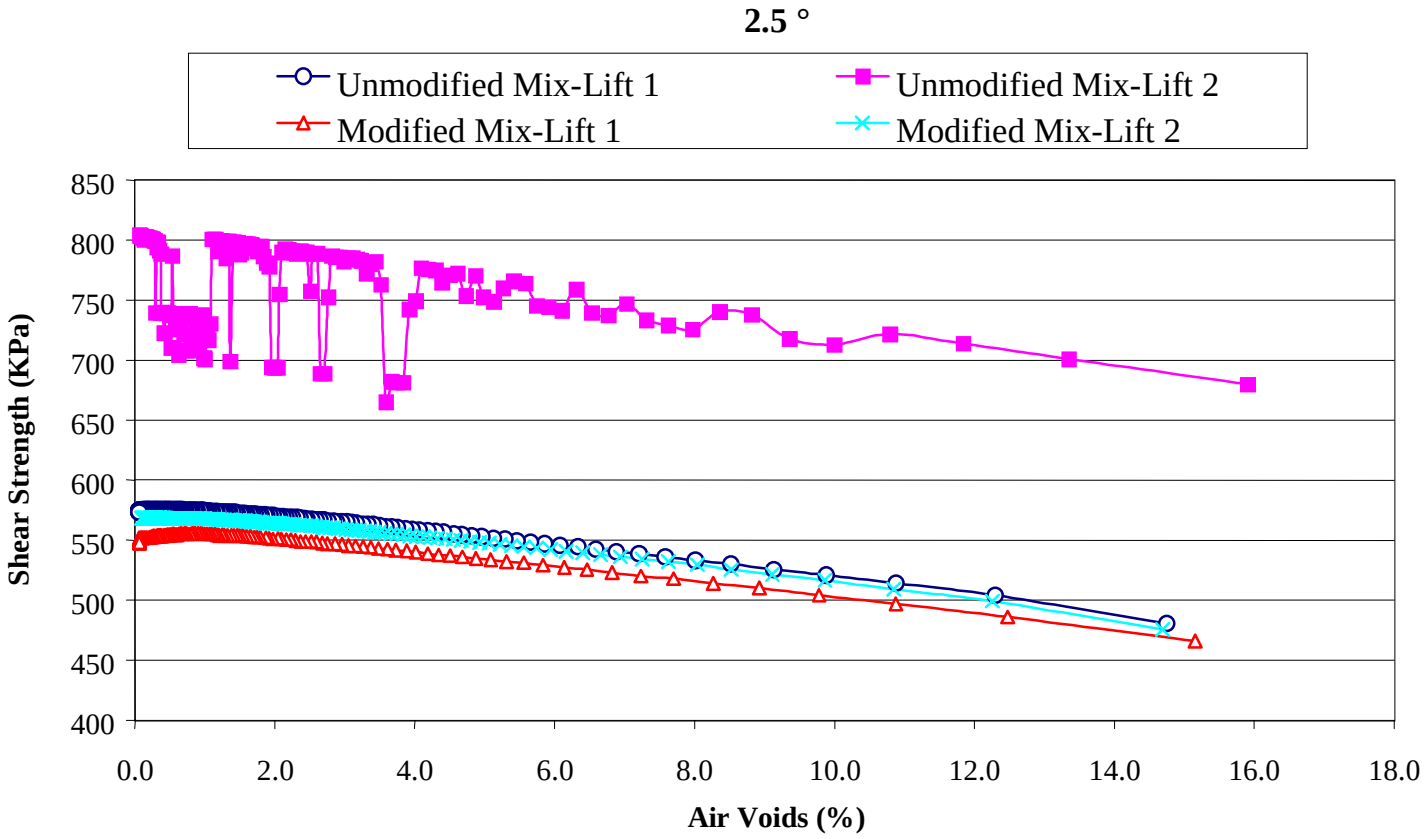

Figure 8.7 Gyratory Shear Strength versus Air Voids at 2.5° Gyratory Angle in the Servopac Gyratory Compactor

the SBS-modified showed lower gyratory shear than the unmodified mixture at the same air void content.

8.4 Asphalt Pavement Analyzer (APA) Results

To evaluate the rutting performance of the asphalt mixtures in the laboratory, cylindrical specimens were compacted to between 6.5 and 7.5% air voids with the Superpave Gyratory Compactor. A 100-lb load was applied by a wheel to a hose placed on top of the specimens in the APA. The rut depth was measured at two locations after 8000 wheel passes. Final rut depth was calculated by subtracting the rut depth after 8000 wheel passes by the rut depth after 25 wheel passes. A total of six specimens of the unmodified mixture-lift 1 and four specimens of each of the other mixtures were evaluated in the APA. From the summary of the rut measurements as shown in Table 8.3, it can be seen that the average rut depths for the unmodified asphalt mixtures (8.7 mm) were about 50% higher than those for the SBS-modified asphalt mixtures (5.75mm).

8.5 Summary of Findings

From the results of the laboratory testing program on the plant-collected mixtures, it appears that the two laboratory test results which correlate with field rutting performance are (1) the rut depth measurement from the APA, and (2) the GSI value as measured in the GTM. A mixture with a higher rut depth in the APA will be likely to rut more in the actual pavement. A mixture with a GSI of more than 1.0 as measured by the GTM will be likely to rut more than one with a GSI close to 1.0.

Table 8.3 Summary of Rut Depth Measurements in the APA Evaluation of the Four Mixtures

Sample No	Measurement No	Unmodified Mix-Lift 1			Unmodified Mix-Lift 2		
		Rut Measurement			Rut Measurement		
		25 Passes	8000 Passes	**Rut Depth**	25 Passes	8000 Passes	**Rut Depth**
1	1	20.2	11.8	8.4	19.8	12.6	7.2
	2	20.6	11.1	9.5	20.3	11.9	8.4
2	1	20.8	10.8	10.0	20.6	12.6	8.0
	2	20.6	11.3	9.3	20.1	13.1	7.0
3	1	20.5	9.4	11.1	20.3	13.0	7.3
	2	20.7	9.6	11.1	20.4	12.6	7.8
4	1	20.8	10.4	10.4	20.4	13.4	7.0
	2	20.0	11.0	9.0	18.5	14.5	4.0*
5	1	20.8	11.1	9.7			
	2	20.4	9.8	10.6			
6	1	20.8	10.6	10.2			
	2	21.0	12.0	9.0			
Overall Average (mm)				**9.9**			**7.5**

Sample No	Measurement No	Modified Mix-Lift 1			Modified Mix-Lift 2		
		Rut Measurement			Rut Measurement		
		25 Passes	8000 Passes	**Rut Depth**	25 Passes	8000 Passes	**Rut Depth**
1	1	20.6	14.4	6.2	21.0	16.1	4.9
	2	20.8	14.5	6.3	21.0	15.8	5.2
2	1	20.7	14.4	6.3	21.2	16.4	4.8
	2	20.9	14.8	6.1	21.0	15.6	5.4
3	1	20.5	15.4	5.1	21.1	16.0	5.1
	2	21.1	14.8	6.3	21.2	15.2	6.0
4	1	21.3	14.3	7.0	21.3	15.7	5.6
	2	20.9	14.8	6.1	21.1	15.6	5.5
Overall Average (mm)				**6.2**			**5.3**

* Not considered in the overall average because the value is an outlier

CHAPTER 9
EVALUATION OF CORED SAMPLES FROM THE TEST SECTIONS

9.1 Introduction

Cores were taken from the test sections after they had been tested by the HVS in order to evaluate (1) the changes in properties of the pavement materials, and (2) the possible relationship between the laboratory-measured mixture properties and the observed rutting performance. For each of the test sections, two cores were taken from the middle of the wheel path, and two cores were taken from the edge of the wheel path. Figure 9.1 shows a picture of the locations of a core taken from the middle of the wheel path and a core taken from the outside edge of the wheel path of a test section. All cores were 6 inches in diameter and contained the two lifts of asphalt mixture, which were bonded together.

These cores were evaluated to determine their (1) thickness, (2) density, (3) resilient modulus at 5 and 25° C, (4) indirect tensile strength at 25° C, and (5) viscosity of recovered binders at 60° C.

9.2 Thickness and Density Evaluation of Cores from the Test Sections

For each of the cores taken from the test sections, the thickness profile in the direction perpendicular to the wheel path was determined. This was done by drawing a line across the face and through the center of the core, in a direction judged to be perpendicular to the wheel path. The thickness of the core along the marked line was then measured with a caliper at a spacing of 0.5 inch.

Figure 9.1 Picture Showing Locations of a Core Taken From the Middle of the Wheel Path and a Core Taken From the Outside Edge of the Wheel Path

Plots of the thickness profiles of the cores tested are shown in Appendix C. The average thickness of the cores from the wheel path and the cores from the outside edge of the wheel path for each test section were calculated and shown in Table 9.1. The density of all the cores were also measured and shown also in Table 9.1. The percents difference in thickness and density between the cores from the wheel path and the cores from the outside edge of the wheel path were also computed and shown in Table 9.1.

The data show that all the cores from the wheel paths are thinner and denser than the cores from the edges of wheel paths. In comparing the percent difference in thickness with the percent difference in density between these two groups of cores, it can be seen

Table 9.1 Bulk Densities of Cores from Wheel Paths and Edges of Wheel Paths of the Test Sections

Section		Bulk Density				Thickness (mm)	
		No.1	No.2	Average	% difference	Average	% difference
7AE	wheelpath	2.140	2.152	**2.146**	**2.49**	**81.33**	**5.40**
	edge of wheelpath	2.090	2.095	**2.093**		**85.97**	
7AW	wheelpath	2.141	2.113	**2.127**	**3.57**	**76.96**	**7.64**
	edge of wheelpath	2.105	1.997	**2.051**		**83.33**	
7BE	wheelpath	2.119	2.126	**2.123**	**1.63**	**76.11**	**11.19**
	edge of wheelpath	2.084	2.092	**2.088**		**85.7**	
7BW	wheelpath	2.119	2.142	**2.131**	**1.85**	**79.79**	**10.56**
	edge of wheelpath	2.093	2.089	**2.091**		**89.21**	
7C	wheelpath	2.171	2.171	**2.171**	**2.56**	**84.58**	**8.16**
	edge of wheelpath	2.109	2.122	**2.116**		**92.09**	
2C	wheelpath	2.181	2.181	**2.181**	**2.61**	**81.06**	**2.06**
	edge of wheelpath	2.129	2.119	**2.124**		**82.77**	
3C	wheelpath	2.134	2.133	**2.134**	**1.03**	**74.66**	**5.24**
	edge of wheelpath	2.119	2.104	**2.112**		**78.79**	
4C	wheelpath	2.168	2.099	**2.134**	**4.78**	**80.84**	**8.59**
	edge of wheelpath	2.092	1.971	**2.032**		**88.44**	
5C	wheelpath	2.154	2.155	**2.155**	**3.30**	**77.84**	**11.36**
	edge of wheelpath	2.071	2.096	**2.084**		**87.82**	
1B	wheelpath	2.164	2.163	**2.164**	**1.57**	**89.33**	**7.78**
	edge of wheelpath	2.134	2.125	**2.130**		**96.87**	
2B	wheelpath	2.184	2.189	**2.187**	**2.68**	**73.53**	**5.17**
	edge of wheelpath	2.125	2.131	**2.128**		**77.54**	
3B	wheelpath	2.175	2.182	**2.179**	**3.37**	**71.62**	**10.10**
	edge of wheelpath	2.097	2.113	**2.105**		**79.67**	
4B	wheelpath	2.184	2.187	**2.186**	**4.35**	**78.08**	**13.08**
	edge of wheelpath	2.080	2.101	**2.091**		**89.83**	
5B	wheelpath	2.178	2.171	**2.175**	**4.02**	**80.95**	**18.06**
	edge of wheelpath	2.099	2.075	**2.087**		**98.79**	
1A	wheelpath	2.193	2.186	**2.190**	**3.47**	**89.90**	**6.98**
	edge of wheelpath	2.109	2.118	**2.114**		**96.65**	
2A	wheelpath	2.203	2.193	**2.198**	**3.18**	**92.01**	**3.16**
	edge of wheelpath	2.141	2.115	**2.128**		**95.01**	
3A	wheelpath	2.173	2.164	**2.169**	**3.30**	**78.59**	**10.35**
	edge of wheelpath	2.092	2.102	**2.097**		**87.66**	
4A	wheelpath	2.183	2.185	**2.184**	**4.72**	**83.20**	**12.67**
	edge of wheelpath	2.07	2.092	**2.081**		**95.27**	
5A	wheelpath	2.193	2.171	**2.182**	**3.71**	**90.83**	**12.09**
	edge of wheelpath	2.101	2.101	**2.101**		**103.32**	

that, except for Sections 2C and 2A (which had two layers of SBS-modified mixture), the percent difference in thickness was much greater than the percent difference in density. If the changes in density of the asphalt mixtures were due primarily to vertical densification, the percent increase in density should be approximately equal to the percent decrease in thickness. The greater difference in thickness as compared with the

difference in density indicate that materials might be shoved from the wheel path to the edge, giving the wheel-path cores a higher density which could not be accounted for by their reduction in thickness.

The bulk densities and air voids of these cores (which were obtained after HVS testing) were also compared with those of the cores obtained at the time of construction. Table 9.2 shows the comparison of the air voids of the cores at the time of construction with those of the cores after HVS testing. The change in percent air voids for each group was also computed and shown in Table 9.2. For all of the test sections, the cores from the wheel paths showed an increase in density (or a reduction in air voids). However, two different trends can be observed on the changes of density of the cores from the edge of wheel path. For the cores from the edges of wheel paths from the test sections with the SBS-modified mixture (2C, 3C, 2B, 3B) with the exception of Section 3A, there was generally a small increase in density (or a small reduction in air voids). Section 3A showed a small decrease in density (or a small increase in air voids).

For the cores from the edges of wheel paths from the sections with two lifts of unmodified mixture with the exception of Section 7C, there was generally decrease in density (or an increase in air voids). Section 7C, which was a trial test section, showed a slight increase in density (or slight decrease in air voids).

From the changes in thickness and density of the cores from these test sections, it can be inferred that, for pavements with the unmodified mixture, rutting was caused by a combination of densification and shoving. For the pavements with the SBS-modified mixture, rutting was due primarily to densification of the mixture. This explains why the SBS-modified mixture rutted less than the unmodified mixture though the SBS-modified

Table 9.2 Comparison of Air Voids of Cores before and after HVS Testing

Section	Sample	Gmb	Gmm	Average Air Voids	% Change in air voids
7AE	Original	2.109	2.264	6.8	
	Tested (edge of wheelpath)	2.093	2.264	7.6	**0.71**
	Tested (wheelpath)	2.146	2.264	5.2	**-1.63**
7AW	Original	2.109	2.264	6.8	
	Tested (edge of wheelpath)	2.055	2.264	9.2	**2.39**
	Tested (wheelpath)	2.123	2.264	6.2	**-0.62**
7BE	Original	2.114	2.264	6.6	
	Tested (edge of wheelpath)	2.091	2.264	7.6	**1.02**
	Tested (wheelpath)	2.131	2.264	5.9	**-0.75**
7BW	Original	2.114	2.264	6.6	
	Tested (edge of wheelpath)	2.088	2.264	7.8	**1.15**
	Tested (wheelpath)	2.123	2.264	6.2	**-0.40**
7C	Original	2.11	2.264	6.8	
	Tested (edge of wheelpath)	2.116	2.264	6.5	**-0.27**
	Tested (wheelpath)	2.171	2.264	4.1	**-2.69**
2C	Original	2.112	2.263	6.7	
	Tested (edge of wheelpath)	2.124	2.263	6.1	**-0.53**
	Tested (wheelpath)	2.181	2.263	3.6	**-3.05**
3C	Original	2.097	2.271	7.7	
	Tested (edge of wheelpath)	2.112	2.271	7.0	**-0.66**
	Tested (wheelpath)	2.134	2.271	6.0	**-1.63**
4C	Original	2.122	2.280	6.9	
	Tested (edge of wheelpath)	2.032	2.280	10.9	**3.95**
	Tested (wheelpath)	2.134	2.280	6.4	**-0.53**
5C	Original	2.118	2.276	7.0	
	Tested (edge of wheelpath)	2.084	2.276	8.4	**1.47**
	Tested (wheelpath)	2.155	2.276	5.3	**-1.65**
2B	Original	2.104	2.268	7.2	
	Tested (edge of wheelpath)	2.128	2.263	6.0	**-1.27**
	Tested (wheelpath)	2.187	2.263	3.4	**-3.87**
3B	Original	2.100	2.275	7.7	
	Tested (edge of wheelpath)	2.105	2.271	7.3	**-0.38**
	Tested (wheelpath)	2.179	2.271	4.1	**-3.64**
4B	Original	2.125	2.278	6.7	
	Tested (edge of wheelpath)	2.091	2.280	8.3	**1.57**
	Tested (wheelpath)	2.186	2.280	4.1	**-2.59**
5B	Original	2.121	2.277	6.9	
	Tested (edge of wheelpath)	2.087	2.276	8.3	**1.45**
	Tested (wheelpath)	2.175	2.276	4.4	**-2.41**
3A	Original	2.104	2.268	7.2	
	Tested (edge of wheelpath)	2.097	2.271	7.7	**0.43**
	Tested (wheelpath)	2.169	2.271	4.5	**-2.74**

mixture was densified by the same amount or even greater amount than the unmodified mixture.

9.3 Evaluation of Cores for Resilient Modulus and Indirect Tensile Strength

The cores obtained from the test sections contained two 2-inch layers of asphalt mixture, which were bonded together. Each core was cut into two slices by a mechanical saw at the interface between the two layers. In this report, the slice from the bottom layer is referred to as "Lift 1" and the slice from the top layer is referred to as "Lift 2". The sliced specimens were tested for resilient modulus at 5 and 25° C and indirect tensile strength at 25° C. The SHRP IDT test system as developed and improved by Roque et al. (1997) was used to measure the resilient modulus and indirect tensile strength of the specimens. The detailed description of specimen preparation, testing procedure and analysis procedure can be found in the report by Roque et al. (1997). It is to be pointed out that while the test system as recommended by Roque et al. called for at least three replicate specimens to be tested, only two replicate specimens were available to be tested in this laboratory study.

Table 9.3 shows the resilient modulus and indirect tensile strength at 25° C of the cored specimens from the test sections. The resilient modulus of the SBS-modified mixture appears to be not significantly different from that of the unmodified mixture. However, the resilient modulus of the specimens from the wheel path appears to be slightly higher than that of the specimens from the edge of the wheel path. For the specimens from the wheel path and lift 2 (top layer), the resilient modulus of the

Table 9.3 Resilient Modulus and Indirect Tensile Strength at 25° C of Cores from the Test Sections

Section	Location		Resilient Modulus		Tensile Strength	
			Gpa	Psi (10^6)	Mpa	Psi
7AW	**Lift 2**	Wheelpath	3.16	0.46	0.68	98.6
		Edge	2.84	0.41	0.67	97.1
	Lift 1	Wheelpath	3.40	0.49	0.75	108.7
		Edge	4.13	0.60	0.85	123.2
7AE	**Lift 2**	Wheelpath	3.08	0.45	0.82	118.8
		Edge	3.04	0.44	0.52	75.4
	Lift 1	Wheelpath	3.75	0.54	0.72	104.3
		Edge	3.33	0.48	0.75	108.7
7BW	**Lift 2**	Wheelpath	2.47	0.36	0.62	89.9
		Edge	2.34	0.34	0.52	75.4
	Lift 1	Wheelpath	2.93	0.42	0.68	98.6
		Edge	2.89	0.42	0.68	98.6
7BE	**Lift 2**	Wheelpath	2.91	0.42	0.60	87.0
		Edge	1.97	0.29	0.53	76.8
	Lift 1	Wheelpath	3.17	0.46	0.67	97.1
		Edge	2.88	0.42	0.68	98.6
7C	**Lift 2**	Wheelpath	3.59	0.52	0.78	113.0
		Edge	2.89	0.42	0.63	91.3
	Lift 1	Wheelpath	4.11	0.60	0.91	131.9
		Edge	3.97	0.58	0.89	129.0
2C	**Lift 2**	Wheelpath	4.27	0.62	0.91	131.9
		Edge	2.05	0.30	0.60	87.0
	Lift 1	Wheelpath	4.22	0.61	0.89	129.0
		Edge	3.90	0.57	0.86	124.6
3C	**Lift 2**	Wheelpath	3.12	0.45	0.57	82.6
		Edge	2.38	0.34	0.70	101.4
	Lift 1	Wheelpath	3.97	0.58	0.71	102.9
		Edge	3.81	0.55	0.72	104.3
4C	**Lift 2**	Wheelpath	3.28	0.48	0.76	110.1
		Edge	1.69	0.24	0.42	60.9
	Lift 1	Wheelpath	3.33	0.48	0.76	110.1
		Edge	2.34	0.34	0.64	92.8
5C	**Lift 2**	Wheelpath	4.38	0.63	0.77	111.6
		Edge	2.75	0.40	0.55	79.7
	Lift 1	Wheelpath	3.63	0.53	0.82	118.8
		Edge	2.50	0.36	0.66	95.7
2B	**Lift 2**	Wheelpath	4.92	0.71	0.93	134.8
		Edge	2.76	0.40	0.73	105.8
	Lift 1	Wheelpath	5.57	0.81	1.04	150.7
		Edge	3.58	0.52	1.00	144.9

Table 9.3 Resilient Modulus and Indirect Tensile Strength at 25° C of Cores from the Test Sections (continued)

Section	Location		Resilient Modulus		Tensile Strength	
			Gpa	Psi (10^6)	Mpa	Psi
3B	Lift 2	Wheelpath	4.88	0.71	0.91	131.9
		Edge	2.85	0.41	0.78	113.0
	Lift 1	Wheelpath	5.65	0.82	1.05	152.2
		Edge	4.10	0.59	0.83	120.3
4B	Lift 2	Wheelpath	4.97	0.72	0.92	133.3
		Edge	2.59	0.38	0.66	95.7
	Lift 1	Wheelpath	5.60	0.81	1.01	146.4
		Edge	3.59	0.52	0.77	111.6
5B	Lift 2	Wheelpath	4.11	0.60	0.88	127.5
		Edge	2.41	0.35	0.60	87.0
	Lift 1	Wheelpath	5.55	0.80	1.01	146.4
		Edge	4.02	0.58	0.91	131.9
3A	Lift 2	Wheelpath	4.25	0.62	0.81	117.4
		Edge	2.51	0.36	0.61	88.4
	Lift 1	Wheelpath	4.91	0.71	0.87	126.1
		Edge	3.46	0.50	0.66	95.7

unmodified mixture varied from 0.36 to 0.72×10^6 psi with an average of 0.49×10^6 psi, while that of the SBS-modified mixture varied from 0.45 to 0.71×10^6 psi with an average of 0.62×10^6 psi. For the specimens from the edge of the wheel path and lift 2, the resilient modulus of the unmodified mixture varied from 0.24 to 0.44×10^6 psi with an average of 0.36×10^6 psi, while that of the SBS-modified mixture varied from 0.30 to 0.41×10^6 psi with an average of 0.36×10^6 psi.

The resilient modulus of the samples from lift 1 appears to be slightly higher than that from lift 2. For the samples from the wheel path, the resilient modulus of the samples from lift 2 varied from 0.36 to 0.72×10^6 psi with an average of 0.54×10^6 psi, while that of the samples from lift 1 varied from 0.42 to 0.82×10^6 psi with an average of 0.62×10^6 psi.

The indirect tensile strength of the SBS-modified mixture appears to be slightly higher than that of the unmodified mixture. The indirect tensile strength of the specimens from the wheel path appears to be slightly higher than that of the specimens from the edge of the wheel path. For the specimens from the wheel path and lift 2, the indirect tensile strength of the unmodified mixture varied from 87 to 133.3 psi with an average of 110.5 psi, while that of the modified mixture varied from 82.6 to 134.8 psi with an average of 119.7 psi.

For the specimens from the edge of the wheel path and lift 2, the indirect tensile strength of the unmodified mixture varied from 60.9 to 97.1 psi with an average of 82.1 psi, while that of the modified mixture varied from 87.0 to 113 psi with an average of 95.4 psi.

The indirect tensile of the samples from lift 1 appears to be slightly higher than that of the samples from lift 2. For the samples from the wheel path, the indirect tensile strength of the samples from lift 2 varied from 82.6 to 134.8 psi with an average of 113.8 psi, while that of the samples from lift 1 varied from 97.1 to 152.2 psi with an average of 123.1 psi.

Resilient modulus test at 5° C was performed only on the cores from Lane 7. The results are shown in Table 9.4. The resilient modulus of the specimens from the wheel path appears to be slightly higher than that of the specimens from the edge of the wheel path. The resilient modulus of the specimens from the wheel path and lift 2 (top layer) varied from 1.27 to 1.73×10^6 psi with an average of 1.52×10^6 psi, while that of specimens from the edge of wheel path varied from 1.35 to 1.54×10^6 psi with an average of 1.42×10^6 psi.

Table 9.4 Resilient Modulus at 5° C of Cores from the Test Sections on Lane 7

Section	Location		Resilient Modulus	
			Gpa	Psi (10^6)
7AW	Lift 2	Wheelpath	8.76	1.27
		Edge	9.62	1.39
	Lift 1	Wheelpath	8.79	1.27
		Edge	11.15	1.62
7AE	Lift 2	Wheelpath	10.51	1.52
		Edge	9.84	1.43
	Lift 1	Wheelpath	10.59	1.53
		Edge	10.22	1.48
7BW	Lift 2	Wheelpath	10.47	1.52
		Edge	10.61	1.54
	Lift 1	Wheelpath	10.69	1.55
		Edge	9.73	1.41
7BE	Lift 2	Wheelpath	10.64	1.54
		Edge	9.48	1.37
	Lift 1	Wheelpath	12.55	1.82
		Edge	11.25	1.63
7C	Lift 2	Wheelpath	11.92	1.73
		Edge	9.34	1.35
	Lift 1	Wheelpath	13.61	1.97
		Edge	11.15	1.62

The resilient modulus of the samples from lift 1 appears to be slightly higher than that from lift 2. For the samples from the wheel path, the resilient modulus of the samples from lift 2 varied from 1.27 to 1.73×10^6 psi with an average of 1.47×10^6 psi, while that of the samples from lift 1 varied from 1.27 to 1.97×10^6 psi with an average of 1.59×10^6 psi.

9.4 Evaluation of Cores for Viscosity Test

Asphalt binder was extracted and recovered from the mixtures to evaluate the binder viscosity. The Reflux Asphalt Extraction procedure in accordance with ASTM D 2171-95 standard test method was used to extract the asphalt binder from the cores. The

asphalt binders were then recovered from the solvent using Trichloroethylene (TCE) in accordance with ASTM D 5404-97 standard test method. The Brookfield viscosity test was performed on the recovered binders at 60° C. The standard testing procedure for the Brookfield viscosity test is described in ASTM D 4402-95. Three replicate tests were run per sample.

Table 9.5 shows the viscosity of the recovered binders from the cored samples. The viscosity of the recovered binders from the SBS-modified mixture are about two to three times) higher than that from unmodified mixture. For the SBS-modified mixtures, the viscosity of the recovered binders from the wheel path appears to be slightly higher than that of the binders from the edge of the wheel path. The viscosity of the recovered binders from the wheel path varied from 33,344 to 52,202 poises with an average of 40,589 poises, while that of the binders from the edge of wheel path varied from 25,514 to 45,510 poises with an average of 36,238 poises.

However, for the unmodified mixtures, the viscosity of the recovered binders from the edge of the wheel path appears to be slightly higher than that of the binders from the wheel path. The viscosity of the recovered binders from the wheel path varied from 12,547 to 17,955 poises with an average of 15,544 poises, while that of binders from the edge of wheel path varied from 12,759 to 16,316 poises with an average of 14,577 poises.

For the unmodified mixture, the viscosity of the recovered binders from lift 2 (top layer) appeared to be about the same as that from lift 1 (bottom layer). The average viscosity of the unmodified binders from lift 1 was 15,016 poises, while the average viscosity of the unmodified binders from lift 2 was 15,104 poises. For the modified mixtures, the viscosity of the recovered binders from lift 2 was higher than that from

Table 9.5 Viscosity of Cores from the Test Sections

Section	Location		Viscosity
			Poise
2C	**Lift 1**	Wheelpath	33344
		Edge	25514
	Lift 2	Wheelpath	45468
		Edge	45510
3C	**Lift 1**	Wheelpath	16438
		Edge	14965
	Lift 2	Wheelpath	34554
		Edge	39265
4C	**Lift 1**	Wheelpath	14576
		Edge	12759
	Lift 2	Wheelpath	17282
		Edge	13761
5C	**Lift 1**	Wheelpath	15303
		Edge	14844
	Lift 2	Wheelpath	17517
		Edge	16316
2B	**Lift 1**	Wheelpath	43716
		Edge	30897
	Lift 2	Wheelpath	52202
		Edge	43032
3B	**Lift 1**	Wheelpath	17955
		Edge	13288
	Lift 2	Wheelpath	34247
		Edge	29604
4B	**Lift 2**	Wheelpath	12547
		Edge	15991
5B	**Lift 2**	Wheelpath	12733
		Edge	14690

lift 1. The average viscosity of the modified binders from lift 1 was 33,368 poises, while that from lift 2 was 40,485 poises.

9.5 Summary of Findings

The following are the main findings from the results of evaluation of cored samples from the test sections:

1. From the density and thickness of cores from the test sections, rutting of the pavement sections with the unmodified asphalt mixture appeared to be due to a combination of densification and shear movement, while rutting of the pavement sections with the SBS-modified mixture appeared to be due primarily to densification.
2. The resilient modulus at 25° C of the SBS-modified mixture was not significantly different from that of the unmodified mixture.
3. The average indirect tensile strength at 25° C of the SBS-modified mixture was higher than that of the unmodified mixture by about 10%.
4. The viscosity at 60° C of the recovered binders from the SBS-modified mixture was two to three times that of the recovered binders from the unmodified mixture.

CHAPTER 10
SUMMARY OF FINDINGS

A research study was conducted to evaluate the rutting performance of a Superpave mixture and a SBS-modified Superpave mixture using a Heavy Vehicle Simulator (HVS) at FDOT's Accelerated Pavement Testing Facility. Before the main field testing program was conducted, trial tests were performed to evaluate the operating characteristics of the HVS and to determine an appropriate HVS testing configuration to be used for the main testing program. A laboratory testing program was also conducted on samples of asphalt mixtures collected from the plant during construction of the test pavements, and cored samples from the test sections after HVS testing, in order to determine the possible relationship between the mixture properties and their rutting performance.

Results from the HVS tests showed that the pavement sections with two lifts of SBS-modified mixture clearly outperformed those with two lifts of unmodified mixture, which had two to two and a half times the rut rate. The pavement sections with a lift of SBS-modified mixture over a lift of unmodified mixture had practically about the same rut rate as those with two lifts of modified mixture when tested at 50° C. The test sections with two lifts of SBS-modified mixture and tested at 65° C still outperformed the pavement sections with two lifts of unmodified mixture and tested at 50° C.

Results from the laboratory testing program showed that a mixture with a higher rut depth in the APA will be likely to rut more in the actual pavement. A mixture with a GSI of more than 1.0 as measured by the GTM will be likely to rut more than one with a GSI close to 1.0.

From the observation of the changes in thickness and density of the cores from these test sections, it can be inferred that, for the pavements with the unmodified mixture, rutting was caused by a combination of densification and shoving. For the pavements with the SBS-modified mixture, rutting was due primarily to densification of the mixture. The resilient modulus at 25° C of the SBS-modified mixture was not significantly different from that of the unmodified mixture. The average indirect tensile strength at 25° C of the SBS-modified mixture was only slightly higher than that of the unmodified mixture (by about 10%). The viscosity at 60° C of the recovered binders from the SBS-modified mixture was two to three times that of the recovered binders from the unmodified mixture. The higher viscosity of the SBS-modified binder was one of the main reasons for the higher rutting resistance of the SBS-modified mixture.

LIST OF REFERENCES

Asphalt Institute, *Superpave Level 1 Mix Design*, Superpave Series No.2 (SP-2), Lexington, Kentucky, 1994.

Bonaquist, R., Sherwood, J., and Stuart, K., "Accelerated Pavement Testing at the Federal Highway Administration Pavement Testing Facility," *Journal of Association of Asphalt Pavement Technologists*, Vol. 67, 1998.

Carpenter, S.H., "Permanent Deformation: Field Evaluation," *Transportation Research Record 1417*, Transportation Research Board (TRB), National Research Council (NRC), Washington, D.C., 1993, pp 135-143.

Coetzee, N., Harvey, J.T., Nokes, W.A., Rust, F.C., Stolarski, P.J., "Establishing the California Department of Transportation Accelerated Pavement Testing Program," *Transportation Research Record 1540*, TRB, NRC, Washington, D.C., 1996, pp 92-96.

Coetzee, N., Nokes, F., Monismith, W., Metcalf, J.B., Mahoney, J., "Full-Scale/ Accelerated Pavement Testing: Current Status and Future Directions," *Transportation in the New Millennium*, TRB, NRC, Washington, D.C., 2000, pp. 4.

Coetzee, N., Harvey, J.T., Monismith, C.L., "(CAL/APT) Program Summary Report," Institute of Transportation Studies, University of California, Berkeley, June 2000.

Dynatest International, *Technical Specification for Heavy Vehicle Simulator (HVS Mark IV)*, HVS Technical Manual, South Africa.

Franklin Associates, Ltd., Hershey, R.L., "Markets for Scrap Tires," *Report EPA/530-SW-90-074A*, Office of Solid Waste, Environmental Protection Agency, October 1991.

Gisi, A.J., Hossain, M., Wu, Z., "Performance of Superpave Mixtures Under Accelerated Load Testing," *Transportation Research Record 1325*, TRB, NRC, Washington, D.C., 2000, pp 126-134.

Gramling, W.L., Hunt, J.E., Suzuki, G.S., "Rational Approach to Cross-Profile and Rut Depth Analysis," *Transportation Research Record 1311*, TRB, NRC, Washington, D.C., 1991, pp 173-179.

Heitzman, M., "Design and Construction of Asphalt Paving Materials with Crumb Rubber Modifier," *Transportation Research Record 1339*, TRB, NRC, Washington, D.C., 1992, pp 1-8.

Hoot, S., "Ohio State helps open nation's only indoor pavement test facility," *News in Engineering*, The Ohio State College of Engineering, Vol. 69, No. 5, September 1997.

Huang, Y.H., *Pavement Analysis and Design*, Prentice-Hall, Eaglewood Cliffs, New Jersey, 1993.

Hugo, F., McCullough, F., van der Walt, B., "Full-Scale Accelerated Pavement Testing for Texas State Department of Highways and Public Transportation," *Transportation Research Record 1293*, TRB, NRC, Washington, D.C., 1991, pp. 52-60.

Kluttz, Q., "SBS polymers affect mix characteristics," *Asphalt Contractor Magazine*, Independence, Missouri, October 1999.

McNamara, W.M., Sebaaly, P.E., Epps, J.A., Weitzel, D., "Evaluation of Superpave Mixtures in Nevada," *Journal of Association of Asphalt Pavement Technologists*, Vol. 69, 2000.

Metcalf, J.B., "The Development of Proposals for an Australian Full-Scale Accelerated Loading Pavement Testing Facility," Institute fur Strassen-, Eissenbahn-und Felsbau an der Eidgenossischen Technischen Hochschule, Zurich, Switzerland, 1982, pp. 35-53.

Metcalf, J.B., "Application of Full-Scale Accelerated Pavement Testing," *NCHRP Synthesis of Highway Practice 235*, TRB, NRC, Washington, D.C., 1996, pp. 116.

Metcalf, J.B., "Accelerated Pavement Testing, a Brief Review Directed Towards Asphalt Interests," *Journal of Association of Asphalt Pavement Technologists*, Vol. 67, 1998.

Metcalf, J.B., Li, Y., Rasoulian, M., Romanoschi, S.A., "Assessment of Pavement Life at First Full-Scale Accelerated Pavement Test in Louisiana," *Transportation Research Record 1655*, TRB, NRC, Washington, D.C., 1999, pp 219-226.

Musselman, J.A., Choubane. B, Page. G.C., Upshaw. P.B., "Superpave Field Implementation," *Transportation Research Record 1609*, TRB, NRC, Washington, D.C., 1998, pp. 51-60.

Othman, A., Figueroa, L., Aglan, H., "Fatigue Behavior of Styrene-Butadiene-Styrene Modifier Asphaltic Mixtures Exposed to Low-Temperature Cyclic Aging," *Transportation Research Record 1492*, TRB, NRC, Washington. D.C., 1995, pp. 129-134.

Pidwerbesky, B.D., "Accelerated Dynamic Loading of Flexible Pavements at the Canterbury Accelerated Pavement Testing Indoor Facility," *Transportation Research Record 1482*, TRB, NRC, Washington, D.C., 1995, pp. 79-86.

Solaimanian, M., T.W. Kennedy, R. Tripathi, "Performance Characteristics of Asphalt Binders and Mixtures Modified by Waste Toner," *Transportation Research Record 1638*, TRB, NRC, Washington, D.C., 1998, pp 120-128.

Terrel, R.L., "Asphalt Modifiers," *A User Manual for Additives and Modifiers in Hot Mix Asphalt*, National Asphalt Pavement Association, Lanham, Maryland.

Texas Transportation Institute, *AASHTO Innovative Highway Technologies*, College Station, Texas, 1998.

White, T.D., Albers, J.M., Haddock, J.E., "Limiting Design Parameters for Accelerated Pavement Testing System," *Journal of Transportation Engineering*, Vol. 118, 1992.

Witczak, M.W., Hafez, I., Qi, X., "Laboratory Characterization of *Elvaloy*® Modified Asphalt Mixtures," *Technical Report*, Vol. 1, University of Maryland, College Park, Maryland, June 1995.

APPENDIX A
SUPERPAVE MIX DESIGN

Table A.1 Summary of Aggregate Blending for Superpave Mix Design

Blend		12%	25%	48%	15%	Job Mix Formula	Control Points	Restricted Zone
Sieve Size		S-1-A Stone	S-1-B Stone	Screenings	Local Sand			
3/4"	19.0 mm	99	100	100	100	100	100	
1/2"	12.5mm	45	100	100	100	93	(90 - 100)	
3/8"	9.5mm	13	99	100	100	89	-90	
No. 4	4.75mm	5	49	90	100	71		
No. 8	2.36mm	4	10	72	100	53	(28 - 58)	39.1 - 39.1
No. 16	1.18mm	4	4	54	100	42		25.6 - 31.6
No. 30	0.600mm	4	3	41	96	35		19.1 - 23.1
No. 50	0.300mm	4	3	28	52	22		
No. 100	0.150mm	3	2	14	10	9		
No. 200	0.075mm	2.7	1.9	5.9	2.2	4.5	(2 - 10)	
G_{sb}		2.327	2.337	2.299	2.546	2.346		

Table A.2 Mix Design Data for the Unmodified Superpave Mix

P_b	G_{mb} @ N_{des}	Gmm	V_a	VMA	VFA	P_{be}	$P_{0.075}$ / P_{be}	$\%G_{mm}$ @ N_{ini}	$\%G_{mm}$ @ N_{design}	$\%G_{mm}$ @ N_{max}
7.2	2.159	2.306	6.4	14.6	56	3.94	1.1	86.7	93.6	94.7
7.7	2.168	2.281	5.0	14.7	66	4.66	1.0	88.1	95.0	96.3
8.2	2.185	2.276	4.0	14.5	72	4.97	0.9	88.8	96.0	97.0
8.7	2.193	2.232	1.7	14.7	88	6.09	0.7	91.0	98.3	99.5

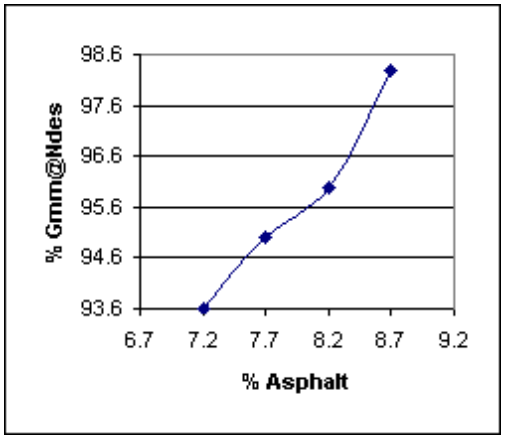

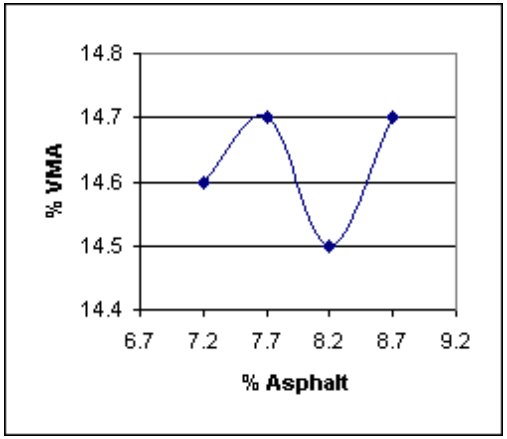

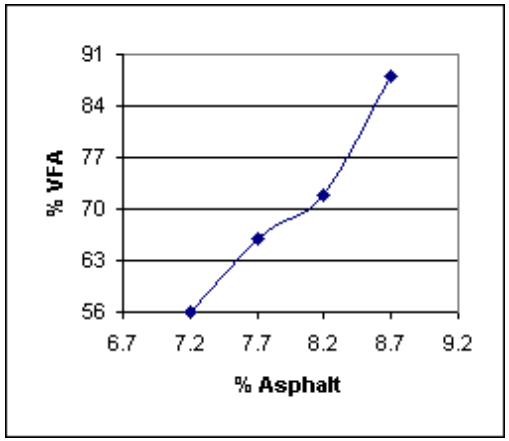

Optimum Asphalt Content	8.20%
Lab Density	136.3 lbs/ft%
	=2185 kg/m^3
VMA	14.50%

FAA	47.00%
%Gmm @ Ndes	96.00%
NCAT Oven Calibration Factor	-0.07%
Mixing Temperature	300°F = 149°C

Table A.3 Mix Design Data for the SBS-Modified Superpave Mix

P_b	G_{mb} @ N_{des}	Gmm	V_a	VMA	VFA	P_{be}	$P_{0.075}$ / P_{be}	$\%G_{mm}$ @ N_{ini}	$\%G_{mm}$ @ N_{design}	$\%G_{mm}$ @ N_{max}
7	2.163	2.300	6.0	14.3	58	3.97	1.1	87.1	94.0	94.7
7.5	2.177	2.285	4.7	14.2	67	4.48	1.0	88.1	95.3	95.8
7.9	2.186	2.273	3.8	14.2	73	4.90	0.9	89.1	96.2	96.7
8	2.185	2.268	3.7	14.3	74	5.04	0.9	89.3	96.3	96.8
8.5	2.195	2.253	2.6	14.4	82	5.56	0.8	90.4	97.4	98.2

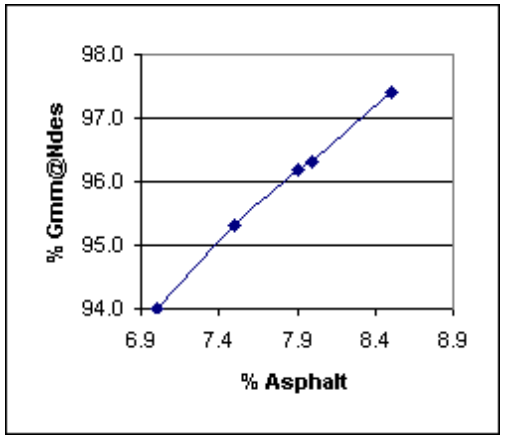

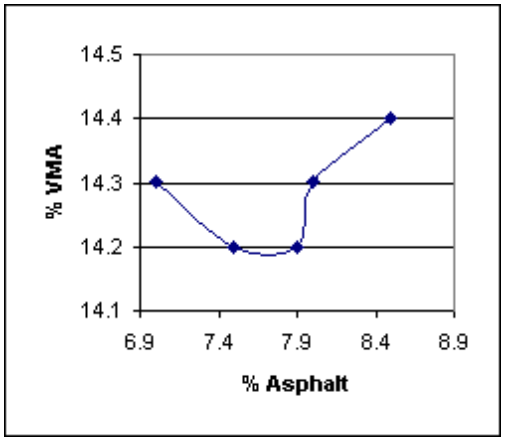

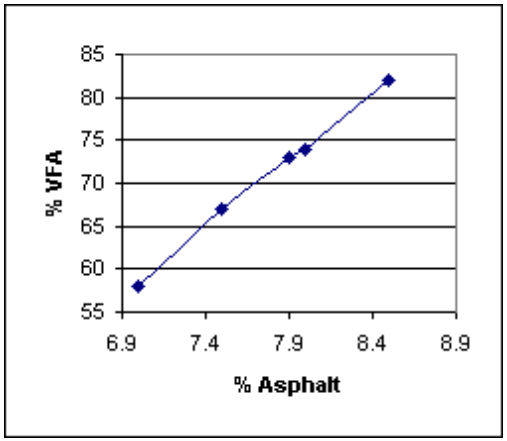

Optimum Asphalt Content	7.90%
Lab Density	136.40%
	=2186 kg/m^3
VMA	14.20%

FAA	47%
%Gmm @ Ndes	96.2%
NCAT Oven Calibration Factor	-6.00%
Mixing Temperature	340°F = 171°C
Compaction Temperature	325°F = 163°C

APPENDIX B
NUCLEAR DENSITY DATA

Table B.1 Nuclear Density Data for Lane 1-Lift 1

	Density (lb/cf)				
Location	1	2	3	4	Average
1	131.7	129.3	131.3	130.2	130.6
2					
3	128.8	129.1	129.4	131.1	129.6
4	129.7	133.4	131.7	131.1	131.5
5	130.2	132.1	130.2	130.3	130.7
6					
7	130.9	131.2	132.8	132.8	131.9
8	131.0	131.4	132.7	132.2	131.8
9	136.8	135.0	134.8	136.3	135.7
10	132.5	132.3	131.6	132.0	132.1
11	134.2	133.0	133.2	133.3	133.4
12					
13	131.7	131.7	130.8	131.3	131.4
14	130.2	129.7	129.3	130.8	130.0
15	130.7	128.8	129.0	129.5	129.5
16					
17	130.6	131.0	130.1	130.7	130.6

Table B.2 Nuclear Density Data for Lane 1-Lift 2

	Density (lb/cf)				
Location	1	2	3	4	Average
1					
2	129.1	128.9	129.6	128.6	129.1
3	129.3	130.1	129.6	130.6	129.9
4	129.6	129.7	131.1	130.9	130.3
5	131.3	130.2	128.8	130.5	130.2
6	135.5	133.5	132.9	135.1	134.3
7					
8	135.1	133.7	132.2	134.5	133.9
9	131.9	131.3	130.2	131.9	131.3
10	132.7	131.8	130.7	131.7	131.7
11					
12	134.3	135.0	134.8	132.0	134.0
13	129.6	130.5	130.3	131.4	130.5
14	131.9	129.4	129.8	130.4	130.4
15	131.6	131.7	127.7	131.9	130.7
16	128.2	131.3	132.6	130.6	130.7

Table B.3 Nuclear Density Data for Lane 2-Lift1

	Density (lb/cf)				
Location	1	2	3	4	Average
1	130.1	128.8	131.2	132.8	130.7
2					
3	130.2	131.2	132.4	132.2	131.5
4	129.2	128.5	130.8	131.4	130.0
5	132.5	129.7	132.6	133.2	132.0
6					
7	126.7	126.7	126.4	129.0	127.2
8	132.9	134.5	132.2	129.5	132.3
9	129.8	129.8	130.4	127.9	129.5
10	132.3	132.4	133.0	130.9	132.2
11	129.9	129.8	131.4	131.5	130.7
12					
13	135.3	132.2	134.4	133.2	133.8
14	133.8	134.2	135.2	133.7	134.2
15	132.6	131.5	132.2	132.9	132.3

Table B.4 Nuclear Density Data for Lane 2-Lift 2

	Density (lb/cf)				
Location	1	2	3	4	Average
1	128.6	128.2	128.4	130.0	128.8
2	132.1	131.9	132.9	131.2	132.0
3	131.1	132.0	133.2	132.4	132.2
4	132.3	132.1	133.4	132.4	132.6
5	131.8	130.5	130.5	131.5	131.1
6					
7	130.1	130.8	130.7	131.0	130.7
8	130.7	132.6	130.8	130.2	131.1
9	133.8	132.9	132.6	133.1	133.1
10					
11	130.0	129.7	130.4	131.4	130.4
12	132.0	130.7	132.1	130.6	131.4
13	132.6	131.0	132.0	130.3	131.5
14	132.1	130.8	133.1	131.5	131.9
15	130.2	130.7	130.0	129.8	130.2

Table B.5 Nuclear Density Data for Lane 3-Lift 1

	Density (lb/cf)				
Location	1	2	3	4	Average
1	127.6	127.6	129.5	127.7	128.1
2					
3	129.8	130.0	128.8	131.4	130.0
4	130.5	131.5	130.0	131.3	130.8
5	129.8	130.7	128.5	129.9	129.7
6					
7	126.2	126.7	128.1	128.1	127.3
8	133.9	133.9	132.4	136.1	134.1
9	130.8	132.0	131.3	132.7	131.7
10	130.8	132.2	132.0	133.8	132.2
11	133.2	132.7	132.4	131.3	132.4
12					
13	130.3	130.9	132.6	132.1	131.5
14	129.5	130.7	130.4	131.6	130.6
15	130.5	129.8	130.8	131.8	130.7
16					
17	129.0	129.6	127.6	127.8	128.5

Table B.6 Nuclear Density Data for Lane 3-Lift 2

	Density (lb/cf)				
Location	1	2	3	4	Average
1					
2	129.2	129.6	131.0	130.7	130.1
3	129.5	130.8	130.4	131.2	130.5
4	132.0	130.1	130.2	131.5	131.0
5	132.4	131.3	129.9	130.0	130.9
6	132.5	132.4	132.0	132.3	132.3
7					
8	133.6	133.1	131.2	132.2	132.5
9	131.3	131.1	131.3	132.2	131.5
10	133.1	132.2	129.5	134.4	132.3
11					
12	128.5	128.6	127.7	128.7	128.4
13	131.9	129.4	128.9	129.6	130.0
14	131.6	131.1	129.9	130.7	130.8
15	136.7	136.2	135.7	136.6	136.3
16	130.1	130.3	131.5	130.5	130.6

Table B.7 Nuclear Density Data for Lane 4-Lift 1

	Density (lb/cf)				
Location	1	2	3	4	Average
1	133.7	129.7	138.6	131.3	133.3
2					
3	130.0	129.0	128.6	130.6	129.6
4	131.3	132.5	131.8	130.9	131.6
5	129.0	129.3	130.0	128.3	129.2
6					
7	127.9	127.2	128.1	127.6	127.7
8	132.5	132.4	133.7	132.3	132.7
9	131.2	130.8	131.7	133.4	131.8
10	132.6	130.7	130.0	132.8	131.5
11	129.9	130.8	130.3	130.2	130.3
12					
13	132.3	133.3	132.2	131.8	132.4
14	129.1	129.1	129.0	130.8	129.5
15	130.0	130.7	131.3	131.3	130.8
16					
17	127.0	125.9	127.2	129.1	127.3

Table B.8 Nuclear Density Data for Lane 4-Lift 2

	Density (lb/cf)				
Location	1	2	3	4	Average
1					
2	131.5	130.6	131.3	130.9	131.1
3	132.1	133.3	130.9	132.3	132.2
4	131.4	133.3	132.7	131.9	132.3
5	130.4	131.5	131.4	132.0	131.3
6	131.5	131.2	131.0	131.5	131.3
7					
8	131.2	130.4	132.1	131.9	131.4
9	131.8	131.7	133.1	132.6	132.3
10	130.8	132.0	132.9	132.8	132.1
11					
12	130.7	132.0	130.8	132.0	131.4
13	131.1	132.9	132.3	131.3	131.9
14	131.5	130.6	131.8	132.3	131.6
15	132.0	131.0	131.0	131.8	131.5
16	133.4	132.2	131.8	132.3	132.4

Table B.9 Nuclear Density Data for Lane 5-Lift 1

	Density (lb/cf)				
Location	1	2	3	4	Average
1	130.3	130.3	132.5	131.6	131.2
2					
3	128.6	129.6	129.3	129.5	129.3
4	129.2	130.4	130.3	129.7	129.9
5	130.8	130.7	130.5	129.2	130.3
6					
7	132.5	132.4	132.1	133.2	132.6
8	131.0	132.8	132.8	133.0	132.4
9	131.4	131.5	131.6	130.9	131.4
10	132.3	131.8	130.6	132.4	131.8
11	134.2	134.2	133.8	135.0	134.3
12					
13	132.0	130.7	131.8	131.5	131.5
14	134.7	134.5	133.3	135.1	134.4
15	132.4	132.0	132.3	132.0	132.2
16					
17	131.0	131.0	130.1	130.6	130.7

Table B.10 Nuclear Density Data for Lane 5-Lift 2

	Density (lb/cf)				
Location	1	2	3	4	Average
1					
2	130.3	130.0	130.4	130.0	130.2
3	131.6	132.0	132.4	132.1	132.0
4	132.5	132.6	131.8	132.7	132.4
5	131.0	130.5	133.3	132.0	131.7
6	131.0	130.9	131.5	130.9	131.1
7					
8	129.3	131.5	131.9	131.4	131.0
9	132.2	131.8	131.5	130.9	131.6
10	132.6	132.4	131.0	132.0	132.0
11					
12	130.5	129.2	130.0	129.5	129.8
13	129.8	130.0	130.5	128.9	129.8
14	130.9	131.5	131.5	131.4	131.3
15	131.3	130.5	130.1	132.4	131.1
16	129.0	131.1	132.3	132.4	131.2

Table B.11 Nuclear Density Data for Lane 6-Lift 1

	Density (lb/cf)				
Location	1	2	3	4	Average
1	128.9	131.4	130.2	130.4	130.2
2					
3	133.7	132.4	131.7	132.9	132.7
4	132.8	132.7	134.6	134.2	133.6
5	129.6	133.4	133.5	133.5	132.5
6					
7	132.0	141.8	133.1	131.8	134.7
8	133.2	133.6	134.1	132.1	133.3
9	135.1	132.7	134.1	135.0	134.2
10	133.0	132.6	132.1	133.0	132.7
11	133.2	131.6	132.6	132.5	132.5
12					
13	132.7	134.8	134.8	132.6	133.7
14	134.0	134.6	136.8	134.0	134.9
15	133.6	133.9	133.5	132.9	133.5
16					
17	135.3	137.0	141.9	141.0	138.8

Table B.12 Nuclear Density Data for Lane 6-Lift 2

	Density (lb/cf)				
Location	1	2	3	4	Average
1					
2	128.6	127.9	128.9	129.1	128.6
3	131.3	128.7	128.8	130.1	129.7
4	132.0	132.8	131.7	131.3	132.0
5	132.8	132.2	133.6	133.9	133.1
6	132.0	132.0	131.6	132.1	131.9
7					
8	132.8	132.6	132.2	131.7	132.3
9	129.7	130.0	130.2	129.3	129.8
10	131.7	130.8	132.6	132.2	131.8
11					
12	131.2	133.4	130.8	132.4	132.0
13	131.9	131.7	130.9	132.8	131.8
14	130.9	132.2	131.9	131.7	131.7
15	129.8	131.0	129.5	131.7	130.5
16	131.1	132.6	132.5	131.6	132.0

Table B.13 Nuclear Density Data for Lane 7-Lift 1

	Density (lb/cf)				
Location	1	2	3	4	Average
1	135.4	134.1	133.9	134.8	134.6
2					
3	131.9	133.6	132.9	131.9	132.6
4	133.5	134.3	132.7	132.4	133.2
5	134.6	133.7	134.3	134.6	134.3
6					
7	136.5	134.7	135.5	135.3	135.5
8	134.9	134.5	135.0	135.5	135.0
9	136.2	135.9	135.5	135.6	135.8
10	134.2	134.3	134.3	133.9	134.2
11	137.0	136.3	136.5	138.0	137.0
12					
13	135.6	136.5	134.5	136.1	135.7
14	136.6	134.3	133.0	135.3	134.8
15	132.3	134.7	133.6	133.3	133.5
16					
17	134.7	133.8	131.9	134.0	133.6

Table B.14 Nuclear Density Data for Lane 7-Lift 2

	Density (lb/cf)				
Location	1	2	3	4	Average
1					
2	131.7	130.8	131.1	130.3	131.0
3	128.3	128.6	128.6	128.7	128.6
4	130.2	128.1	128.2	129.2	128.9
5	131.0	130.0	131.3	129.9	130.6
6	130.0	129.6	131.2	130.8	130.4
7					
8	131.5	131.7	131.8	131.5	131.6
9	129.4	129.4	131.4	131.0	130.3
10	130.8	130.6	130.5	130.7	130.7
11					
12	131.5	130.2	129.1	130.1	130.2
13	127.8	128.5	130.7	130.3	129.3
14	131.3	129.7	128.4	131.4	130.2
15	131.5	130.8	130.9	130.5	130.9
16	133.9	132.7	133.8	131.9	133.1

APPENDIX C
THICKNESS PROFILES OF CORES FROM TEST SECTIONS

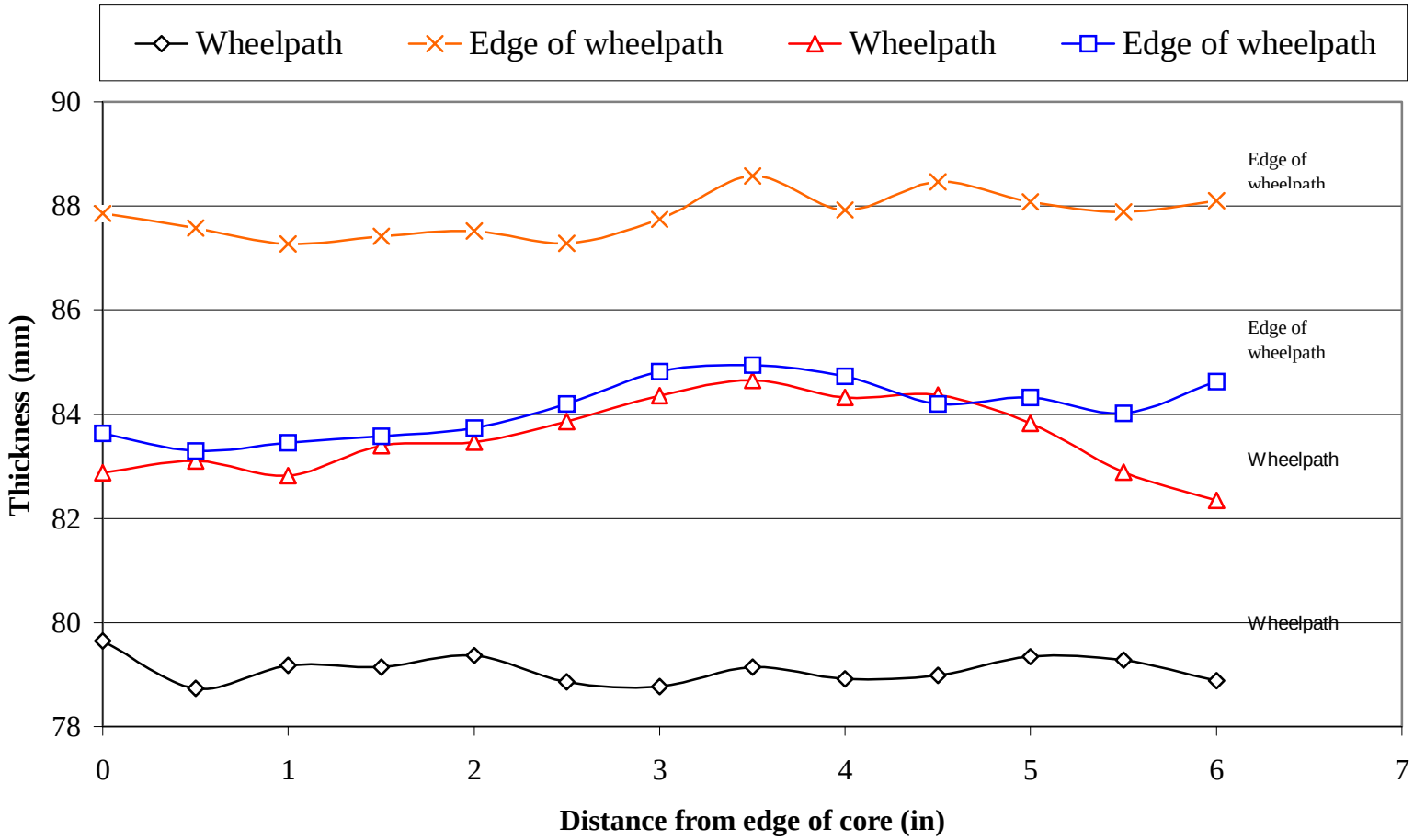

Figure C.1 Thickness Profiles of Cores from Section 7AE (Uni-Directional with 4" Wander in 2" Increments)

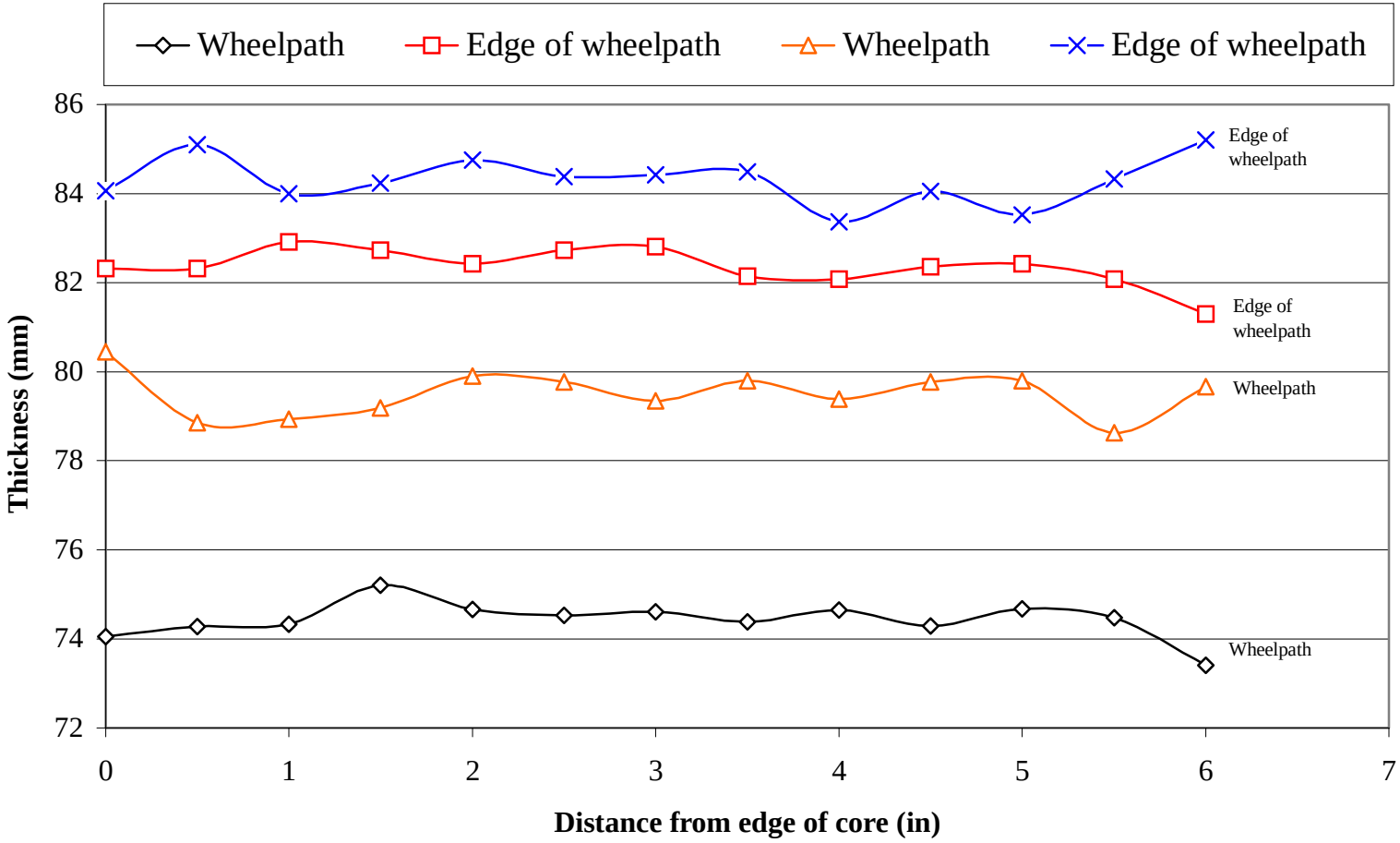

Figure C.2 Thickness Profiles of Cores from Section 7AW (Uni-Directional with 4" Wander in 1" Increments)

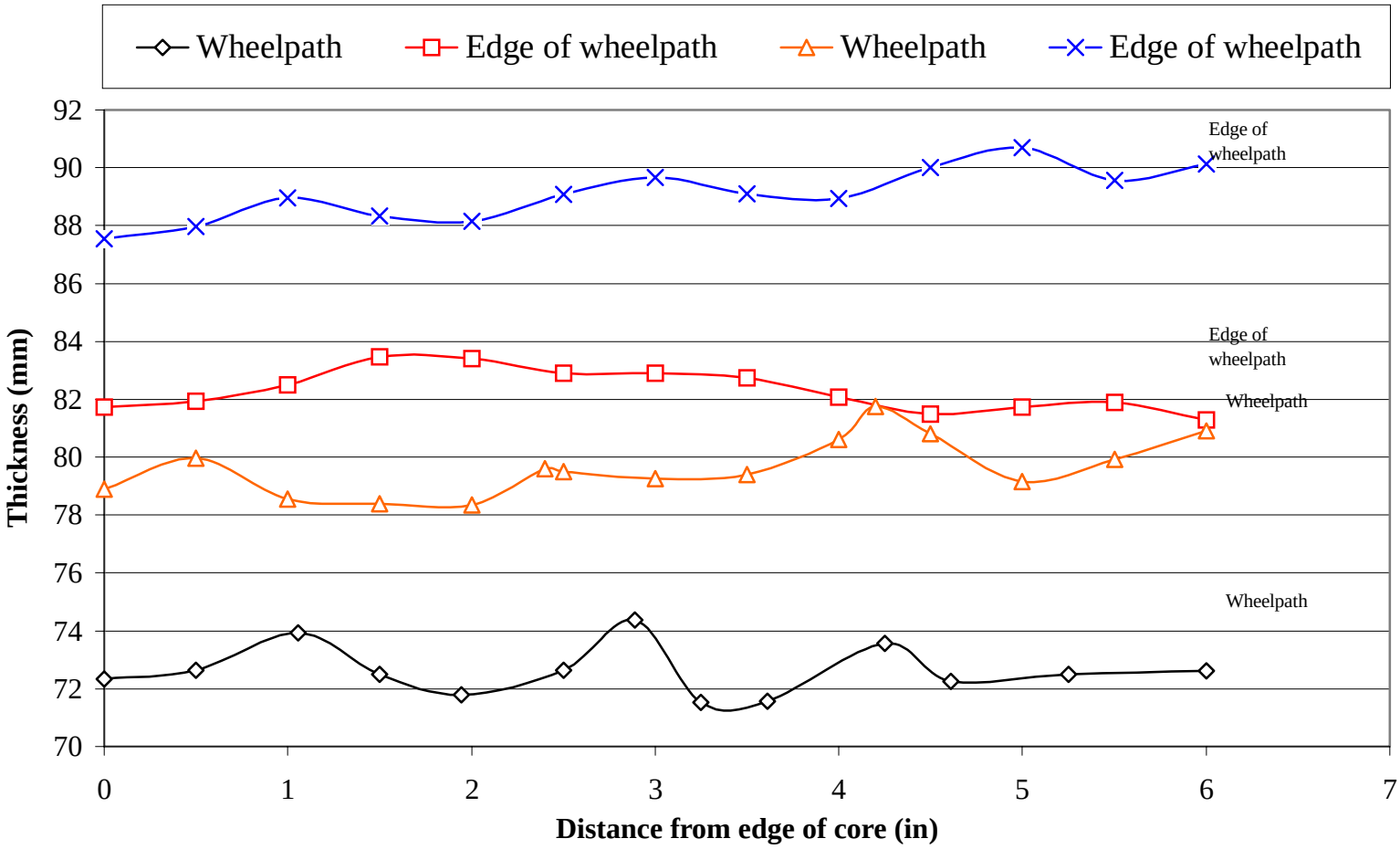

Figure C.3 Thickness Profiles of Cores from Section 7BE (Bi-Directional with 4" Wander in 2" Increments)

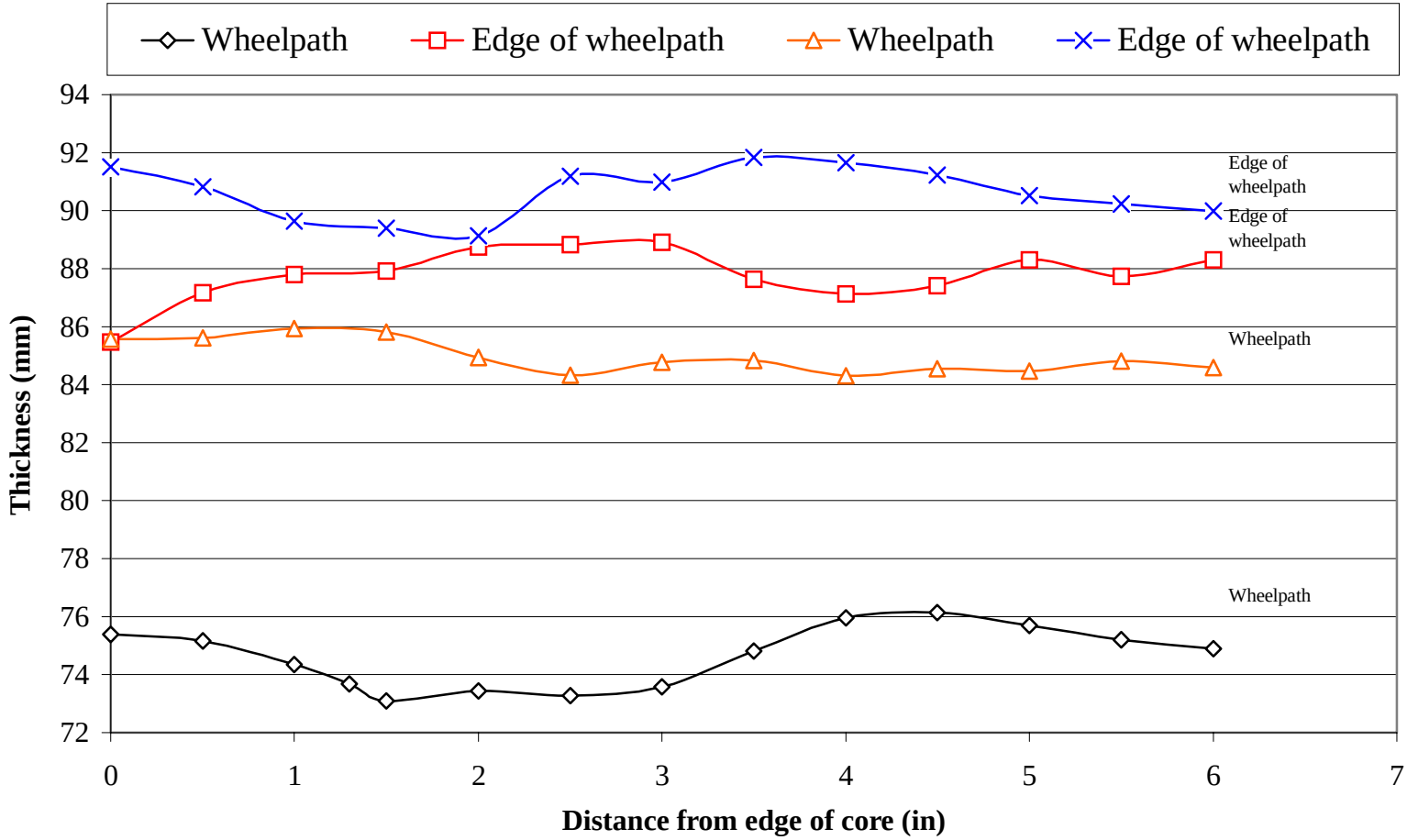

Figure C.4 Thickness Profiles of Cores from Section 7BE (Uni-Directional without Wander)

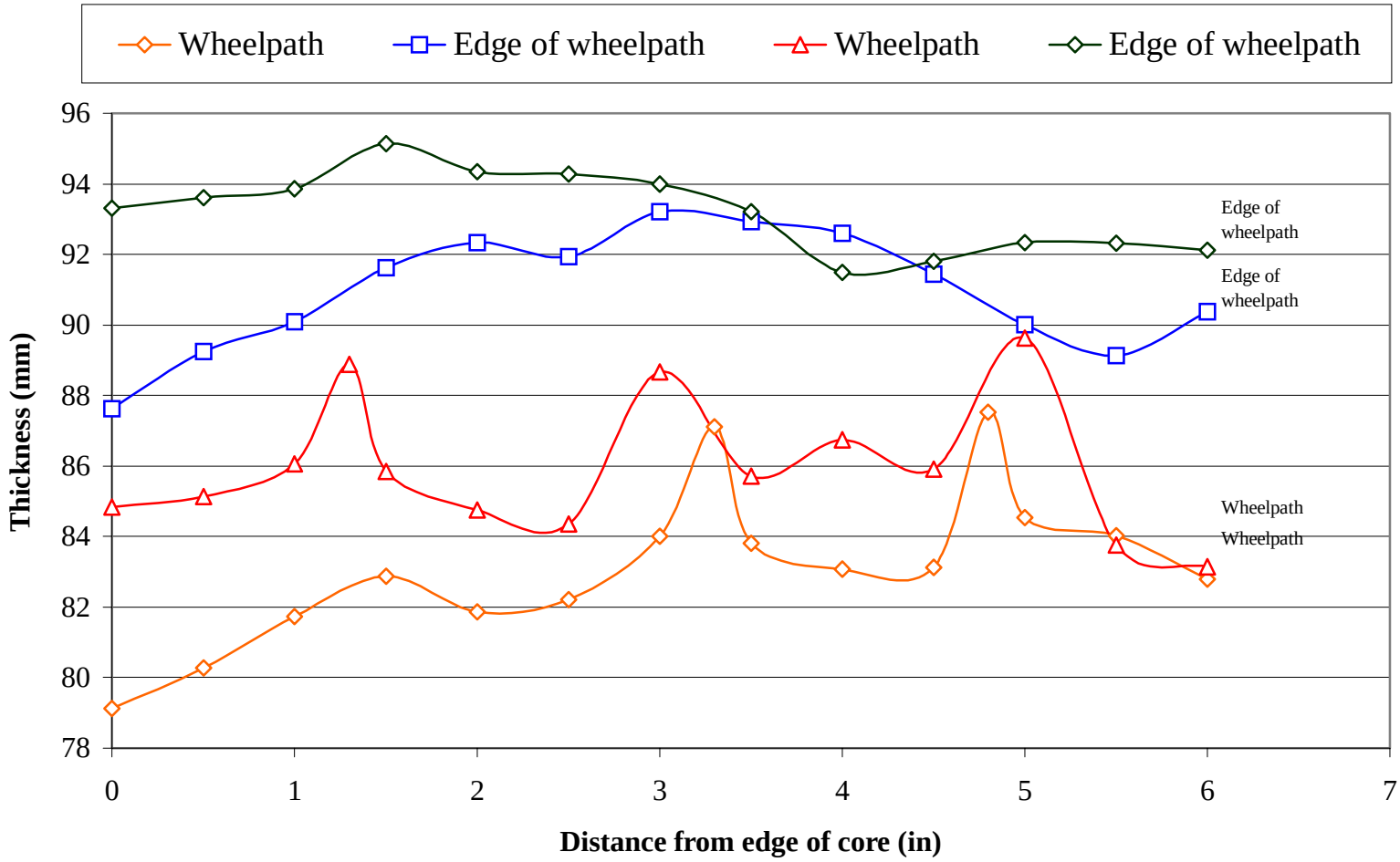

Figure C.5 Thickness Profiles of Cores from Section 7C (Bi-Directional without Wander)

APPENDIX D
LITERATURE REVIEW ON ACCELERATED PAVEMENT TESTING AND FIELD RUT MEASUREMENT

D.1 Full-Scale/Accelerated Pavement Testing

D.1.1 History of full-scale/accelerated pavement testing

Full-scale/accelerated pavement testing (FS/APT) had begun in 1909 with a test track in Detroit, Michigan, as described by Metcalf in *NCHRP Synthesis of Highway Practice 235: Application of Full-Scale Accelerated Pavement Testing*. Various institutions and facilities have invented and developed their own full-scale accelerated pavement testing equipment to pursue this activity. In *NCHRP Synthesis of Highway Practice 235*, it was described as "the controlled application of a prototype wheel loading, at or above the appropriated legal loading limit to a prototype or actual, layered and structural pavement system to determine pavement response and performance under a controlled, accelerated accumulation of damage in a compressed time of period" [Metcalf 1996].

Since 1940, full-scale airfield pavements were experimented at the U.S. Army Corps of Engineers (USACE) Waterways Experiment Station (WES). In the late 1950s, the American Association of State Highway Officials (AASHTO) conducted the full-scale AASHTO Road Test. During the 1970s and 1980s, FS/APT activities had also started to take place in several European countries, Australia and South Africa. In the United States, FS/APT research activities had been initiated and advanced significantly through the efforts from the FHWA, USACE (at both WES and at the Cold Regions

Research and Engineering Laboratory (CRREL)), and the states of California, Louisiana, Minnesota, Texas and others. The state of Florida and the National Center for Asphalt Technology (NCAT) had also initiated FS/APT program with the collaboration of Alabama Department of Transportation. In 2001, for the first time, Florida Department of Transportation (FDOT) acquired a Heavy Vehicle Simulator (HVS), Mark IV model and placed test tracks at the site of the State Materials Research Center in Gainesville, Florida.

D.1.2 Benefits and functions of using FS/APT

Evaluation and validation of new pavement technologies and innovative concepts require assessing their in-service long-term performance. In-service assessments require the consideration of the interaction between traffic loading, material properties, and environmental effects. The primary disadvantage of such an evaluation approach is the extensive time period required before potentially meaningful results can be obtained. In addition, it is difficult, impractical, and expensive to obtain all the data and information required from in-service experimental test sites.

The need for faster and more practical evaluation methods under closely simulated in-service conditions prompted various institutions to consider the adoption of Full-Scale Accelerated Pavement Testing. Generally, APT is defined as a controlled application of realistic wheel loading to a pavement system simulating long-term, in-service loading conditions. However, FS/APT can simulate trafficking under more realistic and severe pavement and environmental conditions than any other APTs. FS/APT can produce early, reliable and beneficial results while improving pavement technology and understanding/predicting pavement systems performance.

D.1.3 Various full-size accelerated pavement testing

Numerous accelerated pavement testing (APT) machines have been manufactured and accepted by various state departments of transportation, institutions, and private companies. In this section, several APT machines and facilities are described along with the Heavy Vehicle Simulator.

D.1.4 Simulated Loading And Vehicle Emulator (SLAVE)

Canterbury Accelerated Pavement Testing Indoor Facility (CAPTIF) carried out the SLAVE, managed by Transit New Zealand, the national highway authority with help from the research staff of the University of Canterbury in 1986. The main feature of CAPTIF is the Simulated Loading and Vehicle Emulator, which can apply a myriad of loading conditions via an array of tire and load configurations at high rates of accelerated loading [Pidwerbesky 1995]. This FS/APT can apply realistic dynamic loads at a high rate (about 20,000 revolutions per 24 hours). The wheels mounted to a trapezoidal leaf, can travel at a speed of 3.1 mph (5 km/h) to 31.1mph (50 km/h), and carry static loads from 21 kN to 60 kN. The SLAVE is able to traffic over the test pavements with up to 1.45 m wander in 1 cm increments.

D.1.5 The Texas Mobile Load Simulator (TxMLS)

This TxMLS was developed by the Center for Transportation Research (CTR) at the University of Texas at Austin in 1988. The development of the TxMLS took over 5 years and cost 3.4 million dollars. For safety and efficiency, the TxMLS is a closed-loop design of six truck bogies linked by a chain-type mechanism. The TxMLS was designed

for 6,000-axle loading per hour, up to 10 in (25.4 cm) wander, and 12.5 mph (20 km/h) [Hugo et al. 1991].

D.1.6 Accelerated Pavement Load Facility (APLF) tester

In 1996, the Ohio University and Ohio State University were awarded from the Ohio Board of Regents for a 1.65 million-dollar project to develop and construct an enclosed accelerated pavement load facility (APLF) at Ohio University's Lancaster campus. The 4,100-square-foot APLF has the width capacity for two 12-foot wide adjacent lanes with four 10-foot shoulders, and a 8-foot deep pit for construction of desired pavement structures. The wheel travels at a speed of 5 mph (3.1 mph) with a lateral wheel wander of up to 10 inches (25.4 cm). The APLF can apply reciprocating wheel loads of 9,000 lbs to 30,000 lbs. The range of test air temperature is 10° F (-12° C) to 110 °F (43° C) [Hoot 1997].

D.1.7 INDOT/PURDUE accelerated pavement tester

In 1992, the Indiana Department of Transportation and the Purdue University designed and constructed an approximately 2000-square feet environmentally controlled building consisting of 20 by 20 feet wide and 6 feet deep test pit. A radiant heating system was added to circulate the heat up to 50° C (122° F). This facility can apply test loads up to 20,000 lbs in either static or dynamic mode with a speed of 10 mph (16 km/h) [White et al. 1992].

D.1.8 Advanced Transportation Loading System (ATLaS)

Advanced Transportation Research Engineering Laboratory (ATREL) in former Chanute Air Force Base was awarded a 2-million-dollar research project to build a full-

scale APT equipment by the Illinois Department of Transportation and the State of Illinois in 2002. The ATLaS was manufactured by Applied Research Associate, Inc. (ARA). It is approximately 124 ft. long, 12 ft. high, and 12 ft. wide. The length of test area to be trafficked with constant velocity loading is approximately 65 feet. The approximate weight of the machine is 156 kips. The ATLaS can transmit a load of up to 80,000 pounds to the test pavement through a hydraulic ram attached to a wheel carriage. The ATLAS can apply up to 10,000 repetitions over the test pavements per day with bi-directional mode. The machine's maximum speed is 10 miles per hour under all kinds of daily environments [Mitchell 2002].

D.1.9 Accelerated Loading Facility (ALF) tester

The ALF is a transportable linear full-size accelerated pavement tester invested and developed by the Department of Transportation and Development (DOTD) in cooperation with the Federal Highway Administration (FHWA). The FHWA has been conducting research associated with flexible pavement performance using ALF pavement testing machine for over one decade [Bonaquist 1998]. The ALF was stationed at and operated by the Louisiana Transportation Research Center (LTRC) Pavement Research Facility in 1998, and Turner-Fairbank Highway Research Center (TFHRC) in Virginia. The ALF simulates dual tires of a single truck axle and wheel loads of 10,000 lbs up to 21,000 lbs. The uni-directional trafficking tester operates 8,100 passes per day over 12 by 1.2-meter test pavements. The cost of the ALF was approximately 1.9-million dollars.

D.1.10 Kansas Accelerated Testing Laboratory (K-ATL) Tester

The Kansas Department of Transportation (KDOT) awarded a contract to Kansas State University (KSU) and the Kansas Technology Enterprise Corporation to develop

the Kansas Accelerated Testing Laboratory (K-ATL) in 1996. This APT is equipped with a tandem axle trafficking at 5 mph (8 km/h) and up to 40,000 lbs of loads on test pavement 20 ft long and 20 ft wide in this facility. The test pit can be constructed in 6-foot depth. Test temperatures can be controlled anywhere between –10° F (12° C) and 150° F (65.5° C).

D.1.11 Heavy Vehicle Simulator (HVS)

The Heavy Vehicle Simulator (HVS) is a mobile machine used to subject test pavements to accelerated trafficking. The HVS is developed and marketed by the Dynatest Company in South Africa. Currently, three HVS Mark IIIs are operational. Two of them were purchased by the California Department of Transportation (Caltrans), and the other is used in South Africa. Dynatest has upgraded the HVS Mark III to the fully automated HVS Mark IV. Two HVS Mark IVs are owned and operated by the Cold Regions Research & Engineering Laboratory (CRREL) of the U.S. Army Corps of Engineers, and VTT in Finland and VTI in Sweden (joint project). The upgraded version of the HVS Mark IV Plus has been purchased by CSIR, and Florida Department of Transportation (FDOT). Dynatest has developed a super-heavy HVS, the HVS-A Mark V used in the Waterways Experiment Station of U.S. Army Corps of Engineers. This HVS-A is capable to simulate aircraft wheel loads up to 440 kN (100 kips).

The FDOT has employed the HVS machine due to its mobility, and high testing ability. The benefits of using the HVS include cost-effective research, quick and highly reliable test results that lead the FDOT and other institutions to fast implementation for developing and validating lower-cost and better performing pavement technology. The HVS, which costed approximately 1.9 million dollars, is capable of providing the service

either on indoor test pavements or in-service pavements. The HVS has the advantage of being more mobile than any other APT machines. It can be transported between long-distance test sites by means of towing with a trailer truck. It can be moved from one test section to the other under its own power. The other advantage of choosing the HVS is its numerous capabilities for accelerating pavement testing with temperature control. The HVS was designed to provide wheel trafficking over a test pavement up to 20 ft (6 m) long and 5 ft (1.5 m) wide. The HVS can apply wheel loads between 30 kN and 200 kN (7 kips and 45 kips) at a speed of up to 8 mph (12 km/h) in either uni-directional or bi-directional mode. Test temperatures can be set up by adding on the temperature control chambers with the installation of radiant heaters [Coetzee 1996].

The detailed technical specifications of the HVS Mark IV Plus are described in Appendix E of this report.

D.2 Field Measurements of Rutting

Testing of permanent deformation in the laboratory and measurement of rutting in the field have been done by pavement engineers and researchers in order to understand the rutting performance of pavements better. The measurement of transverse rut profile and depth has been made by both static and dynamic methods. The static methods have the problems of traffic control, safety of operators and slow work efficiency. They are performed by means of tripod, string-lines, straight edges and dipstick. Unlike the static methods, dynamic methods do not require much traffic control, and provide safer environment, and better efficiency.

D.2.1 Tripod method

The three-legged device is used to measure only rut depth of wheel path in such a manner as to straddle two legs with a width of 4 ft. on the observed location of maximum rut depth. This method tends to be less effective and more erroneous due to its dependence of the operator's skill and judgment. This measurement is also extremely hazardous and slow in on-going traffics [Gramling et al. 1991].

D.2.2 Stringline method

A piece of mason's cord is stretched across the pavement, and the difference in elevation between pavement surface and stringline is measured. The string can be held at any level of pavement and measurements are normally taken at 1-ft intervals. However, this procedure is also extremely slow and hazardous [Gramling et al. 1991].

D.2.3 Straight edge method

A straight wooded or metal beam is placed across the pavement and the elevation difference between pavement surface and the beam is measured at regular intervals. The length of beam should be higher than the width of pavement; therefore, this method can be measured at only one level of pavement above the heaves. Although this method is accepted, it requires extreme care and safety for the operator in all kinds of traffic [Gramling et al. 1991].

D.2.4 Dipstick method

An electronic level and profiler instrument (dipstick) is used to measure the transverse profile of a pavement. Two legs of the device are stretched in 2-in to 1-ft increments. The sequential measurements are read and recorded, and data obtained from

the measurement can be plotted and calculated to determine transverse rut depths. There is the possibility of missing maximum rut depth at large intervals of measurement [Gramling et al. 1991].

D.2.5 Automatic laser sensor system

Either ultrasonic or laser sensors can be adapted to take transverse measurements in this automated system. These sensors are commercially available with numerous manufacturers. Unlike any static devices, these dynamic devices have the ability of taking measurements of full width of lane and shoulder in transverse direction. In addition, the capability of measuring from a moving vehicle with no traffic control is another advantage of using this device. The recorded data can be transmitted to a computer to evaluate the rut depths [Gramling et al. 1991].

D.2.6 Photography system

The Strategic Highway Research Program (SHRP) adopts this system to evaluate and analyze long-term pavement performance. This system is referred as the “wire method” of analysis. The system projects a line onto and across the pavement while the 35-mm film taking photographs of 15-ft. transverse profile from directly overhead. The photographed data can be transmitted to a computer for analysis of the transverse ruts. This system provides permanent records on the surveys conducted [Gramling et al. 1991].

APPENDIX E
HEAVY VEHICLE SIMULATOR

E.1 General Description of HVS Mark IV

The Heavy Vehicle Simulator (HVS) Mark IV is a mobile Accelerated Pavement Testing (APT) machine, which consists of following assemblies:

- Structure Assembly
- Suspension Assembly
- Hydraulic System Assembly
- Electrical System Assembly
- Generator Set

This section presents a description of these assemblies as given in the manual for the HVS Mark IV [Dynatest].

E.2 Structure Assembly

E.2.1 Frame

The Frame consists of a double truss of rectangular tubing members. It serves as the main chassis of the machine. The Main Power Pack, Diesel Power Pack and other components are mounted onto the truss girder. The Frame is also connected to the electrical devices and air brake.

E.2.2 Cabin

The Cabin accommodates the steering wheel, driver's seat, controls and instruments. Vehicle Computer Unit (VCU) is located behind the driver's seat in the Cabin. The steering is operated by means of a conventional power steering wheel. When the HVS needs to be moved or transported to a towing trailer truck under its own power, the controls located on the dashboard of driver seat can be used. The door for the access to the inside of Cabin is located in the front of the Cabin of the HVS.

E.2.3 Test beam

A test wheel mounted in the Test Carriage operates trafficking. The test carriage is also mounted in the Test Beam. The Test Beam is a longitudinal double-flanged steel beam, which contains two sets of longitudinal metal chains at each side of the Test Beam. The Test Beam can move laterally by means of hydraulic side shift cylinders, and the Test Carriage is able to move in longitudinal direction by the action from the chains. The Test Beam is supported by Vertical Shifts, which allow the Test Beam to be raised and lowered vertically. The Vertical Shifts are locked after they are set to be in a certain position. Three possible vertical locked positions are (1) the transport position, (2) the upper load position, and (3) the lower load position.

E.2.4 Test carriage

The Test Carriage mounts either a super single tire or a dual truck tire. The load on the tire is applied by the hydraulic cylinders mounted on the Test Carriage. The Carriage Control Unit (CCU) controls all the operations of Test Carriage.

E.3 Suspension Assembly

E.3.1 Undercarriage cabin end

The four bogeys are connected to the Undercarriage Cabin End, and each bogey is also fitted with two wheels. Two hydraulic cylinders and a system of cranks and links operate the wheels. The vacuum air brake is mounted onto the bogey axles. These bogeys are capable of being raised and lowered by means of the hydraulic system.

E.3.2 Undercarriage tow end

The Undercarriage Tow End is a welded structure fitted with an axle connecting two wheels. The two wheels are moved by hydraulic motors and drive the HVS when the machine is under its own power.

E.3.3 Steering

The Steering is connected to the bogeys at the Undercarriage Cabin End and steers the HVS when the HVS needs to be carried to a transport truck or be moved by its own power.

E.3.4 Brakes and Pneumatics

The operation of the brakes and the inflation of tires are operated by the Brakes and Pneumatics System. The compressed air, which is supplied by the diesel engine's compressor, gives power to the air brakes. When the compressed air is switched on, the parking brake of the HVS is released. The brakes lock automatically when pneumatic power is lost.

E.4 Hydraulic System Assembly

E.4.1 Main pump

The Main Pump, powered by an 110-kW 480-V electric motor, drives the Test Carriage. The pump is a variable displacement axial piston pump, which uses pilot pressure to alter the angle of the swash plate. This boosts up the pump to supply hydraulic fluid. Unlike the pump, the test carriage motors are fixed displacement and radial type motors. They control the speed and direction of the test carriage.

E.4.2 Main reservoir unit

The Main Reservoir Unit (1) provides oil to the Main Pump and Carriage Drive, (2) cools and filters hydraulic oils, and (3) interlocks the level of temperature and oil.

E.4.3 Carriage Hydraulic System

The Carriage Hydraulic System provides hydraulic power to apply the test load to the test wheel. The variable displacement axial piston hydraulic pump powers the system with component supports of a 30-kW electric motor, a fluid reservoir, a hydraulic load cylinder, a manifold block, four accumulators and a hydraulic oil cooler.

E.4.4 Auxiliary hydraulics cabin end

The auxiliary pump from the Main Reservoir Unit supplies the hydraulic power to allow the Auxiliary Hydraulics Cabin End to raise and lower the cabin end outriggers and cabin end suspension bogeys.

E.4.5 Auxiliary Hydraulics Tow End

The Auxiliary Hydraulics Tow End is designed to adjust the height of the tow end outtriggers, powered by the auxiliary pump from the Main Reservoir Unit.

E.5 Electrical System Assembly

E.5.1 Outside Computer Unit (OCU)

The functions of OCU are the followings:

- The automated operation of the HVS.
- Continuous reading and recording of test parameters during the test.
- Continuous reading and recording of fault operations of the HVS
- The recording of log file of all fault and operation conditions.
- Assistance to provide tools with operation and maintenance of the HVS.

E.5.2 Vehicle Computer Unit (VCU)

The VCU communicates directly with the OCU and allows the Carriage Computer Unit (CCU) to operate the test. OCU sends the test parameters to VCU, and the test parameters are downloaded to CCU.

The functions of VCU are the followings:

- Operation of Test Carriage along the Test Beam.
- Lateral movement of the Test Beam.
- Operation of the wheel drive motors.

E.5.3 Carriage Computer Unit (CCU)

The CCU located on the Test Carriage, receives the test parameters from the VCU to enable the Test Carriage to operate the accelerated pavement testing.

The functions of CCU are the followings:

- Application of load on test wheels.
- Lift of the Test Carriage for uni-directional operation.

E.6 Generator Set

The 6-cylinder CAT diesel engine powers a 200kVA, 480 V AC generator. The Generator Set generates the electric power.